HIGHWAY RESEARCH BOARD
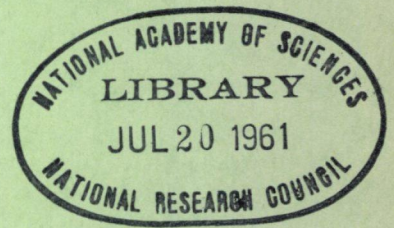
Bulletin 277

Non-Destructive Dynamic Testing of Soils And Highway Pavements

National Academy of Sciences— National Research Council

HIGHWAY RESEARCH BOARD

Bulletin 277

Non-Destructive Dynamic Testing of Soils And Highway Pavements

Presented at the
39th ANNUAL MEETING
January 11-15, 1960

1960
WASHINGTON, D. C.

Department of Soils, Geology and Foundations

Miles S. Kersten, Chairman
Professor of Highway Engineering
University of Minnesota, Minneapolis

COMMITTEE ON STRESS DISTRIBUTION IN EARTH MASSES

D. P. Krynine, Chairman
2960 Pine Avenue
Berkeley, California

Richard G. Ahlvin, Chief Engineer, Special Projects Section, Waterways Experiment Station, Vicksburg, Mississippi

E.S. Barber, Consulting Engineer, Soil Mechanics and Foundations (Bureau of Public Roads and University of Maryland), Arlington, Virginia

B.E. Colley, Portland Cement Association, Chicago, Illinois

Lawrence A. DuBose, Testing Service Corporation, Lombard, Illinois

Austin H. Emery, Associate Soils Engineer, Bureau of Soil Mechanics, New York State Department of Public Works, State Office Building, Albany, N.Y.

Jacob Feld, Consulting Engineer, 60 East 23rd Street, New York, N.Y.

Milton E. Harr, Assistant Professor, School of Civil Engineering, Purdue University, Lafayette, Indiana

Robert G. Hennes, University of Calcutta, Calcutta, India

W.S. Housel, University of Michigan, Ann Arbor

F.N. Hveem, Materials and Research Engineer, California Division of Highways, Sacramento

Robert L. McNeill, Department of Civil Engineering, San Jose State College, San Jose, California

Robert L. Schiffman, Department of Civil Engineering, Rensselaer Polytechnic Institute, Troy, N.Y.

Werner E. Schmid, Assistant Professor, Department of Civil Engineering, Princeton University, Princeton, N.J.

Frank H. Scrivner, Rigid Pavement Research Engineer, AASHO Road Test, Ottawa, Illinois

Contents

ERRATA

BULLETIN 277

n Bulletin 277, in the paper by R. Jones (pages 8-29),

ures 1 to 13, inclusive (pages 11-23), should be replaced

those given here.
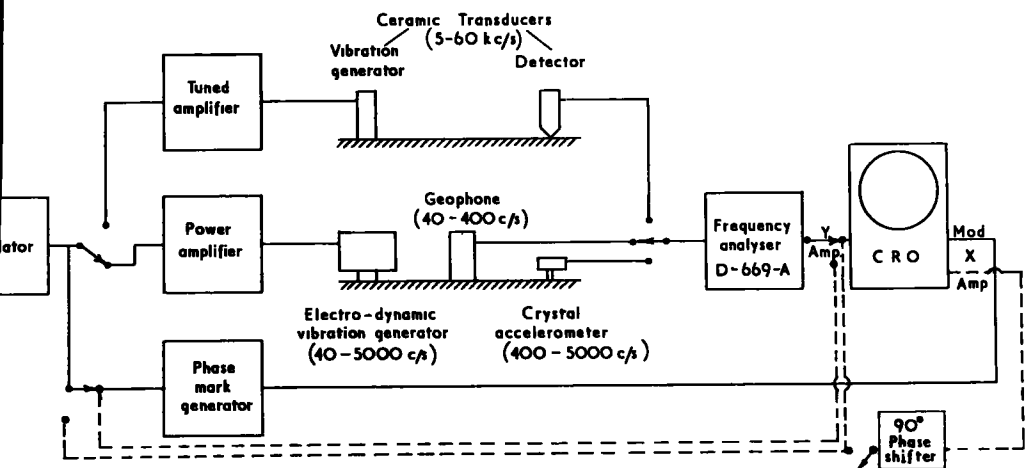
re 1. Schematic diagram of apparatus; switches set for first experimental technique.
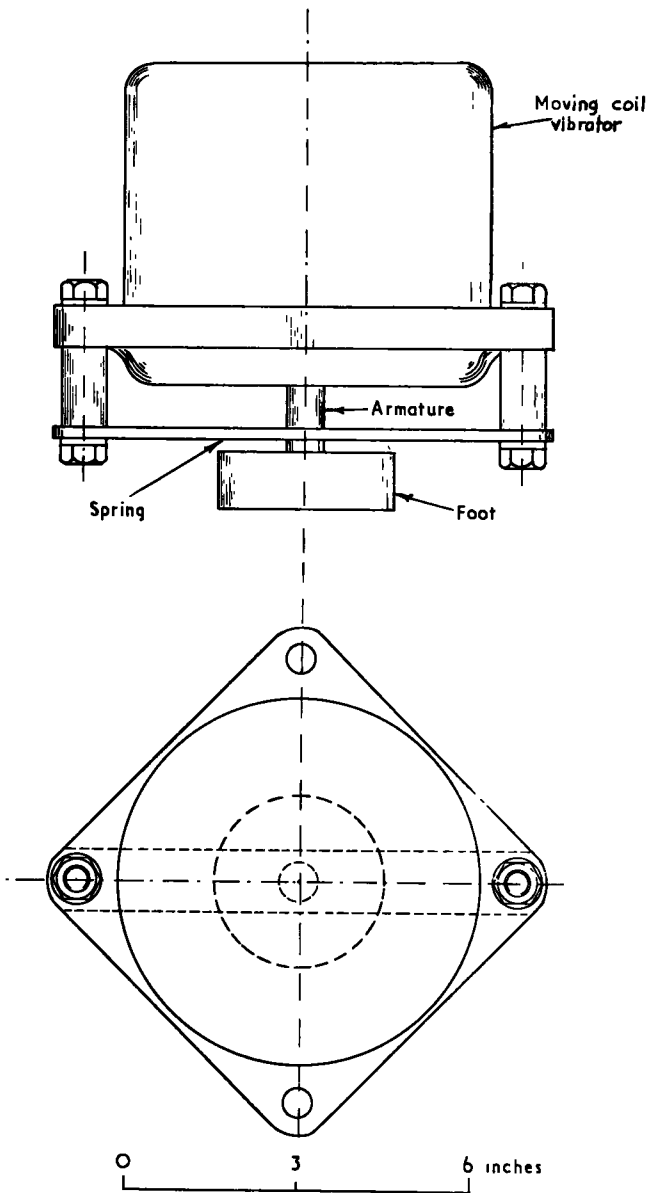
Figure 2. Electro-dynamic .vibration generator.
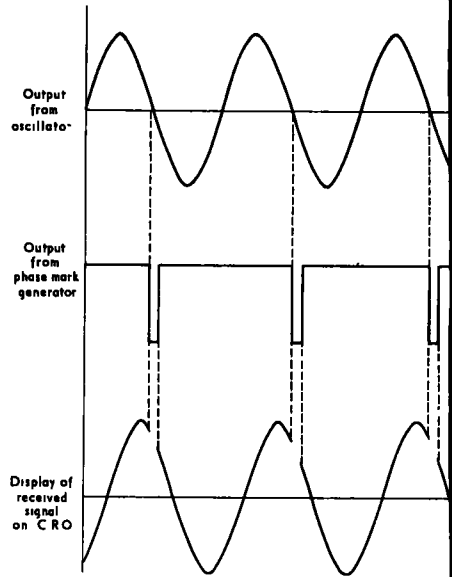
Figure 3. Waveforms illustrating m used for indicating phase of rec signal.

G_1, E_1, d_1, α_1, β_1, γ_1

G_2, E_2, d_2, α_2, β_2, γ_2

G_3, E_3, d_3, α_3, β_3, γ_3

G = Shear modulus of elasticity
E = Young's modulus of elasticity
d = Density
α = Compressional wave velocity
β = Shear wave velocity
γ = Rayleigh wave velocity
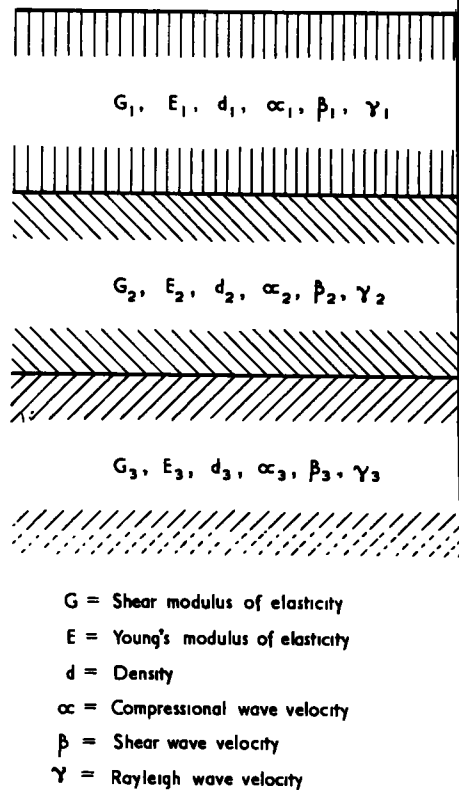
Figure 4. Nomenclature of layers in structure.
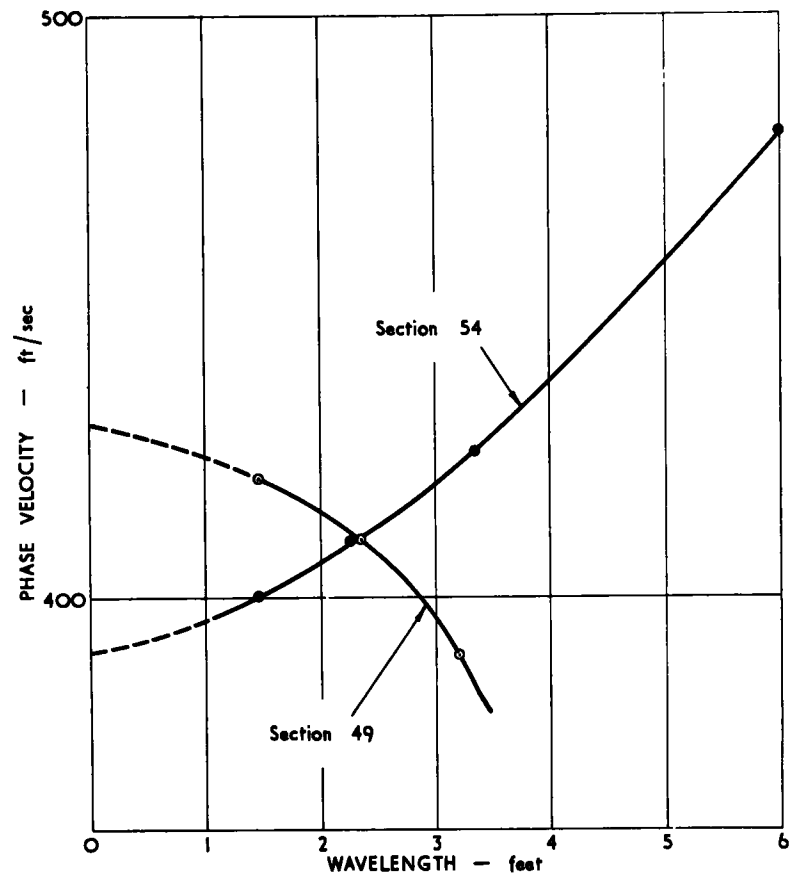
Figure 5. Variation of phase velocity with wavelength on two soils
at Alconbury.
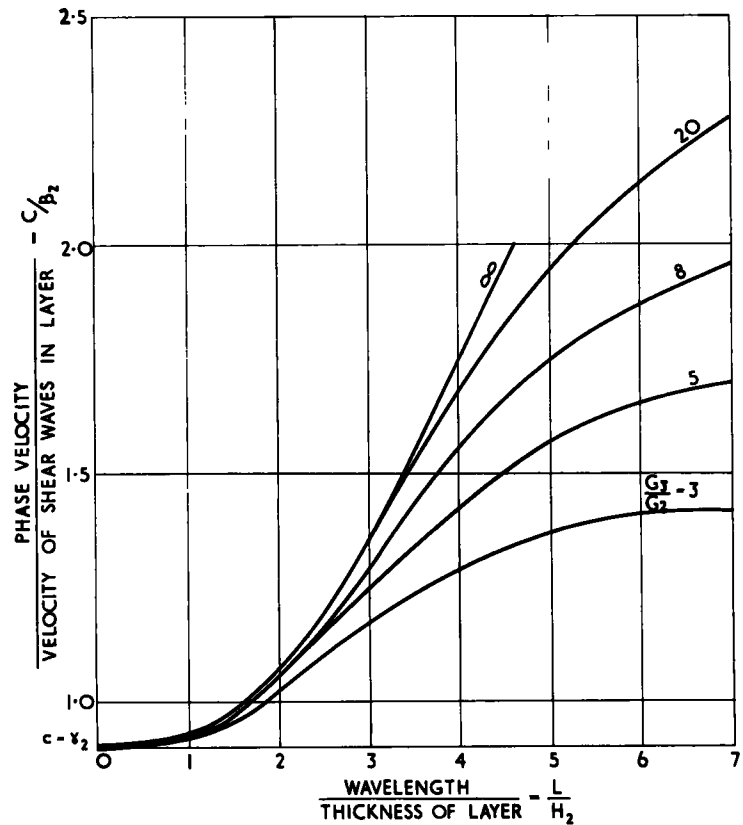
Figure 6. Phase velocity of Rayleigh waves in a single layer
over a semi-infinite medium ($d_2 = d_3$).
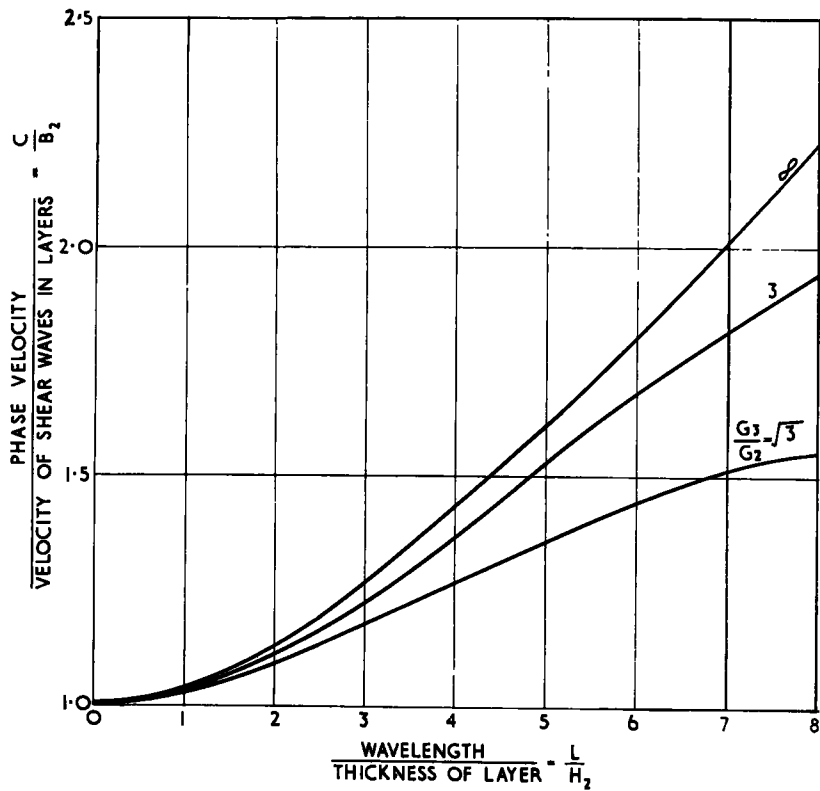
Figure 7. Phase velocity of Love waves in a single layer over a semi-infinite medium ($d_2 = d_3$).
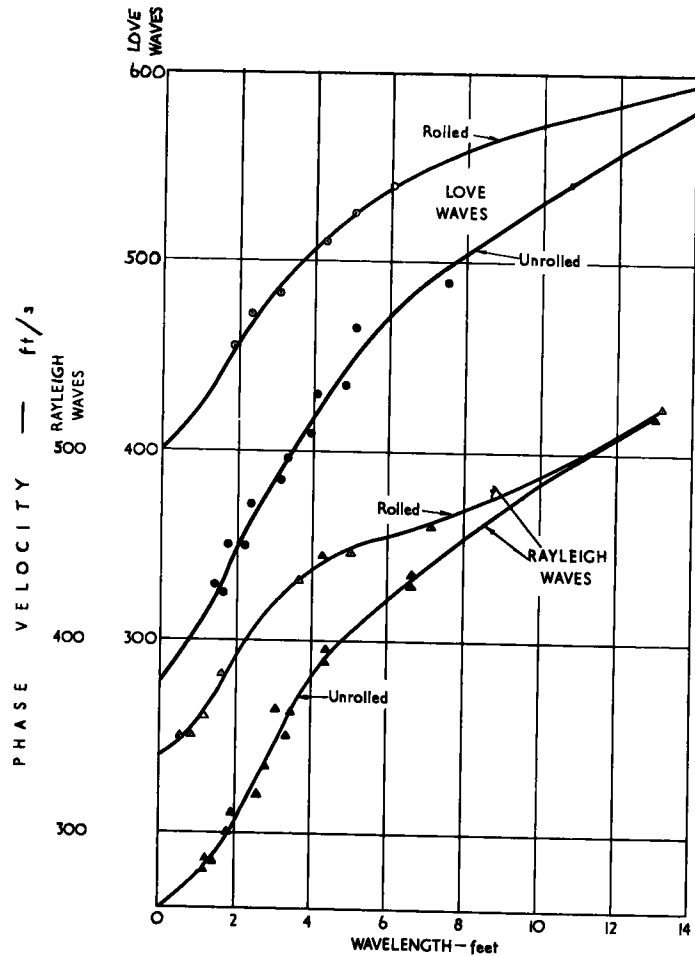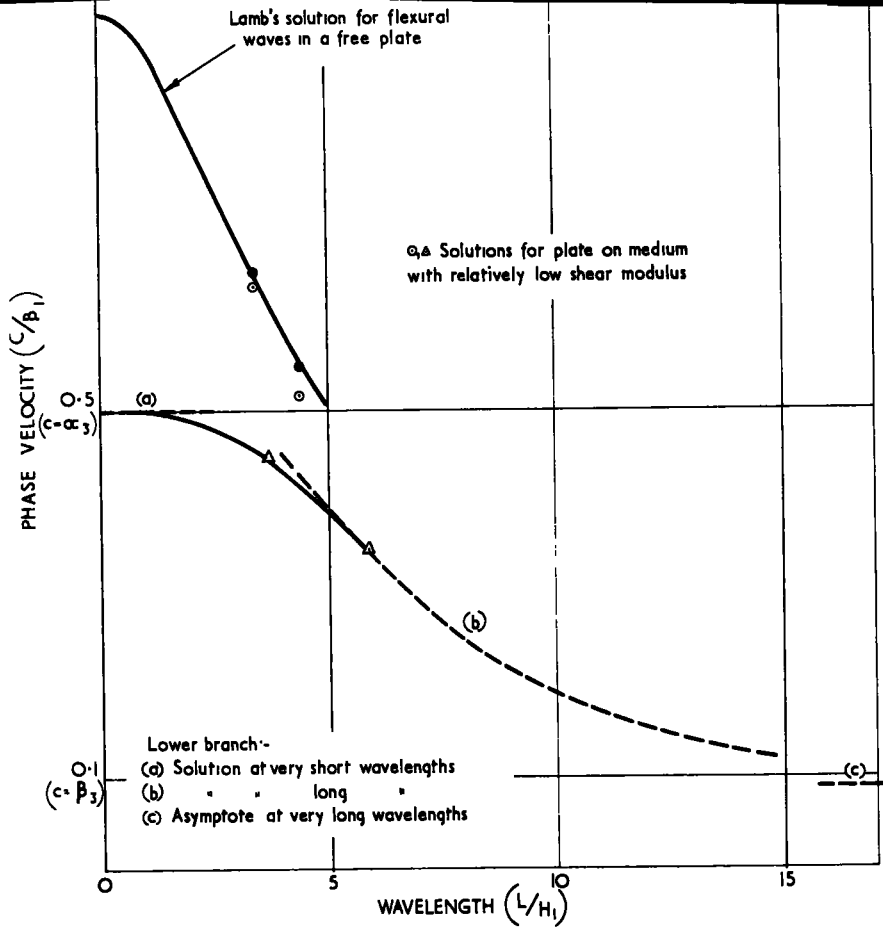
Figure 9. Theoretical relation between phase velocity and wavelength for a plate overlying a medium with relatively low shear modulus ($\beta_1 = 2 \alpha_3 = 10\beta_3$; $d_1 = d_3$; $m_1 = 1/3$).
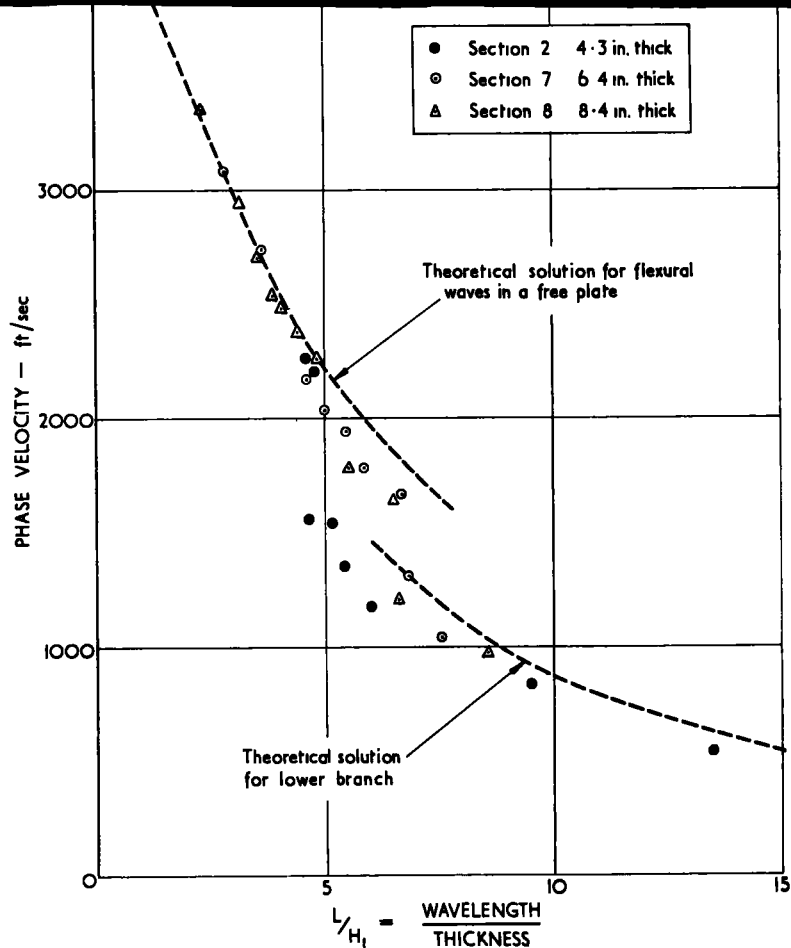
Figure 10. Experimental results obtained from dense asphalt bases laid directly on soil.
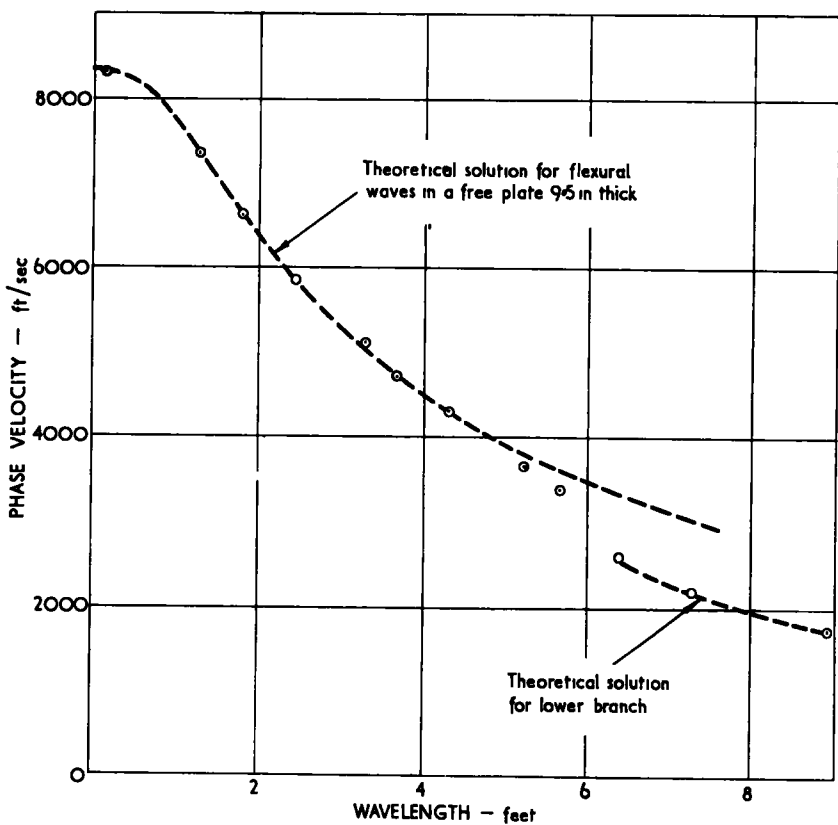
Figure 11. Results from concrete slab nominally 9 in. thick laid on well-compacted hoggin.
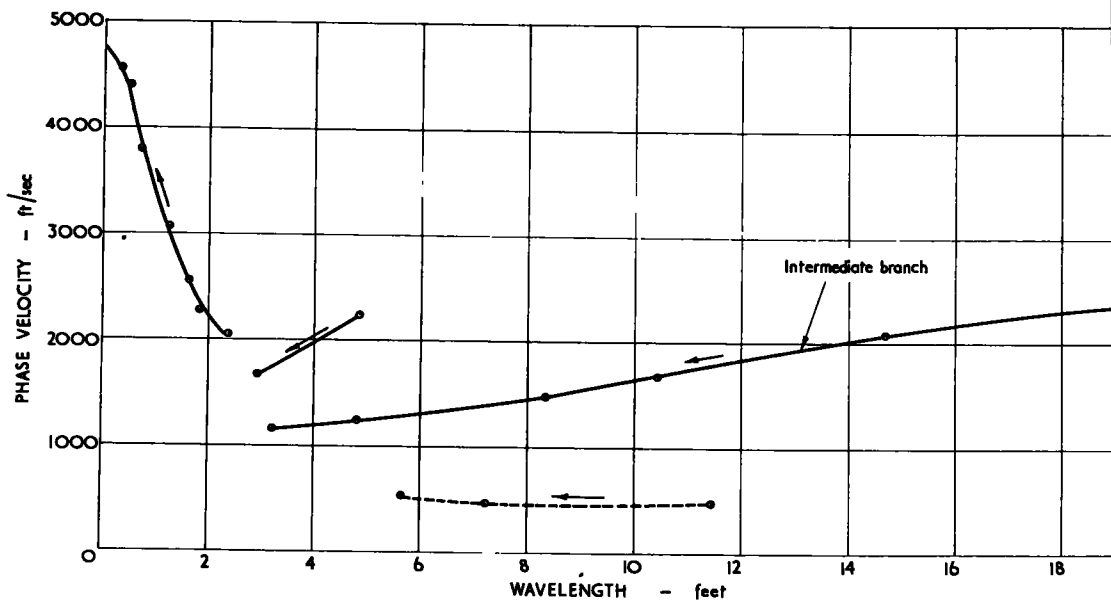
Figure 12. Experimental results from a road construction consisting of 4-in. rolled asphal 13-in. (approx.) sand base on clay subgrade.
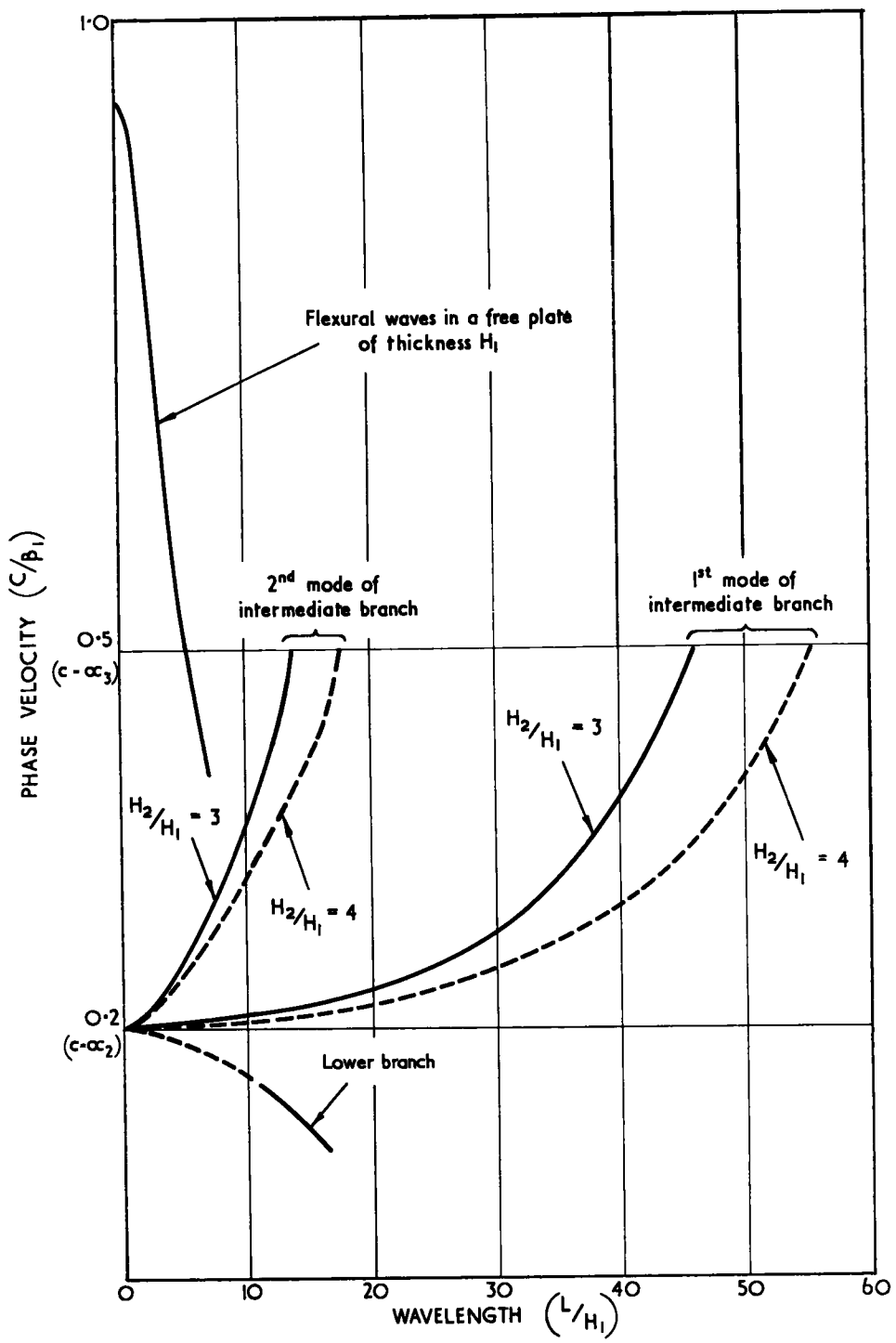
Figure 13. Theoretical solutions for the propagation of vibrations in a system with two surface layers.

$$\left(\begin{array}{c} a_1 = 2\beta_1 = 4\,a_3 = 10\,a_2 \\ d_1 = 1\cdot2d_2 = 1\cdot1d_3 \end{array}\right)$$

A Survey of Dynamic Methods of Testing Roads and Runways

. JONES and A.C. WHIFFIN, Department of Scientific and Industrial Research,
oad Research Laboratory, Harmondsworth, Middlesex, England

The object of this paper is to indicate how far dynamic
methods of testing roads have developed in the various
countries and to summarize the present state of the
work.
The vibrational method of testing roads originated in
Germany where, before World War II, mechanical vibra-
tors were used to investigate the mechanical properties
of different types of soil. During and after World War II,
further developments of the technique were made by the
Royal Dutch Shell Co.'s Laboratory at Amsterdam, and
the method was applied to testing roads and runways. The
dynamic stiffness of the construction was deduced from
the applied vibratory force and the resultant amplitude of
vibration. Tests on a variety of roads indicated that high
values of the stiffness were associated with strong forms
of construction, and low values with weak ones. The ulti-
mate objectives of this form of nondestructive test are
to predict the performance of roads under traffic and to
determine where and when failure of the construction is
beginning. Testing techniques to these ends have been
developed recently in Germany.
The British Road Research Laboratory has been
studying the velocity of propagation of vibrations in layered
constructions using electro-mechanical vibrators covering
a much wider frequency range than is possible with the
rotary machines normally employed. The relations ob-
tained between velocity and frequency are being studied to
deduce the elasticities and thicknesses of the layers partly
to assess the quality of the construction and partly to obtain
data which might be later employed for pavement design.
The application of vibrational testing to pavement design is
still in its infancy and it is too early yet to decide whether
or not such a design technique will ultimately be possible.

THE VIBRATIONAL TESTING of roads and runways originated in Germany, where,
between 1928 and 1939, mechanical vibrators were used to investigate the mechanical
properties of different types of soil. During and after World War II, further develop-
ments of the technique were made by the Royal Dutch Shell Co.'s Laboratory at Amster-
dam, and the method was applied to testing roads and runways. Attempts were made
to correlate the data obtained from vibrational testing with the performance of the
construction under traffic. During the past few years, the Road Research Laboratory
in England has studied the propagation of vibrations in road constructions and has at-
tempted to interpret the relation between the velocity of these vibrations and their
frequency in terms of the elasticities and thicknesses of the various layers forming
the road.
The main purpose of this paper is to indicate how dynamic methods of testing roads

1

have developed in the various countries and to summarize the present state of the wo[r]
There are still divergences of opinion on the interpretation of some of the results in
terms of the mechanical properties of the materials and these are discussed.

OBJECTS OF DYNAMIC TESTING

At present, roads and runways are largely designed on the basis of knowledge of t[h]
performance of other roads under similar traffic and subgrade conditions and by test[i]
the soil to estimate its bearing capacity under the conditions of moisture and density
likely to occur under the completed road. Roads giving a satisfactory performance
under traffic normally take a long time to prove their worth, and one of the objects o[f]
the development of vibrational testing was to provide a rapid, nondestructive testing
technique for assessing the probable performance of a road. By making tests at vari[ous]
ages on the same road, the commencement of changes which might result in failure c[an]
be observed, and, when sufficient experience has been obtained, the technique might [be]
used as the basis of decisions as to where remedial action is necessary. It is shown
later that these objectives have been partially attained.

One of the functions of a road is to spread the loads applied by the wheels of movin[g]
vehicles so that the stresses communicated to the soil subgrade are sufficiently redu[ced]
so as not to cause permanent deformation. Theoretical values of the stresses and de-
formations (1, 2, 3) generated in multi-layered elastic structures have shown that the
stresses applied to the soil subgrade by moving vehicles, and the deflections of the
construction under them, depend on the relative values of the dynamic elasticity of th[e]
layers forming the road and their thicknesses. The dynamic elasticities of the layer[s]
and their thicknesses can be determined in many cases by vibrational tests made both
during and after construction of the road. Because high dynamic elasticity is often
accompanied by good strength in the case of the materials used in flexible constructio[n]
vibrational measurements may be expected to indicate the quality of the construction.

The ultimate objective of the measurement of the dynamic elasticities and thicknes[s]
of the layers forming a road is to develop a method of pavement design based on the
stresses generated by traffic, the mechanical properties of the materials used for co[n]
structing the road, and the properties of the subsoil. Before such a method of design
becomes possible, it will be necessary to check experimentally that the dynamic stre[ss]
generated by traffic can be predicted theoretically from knowledge of the dynamic ela[s]
ticities of the layers and their thicknesses. It will also be essential to obtain informa
tion concerning the dynamic elasticities of the common road-making materials and to
determine their mechanical properties under repeated loading of the form applied by
traffic. Many of the materials employed in road construction, such as granular base[s]
are unsuitable for preparation as laboratory specimens, and there are obvious advan-
tages in determining their dynamic elasticities in situ under the conditions existing in
roads. It may well be many years before all the information required for pavement
design along the lines suggested is accumulated. Some progress will be possible, how
ever, once the theoretical work on the distribution of stress and deformation in multi-
layered elastic structures has been checked experimentally, and when information has
been obtained on the dynamic elasticities of the common road-making materials. For
example, it should then be possible to design a variety of constructions to give the sam[e]
dynamic stress at the soil/base interface with a given soil. When this has been done i[t]
will still have to be proved, however, that equality of this interfacial stress gives
equality of performance of the various types of construction under traffic. It is to be
expected that repeated loading may well cause the different constructions to behave in
different ways if fatigue is an important property, in which case knowledge of this pro[p]
erty will have to be taken into consideration.

The dynamic elasticities and thicknesses of the layers forming roads can be deduce[d]
from the relationship between the velocity of propagation and frequency of vibrations
generated in the surface. This aspect of the work is as yet far from complete, largel[y]
because of difficulties in interpreting these relationships. The theoretical studies of
stress and deformation have been reported and some results of the necessary ancillar[y]
computational work are available (2, 3). The computations are being extended. Meas[u]

ents are being made of the dynamic stresses generated in roads by moving vehicles, t it is too early yet to say whether the theoretical values of these stresses have been nfirmed. It will be apparent that the application of the results obtained from vibra- nal testing to pavement design is thus still in its infancy and it is too early to decide ether or not such a design technique will become an engineering method.

DEVELOPMENT OF VIBRATIONAL METHODS

The vibrational technique originated in Germany during the period from 1928 to 1939, d the publications (4, 5, 6) of the Deutsches Gesellschaft fur Bodenmechanik (DEGEBO) e well known to workers in this field. A mechanical oscillator of the rotary out-of- lance mass type was employed and its vibratory characteristics were studied while was operated on many different types of soil. Attempts were made to deduce the echanical properties of the soil from the results. The resonant frequency of the brator varied with the bearing capacity of the soil but attempts to explain the results terms of a simple mass and spring system were unsuccessful. It was concluded that e properties of the soil could not be represented by a spring or even a damped-spring cause the resonant frequency of the vibratory varied with the applied vibratory force. here was also some conjecture as to whether or not allowance should be made for the ertia of part of the soil in computing the behavior of the mechanical vibrator.

The DEGEBO workers also measured the velocity of propagation of vibrations along e surface of the soil within the frequency range from 10 to 50 c/s (6). They observed at, on most soils, "dispersion phenomena" occurred, that is to say, the meas- ed phase velocity varied systematically with the frequency of the vibrations. ttempts were made to explain the dispersion phenomena in terms of variation of the roperties of the soil with depth and a comparison was made between theoretical predic- ons and the variations of soil type found at boreholes. Although some of these com- arisons were reasonably successful, development of the technique was hampered by ck of information of the types of surface waves being studied and, even within Germany, ere was divergence of opinion on this point. One practical result which emerged was at a qualitative relation was found between the velocity of propagation of the vibrations nd the bearing capacity of soils which were reasonably uniform with depth.

Immediately after World War II, further work on soil was reported from Sweden). In these experiments, the elastic modulus of a fairly uniform clay soil was obtained om the velocity of propagation of sustained vibrations at frequencies between 14 and 2 c/s. Plate-bearing tests were also made on the soil using plates of various diameters nd thicknesses, and a soil constant was derived from the product of the modulus of ubgrade reaction and the radius of the plate. The same constant was also computed om the elastic properties of the soil by assuming Poisson's ratio to be 0.5 and the lastic modulus that derived from the wave propagation measurements. The soil con- tants derived from the plate-bearing tests with plates of 3 meters radius were in good greement with those computed from the elastic modulus derived from the vibration xperiments: results from smaller plates gave poorer agreement. It was concluded hat the dynamic method of test gave a correct impression of the deformational charac- eristics of the clay soil under the action of a distributed load and could, therefore, rovide the appropriate value of the elasticity of the soil subgrade beneath roads where onsiderable load-spreading had resulted from the action of the upper layers.

Since 1948, the development of vibrational testing has been considerably influenced y the work of Van der Poel (8) and Nijboer (9) of the Dutch Shell Laboratory at Amster- am. Van der Poel devised a machine, now well-known as the "Dutch Shell Vibrator", mploying rotating out-of-balance masses to apply vibrational forces of 2 ± 2 tons to he road surface at frequencies between 5 and 60 c/s. The peak vibratory force (F_p) eveloped in the road was calculated from the masses on the machine and the speed of otation while the peak vibratory displacement (x) was measured under the plate by hich the force was applied to the road surface. Van der Poel introduced the concept f the dynamic stiffness of the construction (S), given by $S = F_p/x$, which is a function f the mechanical properties and thicknesses of the layers forming the construction, ut, unfortunately, it is neither independent of frequency nor force. Measurements on

a variety of roads, however, have shown that the value of S will, under certain conditions, indicate the condition of a flexible road (10). High values of S indicate a strong construction and low values show the construction to be weak.

The Shell vibrator was designed to apply forces to the road similar to those applied by vehicle wheels. There is, however, an important difference between the two types of loading which may affect the relation between dynamic stiffness and the performance of the road under traffic. A vibrating machine loads both the surface and the lower layers at the same rate of loading. A moving wheel loads the surface with a stress pulse which rises from zero, reaches a peak, and returns to zero again in the time taken for the tire contact area to travel over a point on the road surface. Due to the load-spreading action of the road construction, the moving wheel applies a stress pulse to the soil subgrade which is of longer duration and lower intensity than that applied to the road surface, while intermediate rates of loading and peak stresses occur in the various layers forming the road. Soil and many of the materials employed in road construction have mechanical properties dependent on the rate of loading, and this is particularly true of the dynamic elasticity of the bituminous layers which play an important part in spreading wheel loads. Measurements of the transient deformation of the road surface under a loaded wheel (11) during the American WASHO tests showed that the deformation was greatest under a stationary load and decreased with increase of vehicle speed up to about 15 mph, beyond which it hardly varied. The transient deformation under a nearly stationary vehicle agreed with data given by the Benkelman beam. The stiffness at zero frequency, deduced from measurements made with the Shell vibrator, has been found not to agree with data obtained from tests with the Benkelman beam; different relationships have, in fact, been found for each type of road construction. These differences are probably due to differences in the rates of loading produced by the two methods of test which affect the elasticities of the various layers forming the road.

The Bundesanstalt fur Strassenwesen at Cologne (12) has developed a vibrator similar to that devised by Van der Poel and covering the frequency range from 10 to 80 c/s. The road is assumed to consist of a surface layer acting as a plate and resting on a lower semi-infinite layer, and analysis of the results gives the spring constant and damping factor of each layer. Measurements made on experimental roads have shown that decrease of the spring constant and increase of the damping factor of either layer are usually associated with failure of that layer under traffic. The German workers state that one of their objectives, when they have obtained sufficient practical data by testing a wide range of roads, is to include spring constants and damping factors in their road specifications.

Although there has always been agreement on the qualitative significance of stiffness when used as an approximate index for comparing roads, there are divergences of opinion between workers when an attempt is made to relate stiffness to the mechanical properties of the layers. As has been said already, the Dutch and German workers analyze their data in different ways and derive different quantities as indicative of the quality of the road construction. The U.S. Waterways Experiment Station has used the Dutch Shell Vibrator and has followed the Dutch method of analysis. The non-linear behavior of the stiffness with applied force and its anomalous variation with the test frequency have always been stumbling blocks in deriving a simple interpretation of the test results. Simplifying assumptions have had to be made to achieve this purpose and consequently, the deductions depend on these assumptions. Moreover, a single value of dynamic stiffness may be given by a number of constructions having different thicknesses of layer and elasticities, so that prior knowledge of these quantities is essential when attempting to interpret the data. Nijboer has made most progress in this direction (13) and has computed the strain occurring in the road surface under a given wheel load from the measurements of stiffness, the thicknesses of construction and the elastic properties of the layers. Measurements of the surface strain under moving vehicles agreed with those predicted by this method.

The Shell machine has also been used as the source of vibrations within the range from 10 to 60 c/s while measurements were made of the velocity of propagation of vibrations along the road surface. At these frequencies, it is primarily the charac-

ristics of the soil subgrade under the road which determine the velocity of propagation
the vibrations and Nijboer has attempted to deduce the shear modulus of elasticity of
e soil from these results.

The Road Research Laboratory in England collaborated with the Dutch Shell Labora-
ry in making vibrational experiments on a number of British roads (10) and later
veloped apparatus to measure the phase velocity of vibrations over a much wider
equency range (to at least 30 kc/s) so enabling data to be obtained for estimating the
astic properties and thickness of the various layers forming roads. The objects of
is work were to develop tests for assessing the quality of existing roads and to obtain
formation concerning elasticities of road materials for later use in computing stresses
der moving vehicles. The portable vibration equipment constructed at the Road Re-
arch Laboratory is described fully by R. Jones elsewhere in this Bulletin. Part of
is apparatus, extending the frequency range up to about 5 kc/s, has also been in-
rporated into the equipment now used by the Shell Laboratory and it is likely that
eir equipment will be further supplemented to cover the higher range of frequencies.

The Road Research Laboratory has studied the variation of surface wave velocity
ith frequency (or wave length). Because such relationships are complex, theoretical
terpretation of the results is difficult. Data derived from simple types of construction
n often be evaluated satisfactorily and progress is being made in interpreting the
sults obtained in the more complicated cases. The theory has been based on the
ropagation of vibrations in plates (or multiple plates) lying on uniform layers of other
aterials: the results obtained in some of the cases studied are given in the accompanying
aper by Jones.

As far as the authors are aware, the work on vibrational testing in the United States
as been largely confined to the experiments on soil made by Bernhard at Rutgers
niversity and to tests made in collaboration with the team from the Dutch Shell
aboratory. There appears to be growing interest in the United States in these tech-
iques and apparatus for studying surface wave propagation is now being constructed by
he Shell Development Company. Work done in America on the vibration compaction of
oil and the design of machine foundations was described in a symposium organized by
he American Society for Testing Materials in 1953 (15). One feature of this symposium
f particular interest was the development of a theory for the vibration of a mass on a
emi-infinite elastic subgrade.

So far, the vibrational testing of roads has been largely restricted to the measure-
ent of their stiffness under traffic stresses and then attempting to predict their per-
ormance under traffic from comparison of this stiffness with the values attained on
oads of known performance. However, the work of Nijboer indicated that roads behave
easonably elastically under the stress conditions imposed by the passage of a vehicle
wheel, and Acum and Fox (3), and others, showed how to compute the stresses and de-
ormations within a multi-layer elastic structure. In consequence, the idea has gradu-
lly developed that it might ultimately be possible to design a road on the basis of the
stresses developed in the road by moving vehicles and those which cause failure.
Vibrational methods can provide details of the elastic properties of the constituent
materials, often at frequencies well above those giving stress-strain relations similar
to those produced by traffic. Before pavement design will be possible along the lines
indicated, it will be necessary to know how the stress-strain relations of the materials
are affected by decrease of the rate of loading down to that occurring under vehicles,
and to obtain data concerning the conditions causing failure of these materials under
such loading. Designs cannot yet be made on the basis of elastic theory because of
lack of information on many points, but such a technique was anticipated at the sympo-
sium organized by the Dutch Shell Co. in Amsterdam, in April 1959, by the inclusion
of papers from England and France reviewing the theories available for computing
stresses and displacements in layered elastic systems together with papers from the
Shell Laboratory discussing the deformation and fatigue properties of bituminous mate-
rials.

NON-VIBRATIONAL TECHNIQUES FOR TESTING ROADS

Much of the work in this group involves measurements on or under the road while vehicles of known wheel load travel along the surface.

In this category may be placed the Benkelman beam which is used to measure the vertical deflection of the road surface resulting from a loaded wheel moving slowly away from the point at which the measurements are made. Considerable research ha been done on this technique in the United States and work is also in progress in Great Britain and France. Because the Benkelman beam test provides a measure of the stiffness of the road, consideration is now being given to its possibilities as an altern tive to the dynamic stiffness as measured by the low frequency rotary vibrators. The Benkelman beam test may be easier to make, particularly now that an automatic versi has been devised by the Department of Highways in California. There may well be a difference between the properties measured by the Benkelman beam and by the vibrati technique because the elastic characteristics of the constituent materials may vary wi the rate of loading. Moreover, the stiffness or deflection value given by the Benkelm test has the same limitation as the dynamic stiffness obtained by vibration tests in tha it cannot provide detailed information about any individual constituent of the road construction.

The dynamic stresses produced in roads by moving vehicles are being measured at the Road Research Laboratory in England (16), largely to compare the load-spreading characteristics of the various common forms of construction. One early result of this work was to show how, with a given thickness of construction, the peak value of the dynamic vertical compressive stress at the soil-base interface depended markedly on the elasticity of the upper layers of the road (17). The stresses in the soil decrease with increase of the vehicle speed from near zero up to about 15 mph and then remain approximately constant (this relation is similar to that mentioned earlier concerning the variation of transient deflection of the road surface). The magnitude of this chang of stress with speed depends on the materials employed in the road, and is probably due to the changes of the relative elasticities of the layers with rate of loading. With bituminous construction, there is an increase of the dynamic stress with increase of the temperature of the road, again probably due to change of the relative elasticities of the layers. Vibration techniques are used to determine the elastic properties of the layers both during and after construction and attempts are being made to compare the measured values of the dynamic stress with those which are computed from the theorie of multi-layered elastic systems.

REFERENCES

1. Burmister, D.M., "The General Theory of Stresses and Displacements in Layere Systems." J. Applied Physics, 16:296-302 (1945).
2. Fox, L., "Computation of Traffic Stresses in a Simple Road Structure." Road Research Technical Paper No. 9, H.M.S.O. (London) (1948).
3. Acum, W.E.A., and Fox, L., "Computation of Load Stresses in a Three-Layer Elastic System." Geotechnique, 2:4, pp. 293-300 (Inst. C.E., London) (Dec. 1951).
4. Hertwig, A., Fruh, A., and Lorenz, H., "The Usage of Vibrational Techniques to Determine the Properties of Soil Important to Structural Work." Published by the Deutsches Gesellschaft fur Bodenmechanik (DEGEBO) (1933)
5. Erlenbach, L., "The Usage of Dynamic Testing of Foundations." DEGEBO (1936).
6. Ramspeck, A., and Schulze, C.A., "The Dispersion of Elastic Waves in Soil." DEGEBO (1938).
7. Bergstrom, S.G., and Linderholm, S., "A Dynamic Method for Determining Average Elastic Properties of Surface Soil Layers." Swedish Cement and Concrete Research Institute at the Royal Technical University, Stockhom, Proc. 7 (1946).
8. Van Der Poel, C., "Dynamic Testing of Road Constructions." J. Appl. Chemistry 1:7.
9. Nijboer, L.W., and Van der Poel, C., "A Study of Vibration Phenomena in Asphal

Road Constructions." Proc., Assoc. Asphalt Pav. Tech., 22:197-231, Discussion pp. 232-7 (1953).

10. Nijboer, L.W., and Jones, R., "Investigation Into the Dynamic Testing of Roads." Roads and Road Construction, 32:202-9 (1954).

11. "The WASHO Road Test — Part 2: Test Data, Analyses, Findings." HRB Special Report 22 (1955).

12. Baum, G., "Dynamic Investigations on Roads." Strasse und Autobahn, 10:8, 277-82 (1959).

13. Nijboer, L.W., "Dynamic Investigations of Road Constructions." Shell Bitumen Monograph No. 2 (1955).

14. Jones, R., "In Situ Measurement of the Dynamic Properties of Soil by Vibration Methods." Geotechnique, 8:1-21 (Inst. C.E. London) (1958).

15. "Symposium on Dynamic Testing of Soils." ASTM Special Tech. Pub., No. 156 (1953).

16. Whiffin, A.C., "Some Special Techniques Developed at the Road Research Laboratory, England, for Testing Roads and Other Structures." R.I.L.E.M. Symposium, Trans. 2:117-143, Lisbon (1955).

17. Lee, A.R., "Recent Research on Some Problems in the Construction and Maintenance of Roads." Proc. 8th Ann. Conf., Inst. Wks. Highw. Supts. (Folkstone), pp. 65-93 (1956). Contractors Record, 67:36,18; 67:37,24; 67:38,12 (1956).

Measurement and Interpretation of Surface Vibrations on Soil and Roads

R. JONES, Department of Scientific and Industrial Research, Road Research Laboratory, Harmondsworth, Middlesex, England

The Road Research Laboratory is developing nondestructive techniques for measuring the dynamic mechanical characteristics and thicknesses of the layers forming a road. The mathematical theory for computing stresses and deformations requires knowledge of these data and the development of these testing techniques is a necessary step towards a system of pavement design based on the stesses encountered in the road and the mechanical properties of the materials. Apart from this, the techniques are already able to provide information of immediate value in that they provide data of assistance in appraising the performance of experimental and other roads under traffic, they can be used to locate areas where variations of mechanical properties or thickness occur, and they can be used to study the changes produced by traffic and weather.

The first part of this paper deals with the experimental technique for measuring the wave length and phase velocity of mechanical vibrations propagated along the surface of soil or road constructions. The vibrations are produced electro-mechanically by apparatus working within the frequency range from 40 to 60,000 c/s and have wave lengths ranging from a few inches to several feet. The results are normally expressed graphically as the relation between phase volocity and the wave length obtained at selected frequencies. This curve has a number of characteristics which depend on the elastic properties and the thicknesses of different parts of the construction: the second part of the paper discusses theoretical analyses to calculate these parameters. So far, most of the work has been limited to experimental constructions and all the relevant data concerning thicknesses and type of material have been known, while vibratory experiments have also been made, where necessary, on laboratory specimens of the materials to determine their elastic properties. These data have enabled checks to be made of the validity of predictions from the vibrational experiments.

●APPARATUS has been developed at the Road Research Laboratory which enables vibrations in the range 40 to 60,000 c/s to be propagated along the surface of soil or road constructions. The purpose of the present paper is to interpret the results in terms of the elastic properties and, where possible, the thickness of the construction.

So far, most of the work has been limited to experimental constructions, and the relevant data concerning thicknesses and types of material have therefore been availal from laboratory records and experiments have also been made to determine the elasti properties of the materials. These data have enabled checks to be made of the validit of predictions from the vibrational experiments.

In the experiments, the wave length of the vibrations is measured at specific frequ cies and their phase velocity is derived from the product of their wave length and frequency. For purposes of analysis, it has been found preferable to express the results

8

s a graph relating phase velocity to wave length and then to fit theoretical curves de-
uced from the propagation of plane waves in an equivalent type of layered construction:
he thicknesses and elastic properties in the theoretical curves are adjusted to provide
he best fit to the experimental results. This method of analysis is applied in this
aper to the following types of construction:

1. Soil formations in which the elastic properties are uniform or have only slight
ariation with depth.
2. Soil formations in which there is a distinct transition with a sudden increase in
lastic modulus at a particular depth: this corresponds to a surface layer of lower
lastic modulus than that of the underlying material. A typical example of this type of
ormation is a layer of soil overlying gravel or rock.
3. Road constructions consisting of a surface layer with considerably greater
lastic modulus than the underlying material. An example of this type of construction
s a concrete slab laid directly on soil or on a deep granular base.
4. Road constructions with a surface layer and an intermediate layer overlying a
niform medium: the material in the surface layer is taken to have an elastic modulus
vhich is considerably greater than in either of the two lower materials while the com-
pressional wave velocity in the material of the intermediate layer is assumed to be less
han that in the underlying material. This system is an idealized representation of a
pituminous surfacing on certain granular base materials overlying clay soil.

There are many more combinations of properties within the three-layer system
vhich need to be considered and the analysis offered here represents a very limited
contribution to what will ultimately be required.

EXPERIMENTAL TECHNIQUES

First Technique

A schematic diagram of the apparatus is shown in Figure 1: different types of vibra-
tor and pick-up are used for different parts of the frequency range.
Below 5,000 c/s, the vibrations are produced by an electro-dynamic vibration generator
driven by an oscillator and a power amplifier; details of the vibration generator are shown in
Figure 2 and specifications for the generator, oscillator and power amplifier appear in Table 1.
The oscillator also feeds into a phase-mark generator which squares and differentiates the
waveform and ultimately produces a voltage pulse once per cycle as shown in Figure 3. The
voltage pulse is used to suppress the beam of the cathode-ray oscilloscope and so provide a ref-
erence mark which is fixed in relation to the phase of the vibrations produced by the generator.
The vibrations are received by a vibration pick-up, whose output is amplified and
applied to the vertical deflection plates of the cathode-ray oscilloscope. Thus, the
waveform of the vibrations is displayed on the oscilloscope with the reference mark
appearing as a short break in each cycle (Fig. 3). In the present apparatus a geophone
is used as the vibration detector at frequencies below 400 c/s, and a crystal accelerom-
eter at frequencies between 400 and 5,000 c/s; details of these pick-ups are given in
Table 1.
Vibrations within the frequency range of 5-24 kc/s are obtained as specific reso-
nances of a ferro-electric ceramic transducer in the form of a hollow cylinder. The
ceramic transducer is driven by the oscillator through a tuned amplifier which has
switched outputs, each tuned to one of the resonant frequencies of the transducer. The
vibrations in the high-frequency range are detected by a hollow cylinder transducer
which is identical with the generator; the specifications of the transducers are given in
Table 1. For convenience, the diaphragm of the receiving transducer has been tapered
to a point to enable the shortest wave lengths (about 2 in.) to be located accurately.
In operation, the generator, which is either an electro-dynamic or a ceramic trans-
ducer, is placed on the road surface and the oscillator is tuned to the required frequency.
The appropriate pick-up is moved progressively away from the generator and successive
positions are found at which the vibrations are alternately in phase and in anti-phase
with the fixed reference phase. These positions are indicated by the phase mark coin-
ciding with a peak or a trough of the waveform display. The distances between succes-

TABLE 1

BRIEF SPECIFICATION OF APPARATUS

Oscillator	Minimum frequency range: 30-60,000 c/s Accuracy better than $\pm$ 1 percent
Power amplifier	Output 50 watts in frequency range from 30 c/s to 5,000 c/s
Oscilloscope	Single beam with amplifier response to at least 60 kc/s and provision for coupling t modulator grid
Electro-dynamic vibration generator	Modified Goodmans, Model 390A
Geophone	Pye. Sensitivity about 2V/in./s
Crystal accelerometer	Rochelle-salt bimorph.
Ceramic transducers	Hollow cylinders of Casonic III (barium titanate) 6 in. long x 1 in. O.D. x $\frac{3}{4}$ in. I.D. on $\frac{3}{16}$-in. thick diaphragm, giving resonant frequencies of about 6, 10, 14 and 24 kc/s. Also solid prisms of Casoni on $\frac{1}{16}$-in. thick diaphragms, 1 in. square x 2 in., resonating at about 38 kc/s, and 1 in. x 1 in. x 1 in. resonating at about 57 kc/s

sive positions are then equal to half wave lengths and, in practice, measurements are made over about four or more wave lengths in order to obtain a reliable average value It must always be realized that the vibrator produces cylindrical waves so that the wave lengths occur at distances corresponding to the roots of a Bessel function and not at equal increments of distance as they do in plane waves. The discrepancy is most marked near to the vibrator and it is sufficiently accurate to regard the first wave length as being 0.75 as long as the equivalent wave length of plane waves with all subsequent wave lengths equal to that of plane waves. The most satisfactory way of analyzing the measurements is to plot the number of wave lengths moved by the pick-up against its distance from the vibrator. If the site is uniform all results beyond the first wave length should be approximately collinear and should extrapolate back to zero distance at the equivalent of about $\frac{1}{4}$ wave length: the slope of the line provides a reliable value for the average wave length (L) of equivalent plane waves. The phase velocity (c) is derived from the relation:

$$c = n L \tag{1}$$

in which

$$n = \text{vibrator frequency.}$$

Second Technique

In this experimental technique the apparatus is basically the same as the foregoing, except that provision is made for a circular time base on the oscilloscope. The apparatus is also shown in Figure 1 and becomes operative when the three switches are thrown over to connect to the dotted part of the circuit. The display on the oscilloscop consists of a single bright spot whose position on the circular time base indicates the relative phase difference between the vibrations at the oscillator and at the pick-up. It is convenient to measure this difference by means of a graduated circle on a graticul in front of the screen of the oscilloscope; divisions at tenths with sub-divisions at twentieths provide adequate measuring points and enable the position of the spot to be

Figure 1. General view of the operation of the vibration apparatus.

stimated to 0.01 of the circumference. The circular time base makes one complete evolution per cycle of the applied vibrations so that the spot of the oscilloscope display moves once round the graduated circle as the pick-up moves one wave length. The elation between the phase change (ϕ) and the distance moved by the pick-up (x) is:

$$\frac{\phi}{2\pi} = \frac{x}{L} \tag{2}$$

To set up the apparatus for operation it is necessary to adjust the circular time base n coincidence with the graduated circle. This is done by turning up the brilliance of he oscillescope to brighten up the complete time-base trace and adjusting its size by means of the X and Y amplifier gains on the oscilloscope. The brilliance control is hen turned back so as to black out the circular trace except for the bright spot due to he modulation arising from the pick-up signal via the phase-mark generator.

In practice it has been found convenient to move the pick-up away from the vibrator by fixed increments of distance and to measure the fractional change in wave length as given by the movement of the spot around the graduated scale. It is necessary, of course, to add one wave length for each complete rotation of the spot and the incremental distance should preferably be chosen to be less than half a wave length. The technique s somewhat simpler and quicker to use than the first technique and has considerable advantages when the test length is so short that it is less than three wave lengths. In his case the incremental distance can be made as small as about 0.1 of a wave length so that a larger number of results are obtained from which to obtain the average wave ength. The measurements are analyzed in the same graphical manner as described nder the first technique and allowance must also be made for the inequality between he first and subsequent wave lengths.
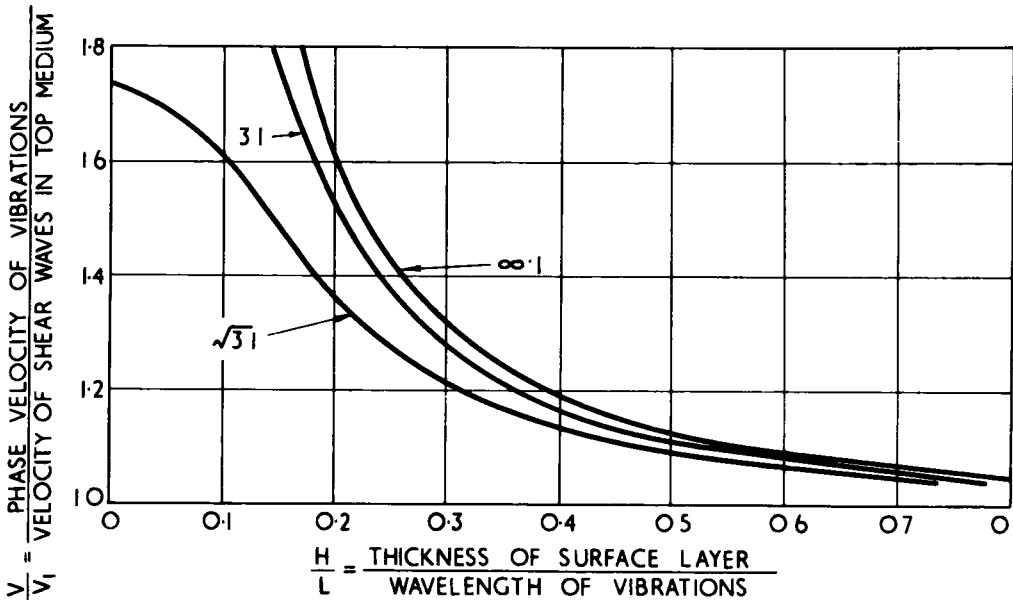
Figure 2.   Theoretical variation of phase velocity of Love waves in a surface layer on a semi-infinite base for different ratios of shear moduli ($G_2:G_1$).

NOTES ON PERFORMANCE

In the original amplifier apparatus the receiver amplifier had a flat response from 15 c/s to 350 kc/s. As a result, vibrations below 40 c/s produced by passing traffic were amplified and formed a background noise. As the pick-up was moved away from the vibrator, the traffic vibrations became so large in relation to the required vibrations that measurements could only be made when there was a lull in the traffic. The frequency analyzer, now used, is tuned to the vibrator frequency and discriminates effectively against traffic noise. The distance to which measurements can now be made is almost double what it was originally and there is now considerably less interference from traffic noise. It is usually possible to obtain measurements over about 6-10 wave lengths throughout most of the frequency range. Thus, at 60 c/s, the distance traversed may be over 80 ft whereas at 24 kc/s it may only be a few feet. The normal practice employed in the present work has been to place the vibrator at one end of the line of measurement at low frequencies (below 360 c/s on bituminous roads) then move the vibrator to the middle of the line and measure on either side at the high frequencies: further subdivision may be made at the highest frequencies. When testing soil alone, vibrations above 400 c/s are usually very highly attenuated and this imposes an upper limit to the practical range of frequencies.

In plotting the number of wave lengths to the pick-up against its distance from the vibrator the results may not be collinear due, it seems, to one of three reasons. First variability in the construction due to differences in materials or cracks: deviations due to this cause usually occur at the same distance from the vibrator for several consecutive frequencies. Second, changes in the contact compliance between the vibrator and surface due to a bedding down process causes a gradual phase change to be superimposed on the measurements: whether this effect is present is easily checked by repeating one or two of the initial measurements. A more usual cause of anomalous results is due to interference between two or more different types of vibration being propagated. When the vibrations are of comparable magnitude the interference may be so great as to make it impossible to obtain the phase velocity of any one of the vibrations. In other cases, one type of vibration may predominate near to the vibrator and another vibration beyond a region of interference: the phase velocity of both types of vibration can then be derived (1).
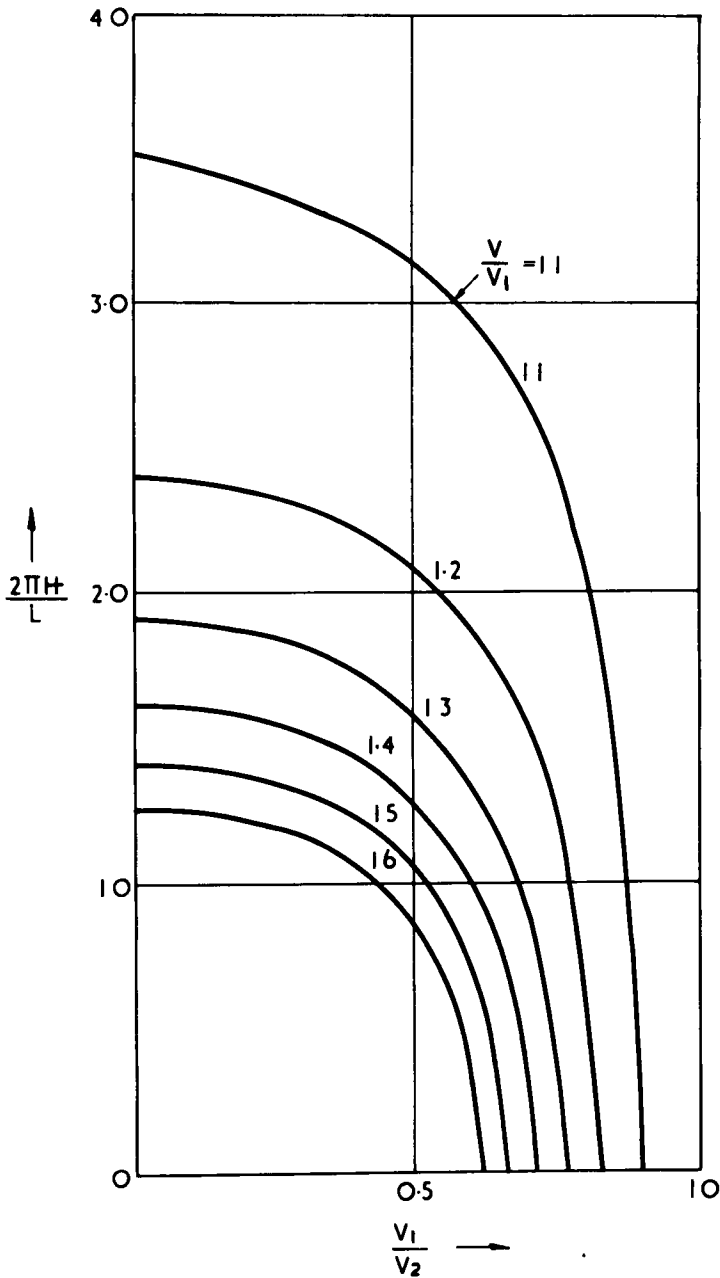
Figure 3. Data for analysis of Love wave results.

PROPAGATION OF SURFACE VIBRATIONS IN SPECIFIC TYPES OF SOIL FORMATION AND ROAD CONSTRUCTION

The nomenclature to be used in this section is given in Figure 4 which applies to the road construction with two surface layers considered in (d). The simpler types of construction considered earlier in this section are merely degenerate cases. For example, the material with subscript 3 always represents soil which is assumed to
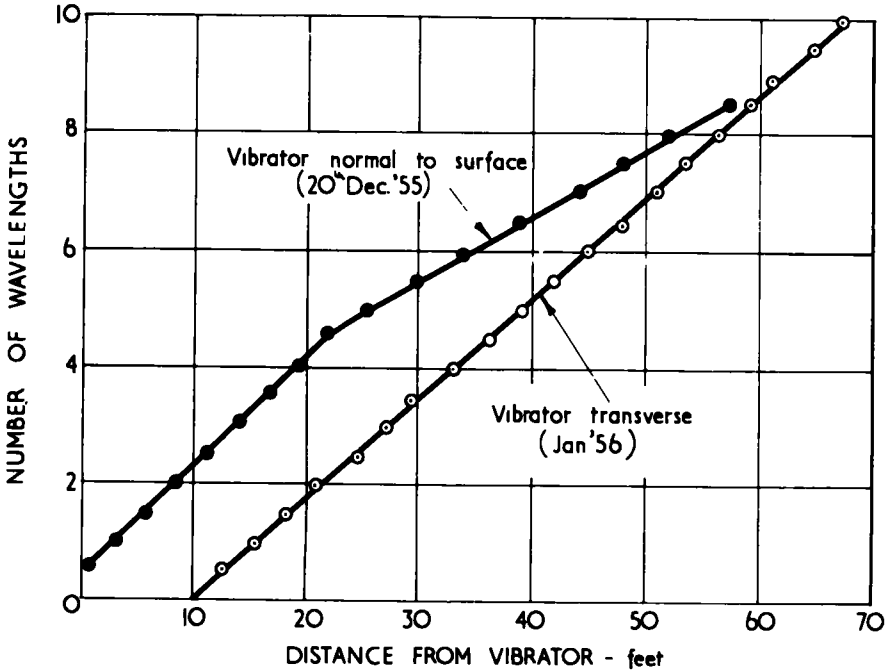
Figure 4. Wave length/distance curves at $80^c/_s$.

have uniform elastic properties down to an infinite depth, so that in case (a) the two surface layers are absent (that is, H_1, $H_2 = 0$). The medium with subscript 2 in the intermediate layer is assumed to have elastic moduli less than those in medium 3, so that for case (b) the surface layer is absent (that is, $H_1 = 0$). The material subscript 1 in the surface layer is considered to have elastic moduli which are considerably greater than in either of the underlying media and in case (c) the intermediate layer is absent (that is, $H_2 = 0$).

(a) Soil Having Uniform Elastic Properties

Miller and Pursey (5) have shown that a vibrator, on a circular base, operating normal to the surface of a semi-infinite elastic solid ($\mu = 0.25$) radiates 67.4 percer of the power as a surface wave. The surface wave here is a Rayleigh wave, which ha its maximum particle displacement normal to the surface with a smaller particle dis placement in the direction of propagation. The velocity (γ_3) of the Rayleigh wave is given by:

$$\gamma_3^2 = p^2 \ \beta_3^2 = p^2 \left(\frac{G_3}{d}\right)$$

(3)

in which

β_3 = velocity of the shear wave,
G_3 = modulus of shear elasticity of the medium, and
d   = density of the medium.

$\mu = 0.2$	$p = 0.911$
$\mu = 0.3$	$p = 0.928$
$\mu = 0.4$	$p = 0.942$
$\mu = 0.5$	$p = 0.955$
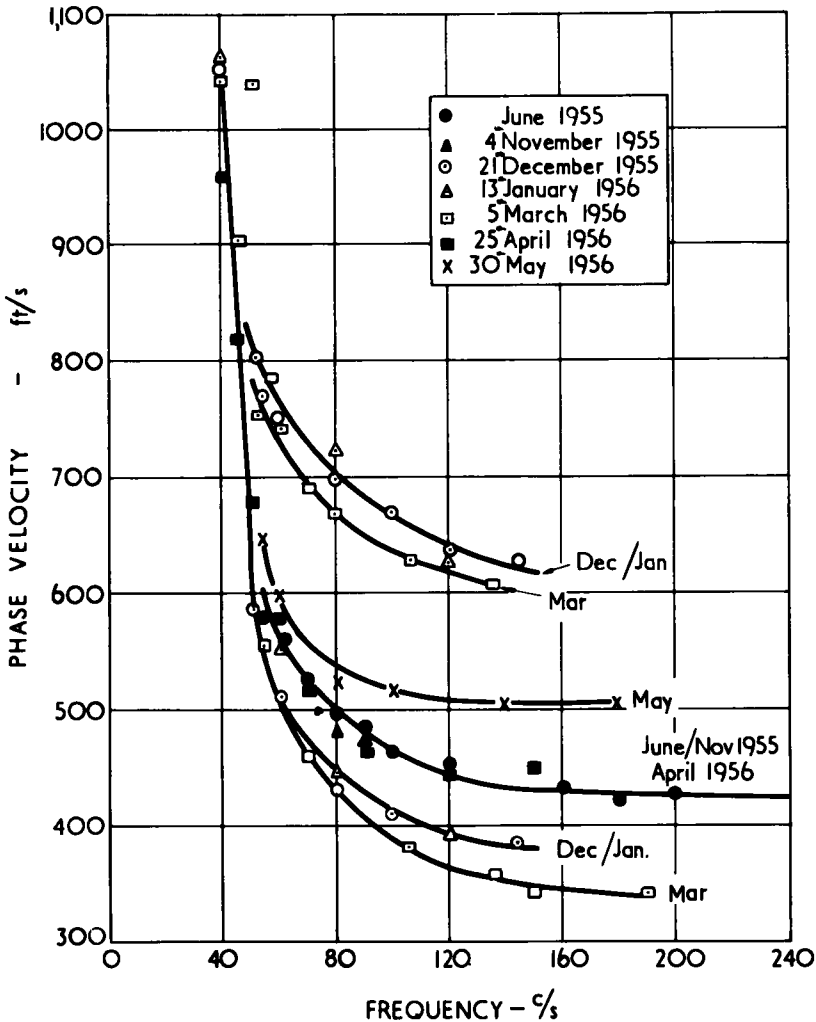
Figure 5. Variation of the phase velocity of Rayleigh waves with frequency on a Harmondsworth soil site (4 ft-10 in. silty clay on gravel).

In the case of soil the value of μ is usually about 0.4 to 0.45 so that the surface ave travels about 5 percent slower than the shear wave.

The shear and longitudinal waves produced by the vibrator are radiated into the ntire volume of the medium and suffer much larger attenuation than the Rayleigh ave, which propagates near the surface. Consequently, the vibrations that are de-ected along the surface of a semi-infinite solid from a vibrator normal to the surface re almost exclusively Rayleigh waves.

Other theoretical work by Miller and Pursey (4) indicates that if the vibrators per-orm rotary oscillations at the surface, the Rayleigh wave is absent and shear waves redominate.

Natural soil formations are rarely uniform with depth and this is reflected in the ibrational measurements by a variation in phase velocity with wave length. In Figure examples are shown of two types of variation of phase velocity which can occur with hange of wave length. The results from section 54 (Alconbury Hill Expt. A.1) indicate iat the shear modulus of the soil decreased towards the surface whereas the inverse
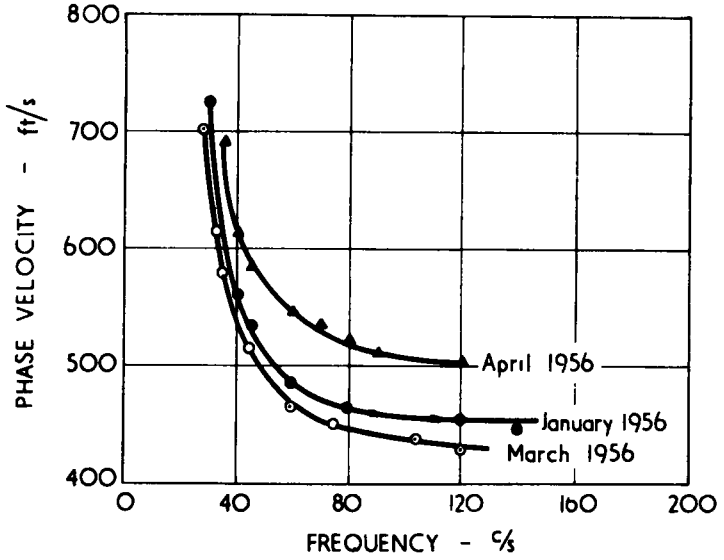
Figure 6. Variation of the phase velocity of Love waves with frequency on Harmondsworth site (4 ft-10 in. silty clay on gravel).
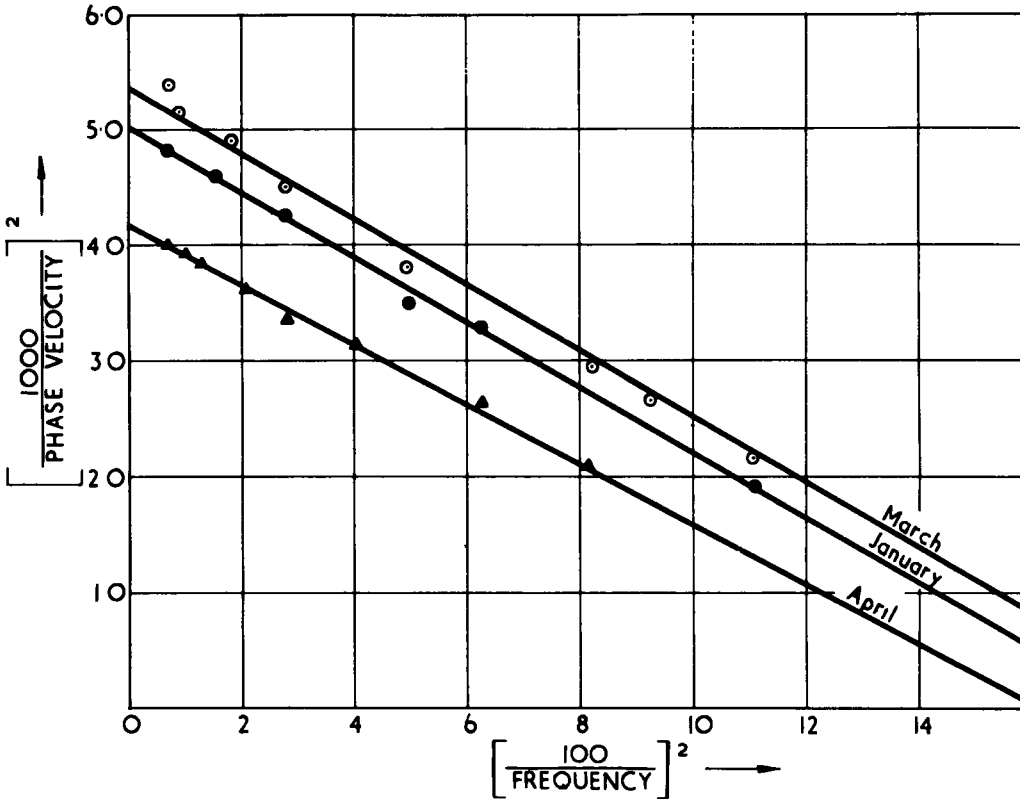
Figure 7. Evaluation of thickness of layer from Love wave data.
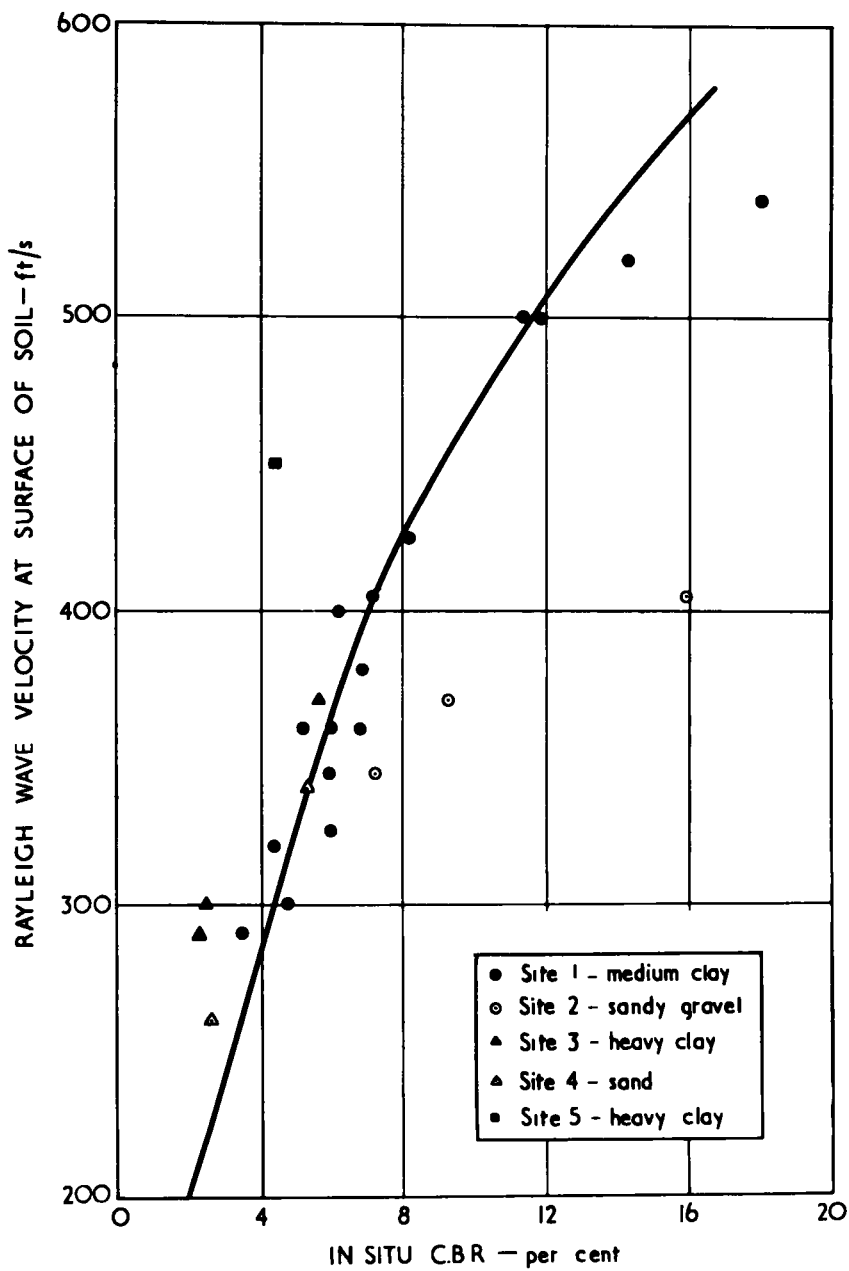
Figure 8. Relation between Rayleigh wave velocity at the surface of soil and the CBR value (in situ).
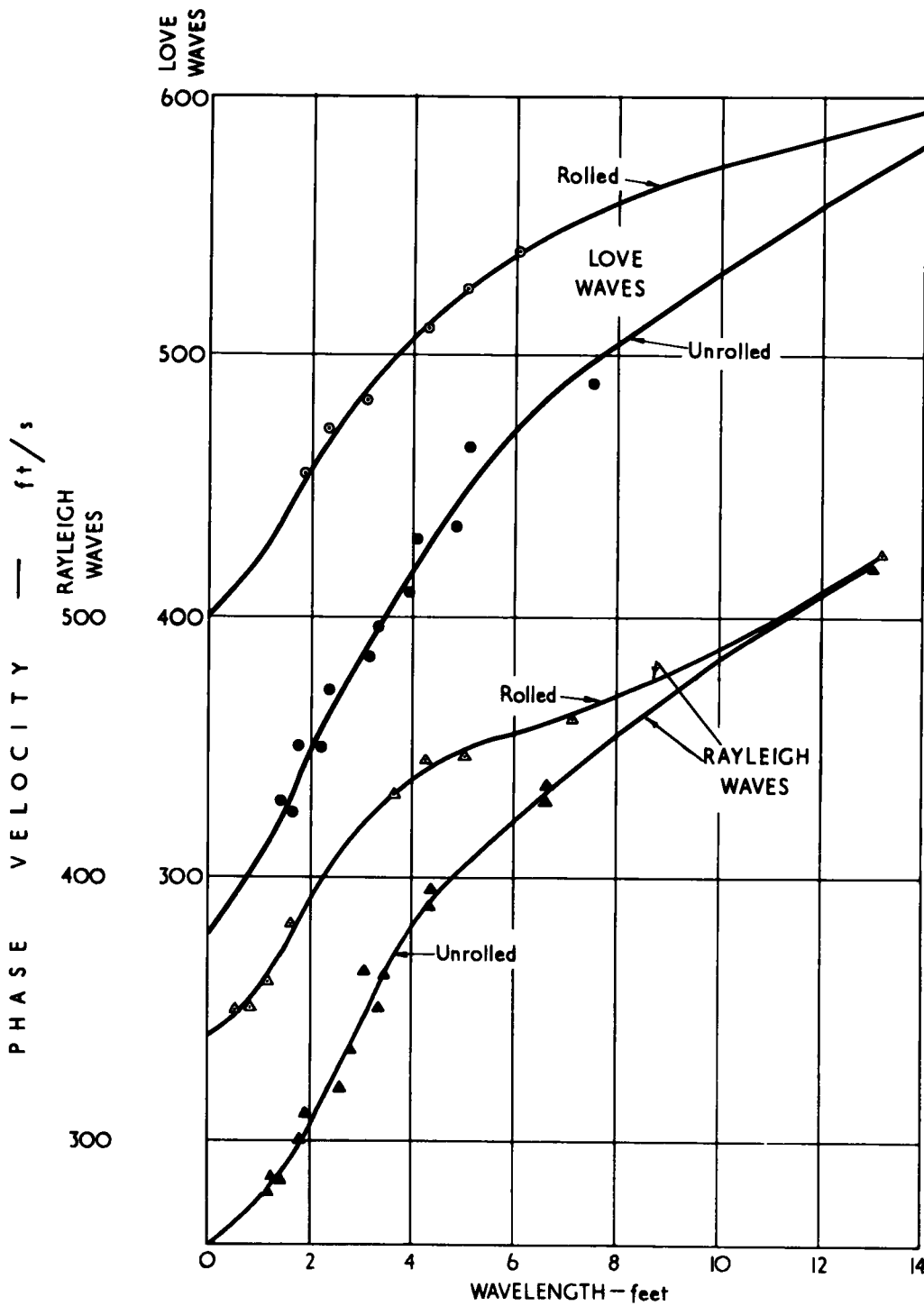
Figure 9. Variation of the phase velocity of Rayleigh waves and Love waves on Site 4 (sand) before and after rolling.
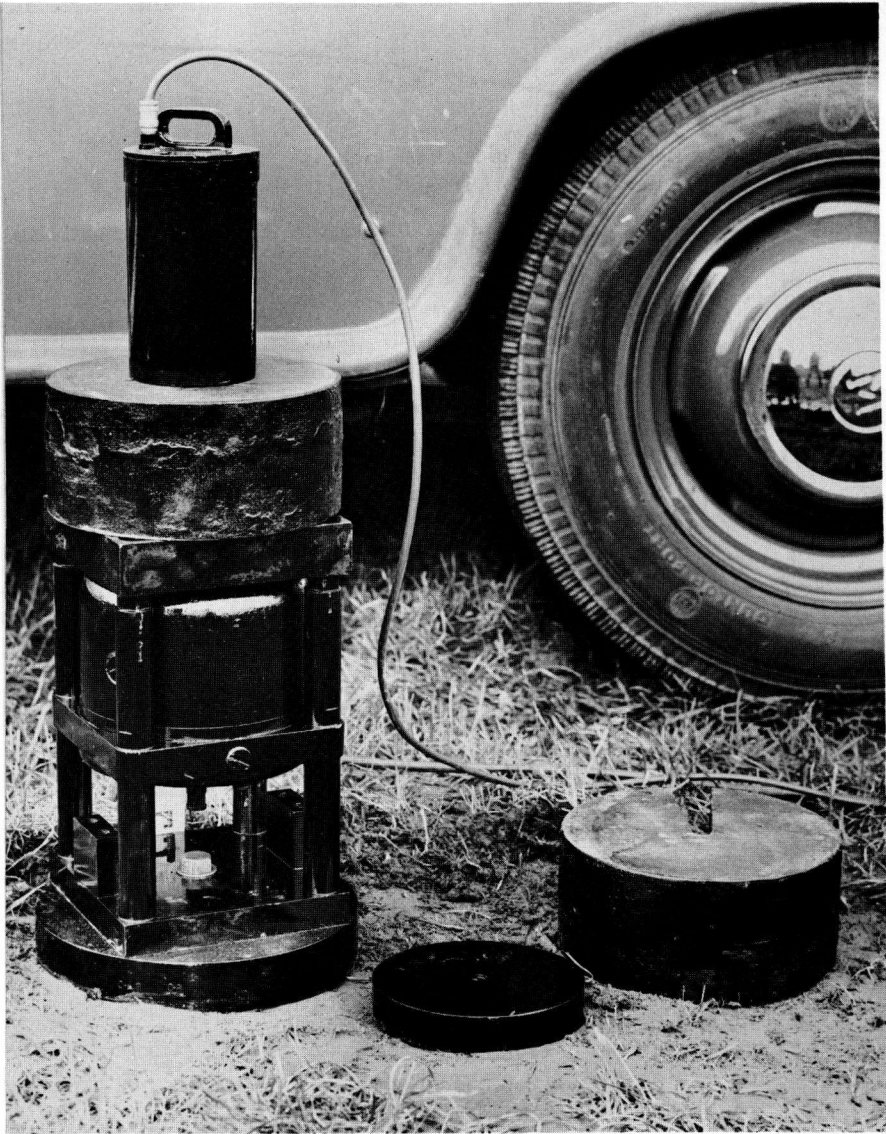
Figure 10.   The vibrator in position.
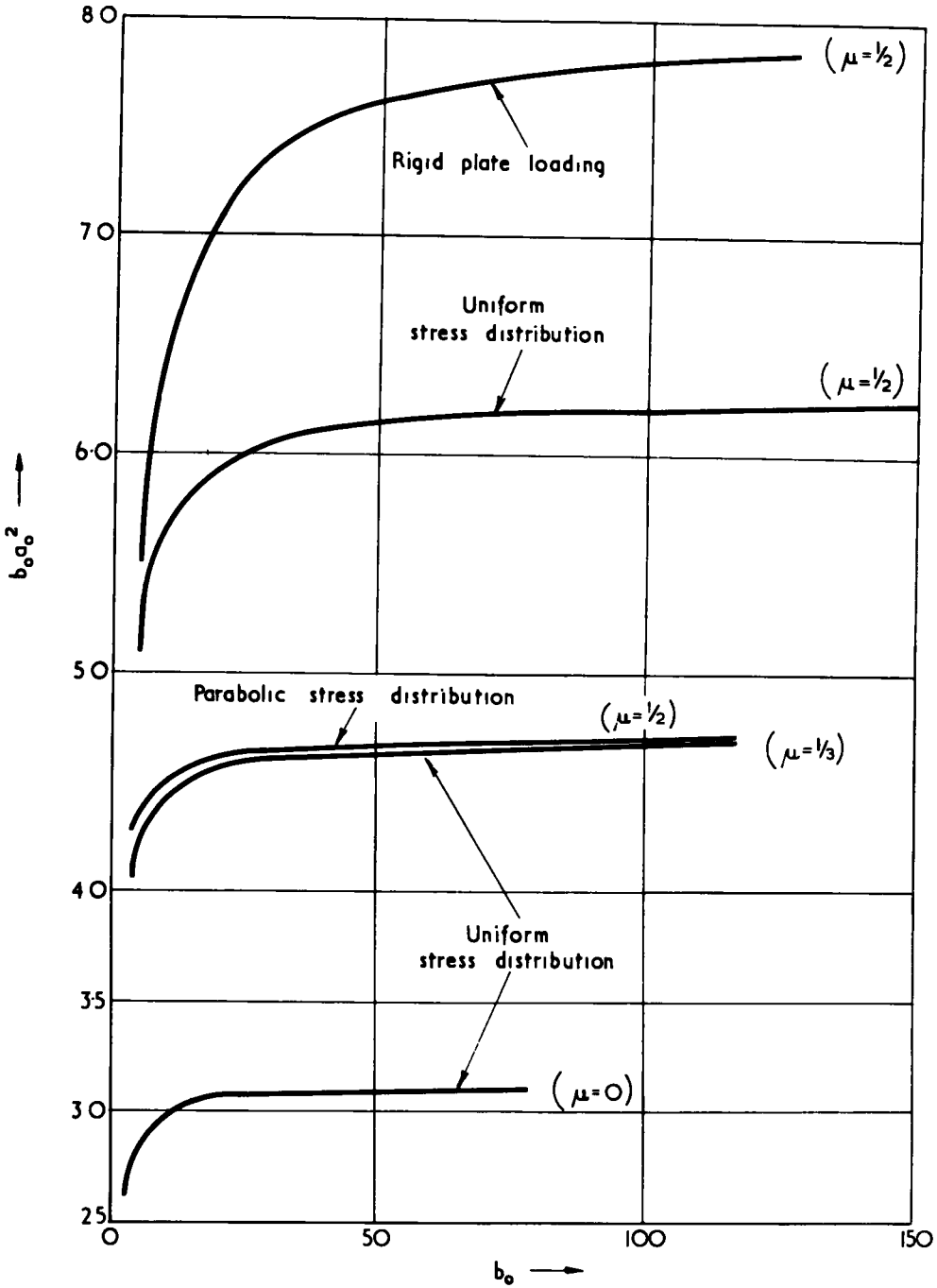
Figure 11. Effect of stress distribution and Poisson's ratio (μ) on the non-dimensional quantity $b_o a_o^2$.
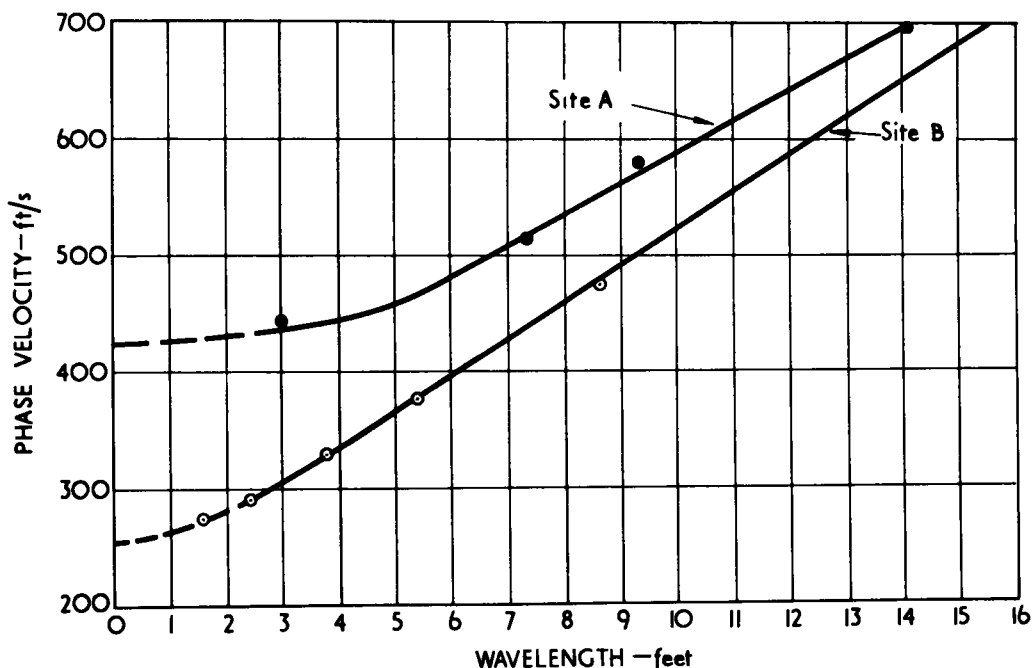
Figure 12. Phase velocity of Rayleigh waves on sites A and B.

ype of variation occurred on section 49 (also Alconbury Hill Expt.). In either case
he data is extrapolated to give the phase velocity (γ_3) at zero wave length and the shear
nodulus (G_3) is calculated from the relation (1):

$$G_3 = 2.4 \ \gamma_3^2 d \times 10^{-4} \ \text{psi} \qquad (4)$$

n which

$$d = \text{density of the soil (pcf)}.$$

The shear modulus (G_3) given by Eq. 4 refers to the soil nearest to the surface
vhich, under a road construction, is subjected to higher stresses than the deeper soil:
his modulus is considered to be one of the properties required in calculations of stress
listribution.

b) Soil Formations Having a Well Defined Surface Layer with a Lower Shear Elastic
Modulus than that of the Underlying Material

The nomenclature for this case (Fig. 4) is as follows:

$$H_1 = 0$$
$$G_2 < G_3$$
$$\beta_2 < \beta_3$$
$$\gamma_2 < \gamma_3$$

Two types of vibration have been studied according to the orientation of the vibrator
and pick-up to the surface of the soil. Rayleigh waves are produced when both vibrator
and pick-up are perpendicular to the surface. Love waves are produced when the vi-
orator and pick-up are placed on their sides so as to operate parallel to the surface
and transversely to the direction of measurement.

When vibrations of the Rayleigh wave type are propagated in a layered medium, their velocity depends on the frequency of the vibrations and the thickness, density, and elastic properties of the strata. The solution of the wave equation for the case of one surface layer of a semi-infinite medium involves the computation of a sixth order determinant, which can yield more than one velocity at each frequency. Here the solution giving the lowest velocity refers to the principal mode of propagation of the Rayleigh waves and computations have usually been derived for this particulare mode. Sezawa and Kanai (8) have also obtained solutions for another mode of propagation, designated as the $\overline{M}_2$ mode. Theoretical results obtained for the principal mode of propagation of Rayleigh waves by Sezawa and Kanai are shown in Figure 6 from which it will be seen that at short wave lengths the phase velocity approaches γ_2: this enable the shear modulus of elasticity (G_2) of the surface material to be calculated as in Eq. It will also be seen from Figure 6 that the shape of the curve relating phase velocity to wave length depends on the thickness (H_2) of the layer and on the ratio of the elastic moduli (that is, $G_3:G_2$). Differences in the density between the media would also intro-duce a further variable into the analysis. At wave lengths which are long in relation to the thickness of the layer, the phase velocity is asymptotic to γ_3 which, if attained, enables the shear modulus (G_3) of the underlying medium to be calculated.

For layered media in which the shear modulus increases with depth, the shear wave (horizontally polarized) gives rise to the type of surface waves known as Love waves. The theory is more tractable than for Rayleigh waves and, in the case of Love waves in a single surface layer, the frequency equation is as follows:

$$\tan \frac{2\pi H_2}{L} \left(\frac{c^2}{\beta_2^2} - 1 \right)^{\frac{1}{2}} = \frac{G_3}{G_2} \left[\frac{1 - \dfrac{c^2}{\beta_3^2}}{\dfrac{c^2}{\beta_2^2} - 1} \right]^{\frac{1}{2}} \tag{5}$$

in which

$$L = \text{the wave length of the vibrations, and}$$
$$c = \text{the phase velocity of the vibrations.}$$

The solution to Eq. 5 indicates that the phase velocity at a particular wave length has different values corresponding to successive branches of the tangent function. The principal mode of propagation corresponds to the lowest branch for which:

$$0 < \left(\frac{c^2}{\beta_2^2} - \right)^{\frac{1}{2}} < \frac{\pi}{2}$$

Limits for higher branches are $\frac{\pi}{2}$ to $\frac{3\pi}{2}$, $\frac{3\pi}{2}$ to $\frac{5\pi}{2}$, etc.

Asymptotic solutions of Eq. 5 show that for high frequencies (that is, short wave lengths) the velocity of the Love waves approaches the velocity of shear waves in the medium of the surface layer (β_2). At low frequencies, the velocity of the Love waves approaches the velocity of shear waves in the base (β_3).

The relation between the phase velocity and wave length for the principal mode of propagation of Love waves has been computed from Eq. 5 for ratios of $G_3:G_2$ of $\sqrt{3}$, 3 and infinity, and for equal densities; that is, $d_2 = d_3$: the results are shown in Figure 7.

Experimental results from the propagation of Rayleigh waves and Love waves have been obtained on several layered soils and some of the more interesting results are shown in Figure 8 for a sandy soil before and after compacting by a roller. On the un-rolled site, measurements at different depths showed a marked transition in soil
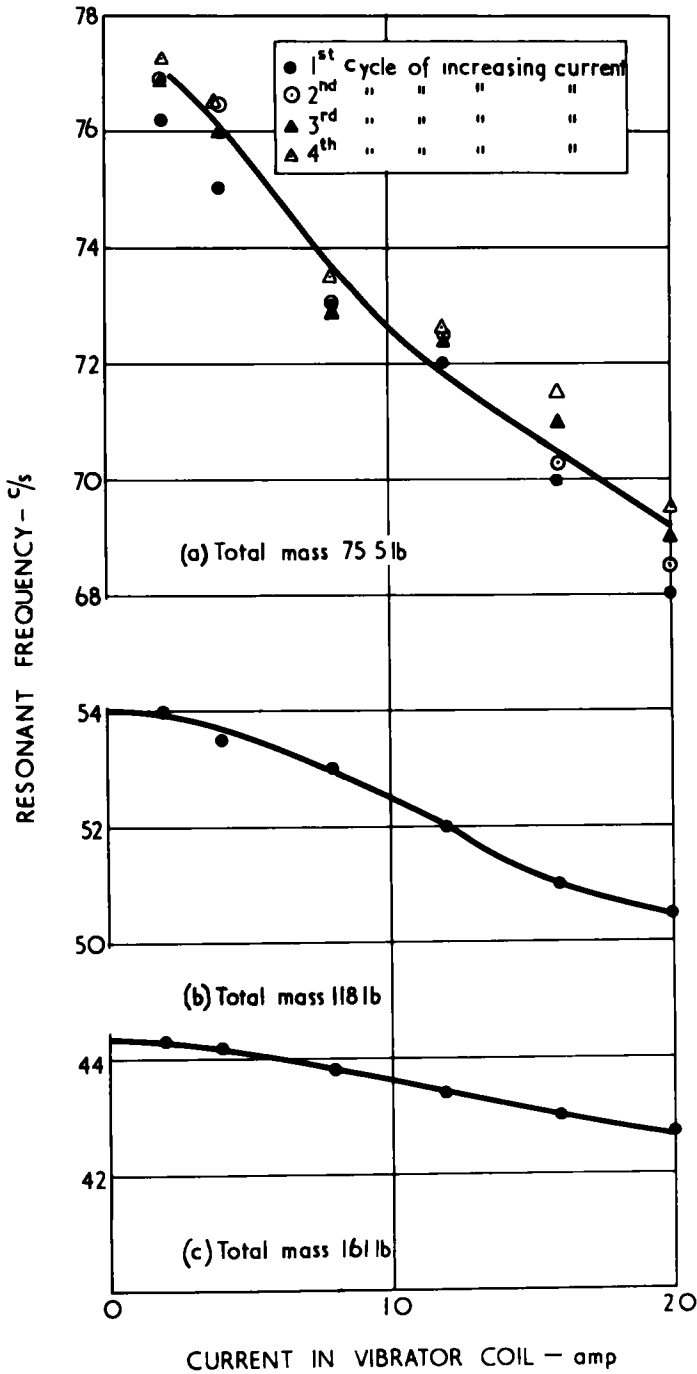
Figure 13. Variation of resonant frequency with current passing through vibrator coil.
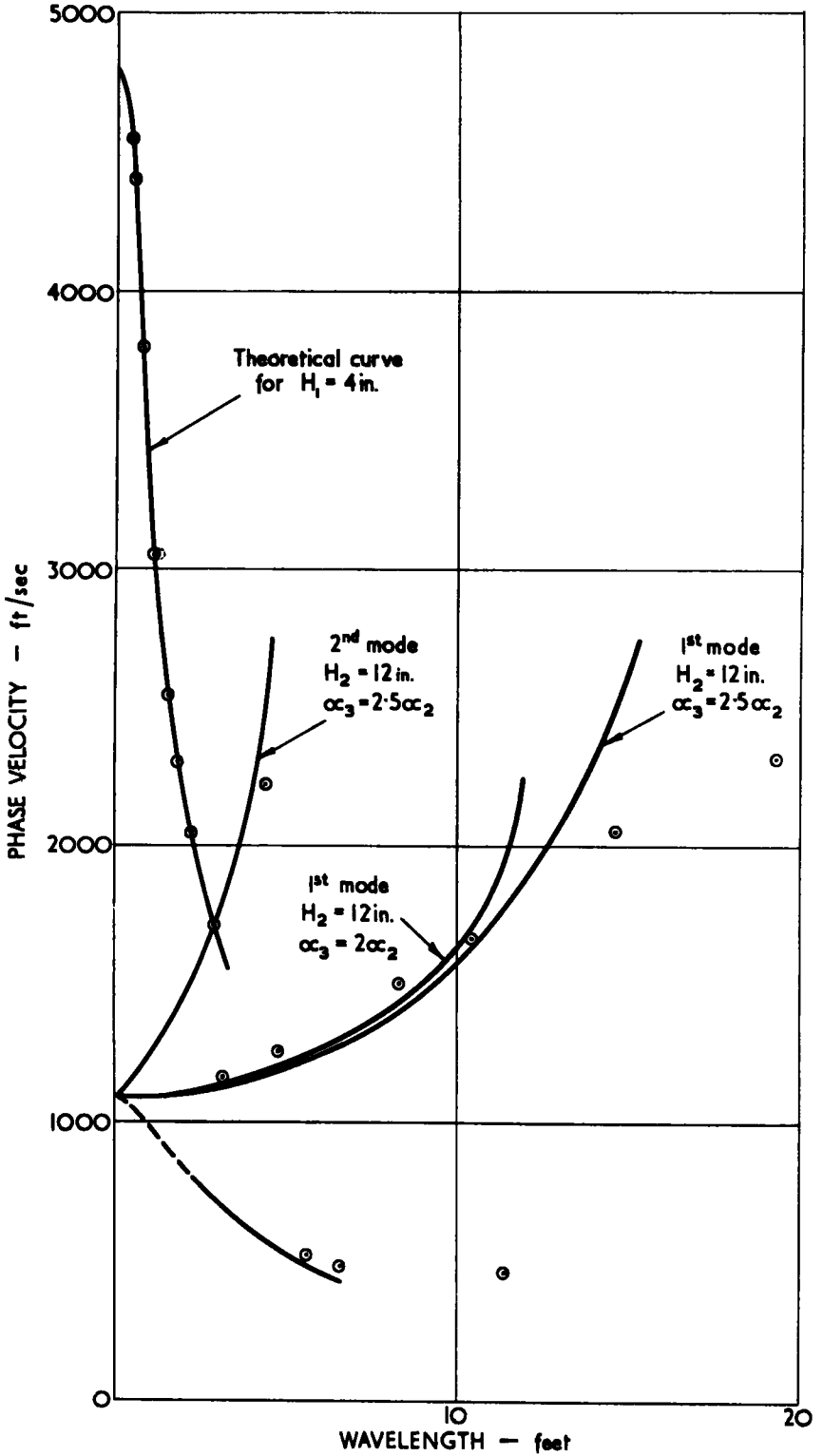
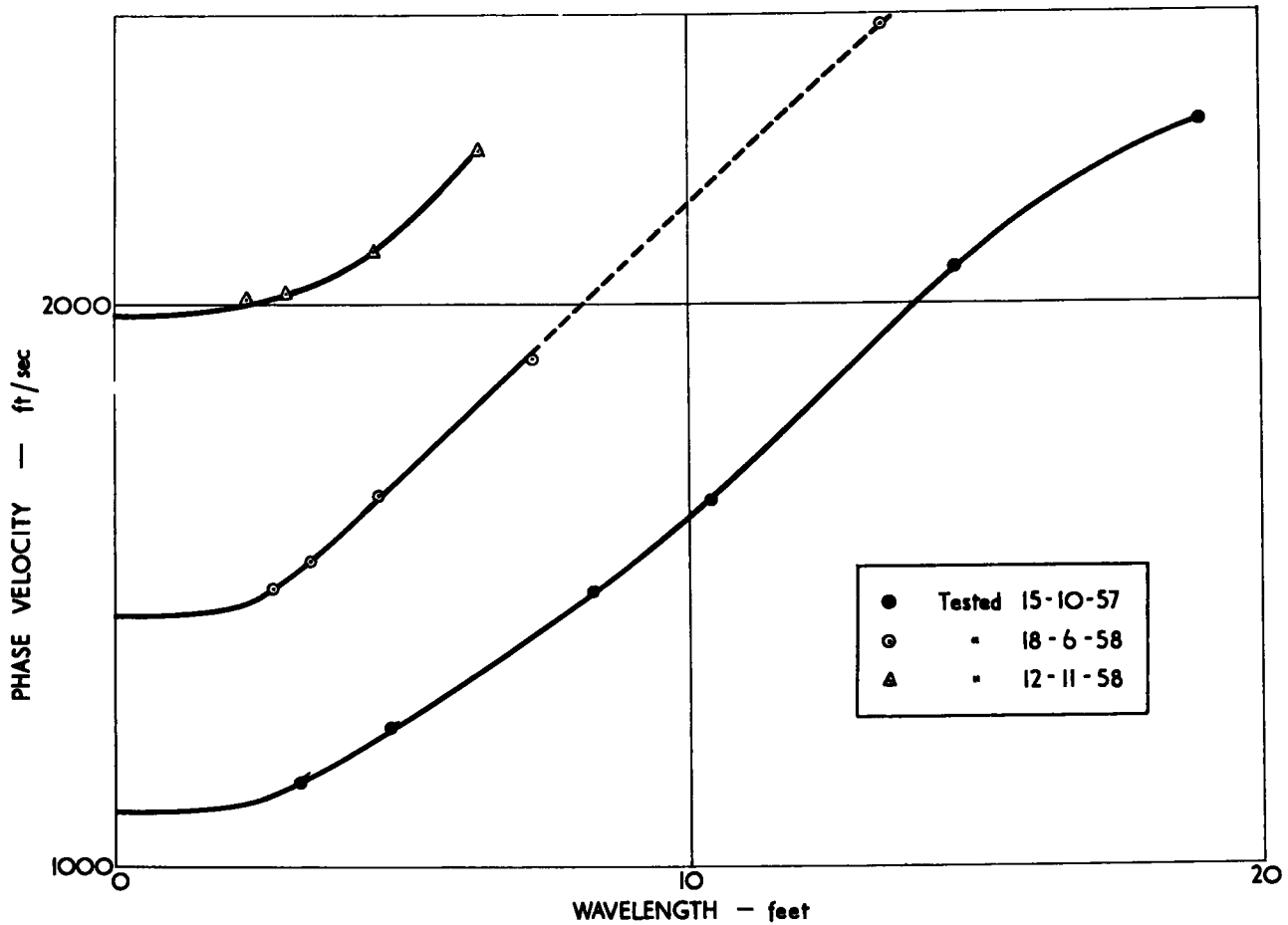Figure 14. Comparison of experimental results of Figure 12 with theory.

Figure 15. Changes in the intermediate branch of the phase-velocity/wave length relation caused by traffic.

properties between 3 and 9 in.: for example, in-situ CBR tests gave average values o 2.6, 13.2, 15.6 and 16.6 at depths of 3, 9, 15 and 21 in. A method of analyzing the experimental results for Love waves using Eq. 5 has been discussed by Jones (1) whic indicated that the transition in elastic properties occurred at a depth of about 7 in.: tł shear modulus of the unrolled surface layer was calculated to be 1,700 psi. After ro ling, analysis of the Love wave data indicated a surface layer 8 in. thick in which the shear modulus was 4,000 psi. Thus, rolling the sand produced compaction primarily in the top 7 to 8 in. of soil.

Analysis of the Rayleigh wave data gave values for the shear modulus of elasticity the surface soil of 1,700 psi before rolling and 3,100 psi after rolling. The discrepaı in the estimation of the shear modulus from Love wave and Rayleigh wave data after rolling was considered to be due to anisotropy produced by the compaction of the sand It is also possible to analyze the experimental results for the Rayleigh wave data usin the curves of Figure 6 so as to calculate the thickness of the surface layer: the result are in good agreement with similar deductions from the Love wave data.

Other cases of the propagation of vibrations in clay soil overlying gravel have beeп studied in which the thickness of the clay layer was about 5 ft. Estimation of the thicl ness from the Love wave data gave extremely good agreement with the actual thicknes as measured at boreholes (1). In some of these experiments, there were two distinct types of vibration present in the Rayleigh waves of which the one corresponding to the Principal Mode predominated nearer the vibrator. Once this wave had decayed, a second faster wave was obtained which was attributed to another mode of propagation of the vibrations (1).

(c) Road Constructions with a Single Surface Layer of Considerably Higher Elastic Moduli than the Underlying Material

In this case:

$$H_2 = 0.$$

$$\alpha_1 > \beta_1 > \alpha_3 > \beta_3$$

Under these conditions, surface vibrations of the Rayleigh wave type can only exist for a limited range of phase velocity (c) given by

$$\beta_3 > c > \gamma_3.$$

The solution for c within this range is obtained from an eight order determinant (9) and the computation is somewhat laborious. At very long wave lengths the phase velocity will approach γ_3 but it is difficult to predict what will happen when the phase velocity becomes comparable with or exceeds β_3. In order to simplify the problem it has been assumed that, once the phase velocity exceeds β_3, the underlying material may be treated as a liquid. This is not a particularly drastic assumption since the Poisson's ratio of most soils is of the order of 0.45 so that α_3 is 5 to 10 times β_3. The most convenient form for the solution of the problem of the propagation of plane waves in a plate resting on a liquid has been given by Press and Ewing (7) and the analysis for the propagation of flexural waves has now been obtained (Jones unpublishe The results of the analysis are shown in Figure 9. It will be seen that the phase veloci wave length curve has at least one discontinuity which occurs near the velocity of com-pressional waves (α_3) in the underlying medium. Above α_3, the results are generall in very good agreement with the solution obtained by Lamb (3) for the propagation of flexural vibrations in a free plate. As the phase velocity approaches α_3, the discrep-ancy between the phase velocity in the free plate case and in the case of an underlying liquid becomes greater and there is also a considerable increase in attenuation of vibrations. Below α_3, the branch of the curve denoted by (b) is expected to account best for the propagation of the vibrations. The short wave length part (a) of this branc represents a type of vibration which has its maximum amplitude at the interface betwe media 1 and 3 and which will not be found experimentally in the presence of the surfac vibrations characterized by the upper branch. The analysis does not give any indicatio

the nature of the transition between part (b) of the curve and the Rayleigh wave
lution (c) for the propagation of very long waves and phase velocities less than β_3.
is considered likely from theoretical considerations that there will be a discontinuity
ar β_3.

The theoretical analysis indicates that over most of the frequency range there is
ely to be more than one type of vibration being propagated and the question arises as
how this will affect the experimental observations. Van der Poel (10) has shown that
e wave with the greatest amplitude will be detected and that it is only when there is a
ar equivalence in amplitude that destructive interference occurs. Thus, the discontin-
y between the upper and lower branches of Figure 9 is expected to be characterized
perimentally by a narrow range of frequencies within which there will be strong inter-
ence and ill-defined propagation of the vibrations.

It is only rarely that a practical road construction approximates to the case of the
igle surface layer considered previously. However, three such constructions were
et with when, in an experimental road, sections were laid with dense asphalt bases
4.3, 6.4 and 8.4 in. thickness. Results obtained from these bases are shown in
gure 10 in which the phase velocity is plotted against the ratio of wave length to thick-
ss. Unfortunately, the length of each section was only 15 ft so that the longest wave
igth which could be measured with reasonable accuracy was 5 ft.

The theoretical curves shown in Figure 10 were obtained directly from Figure 9 and
re adjusted to fit the experimental results at an L/H_1 ratio of 3. It will be seen that
e experimental results deviate progressively from the theoretical curve for flexural
ves in a free plate when L/H_1 exceeds 5. Although part of this disprepancy has been
counted for in the theory given, it is considered that a major contribution arises from
e change in the elastic shear modulus of the asphalt with the frequency of the vibrations.
is effect is also considered to account for the remaining experimental results falling
low the lower branch of the theory.

A practical construction which is free from visco-elastic effects within the experi-
ental range of frequencies is that of a concrete slab laid directly on soil or on a thick
anular base. The results shown in Figure 11 were obtained from experiments on a
ncrete slab, nominally 9 in. thick, laid on a well-compacted hoggin base 2 ft thick.
le theoretical curves shown in Figure 11 have been calculated from the following data:

1. The value of γ_1, for concrete has been taken as 8,350 ft/sec: this is fixed by
e experimental results at about 60 kc/s (that is, $L = 0.139$ ft).

2. Poisson's ratio for concrete has been taken as 0.25. This value was deduced
om γ_1 in conjunction with the compressional wave velocity α_1, measured by an
trasonic pulse method (2) at the surface of the slab.

3. The ratio of the densities of the hoggin to concrete was assumed to be 2:3.

An excellent fit with experimental results is given in Figure 11 when the thickness
assumed to be 9.5 in. Subsequently, two cores were drilled from the slab and indi-
ted thicknesses of 9.55 in. at the center and 9.85 near one corner.

It will be seen from Figure 11 that the experimental results at wave lengths of 5.4
d 5.65 ft deviated from the theoretical curve for flexural vibrations in a free plate.
his deviation is predicted by the theory given earlier and indicates that the phase
locity at these wave lengths is just above the velocity α_3 of compressional waves in
e hoggin (about 3,000 ft/sec).

) Road Construction with a Surface and an Intermediate Layer

In the case to be considered below the nomenclature is as Figure 4 and the magnitudes
the phase velocities were as follows:

$$\alpha_1 > \beta_1 > \alpha_2 > \beta_2 \approx \beta_3$$

This particular problem was analyzed because of some very anomolous results ob-
ined in experiments on a section consisting of an asphalt surfacing 4 in. thick on a
nd base about 13 in. thick overlying clay. The experimental results are shown in

Figure 12 in the form of the phase-velocity-wave length curve. Experimentally, the measurements commenced at a frequency of 40 c/s and the frequency was increased increments up to 13,750 c/s. At frequencies of 40, 70 and 90 c/s the phase velocitie were 460, 462 and 504 ft/sec as indicated on the lowest branch of Figure 12. A furth increase of frequency to 120 c/s caused a very large increase in wave length and a jump in the phase velocity to 2,320 ft/sec. Subsequent increases in frequency to 360 c/s produced decreasing phase velocities and gave rise to what will be called the inte mediate branch of the phase-velocity-wave length curve. Between 360 c/s and 460 c there was another jump in phase velocity from 1,150 to 2,220 ft/sec followed by a de crease to 1,680 ft/sec when the frequency increased to 575 c/s. At frequencies high than 875 c/s, the results gave the well-defined upper branch.

The intermediate branch of the curve of Figure 12 bears a strong resemblance to the dispersion of longitudinal waves in a liquid layer on a liquid substratum (6) and it was considered that this branch represented longitudinal waves in a form of wave-gu For this to be possible requires that the velocity of compressional waves in the sand should be about 1,000 ft/sec and should be less than the velocity of compressional waves in the clay (about 2,300 ft/sec). Samples of the sand and clay were molded into specimens suitable for test by the ultrasonic pulse method (2) and it was found th the pulse velocities were consistent with these values.

The theoretical analysis has been carried out treating the sand and clay as liquids (Jones unpublished). The results of the analysis are therefore not applicable when th velocities become comparable with β_2 or β_3 but it is expected to apply to phase ve- locities which exceed β_2 or β_3 by 25 percent or more. Computations have been ma for ratios of wave velocities and thicknesses consistent with the experimental constr ction (that is, $a_1 = 2$ $\beta_1 = 4$ $a_3 = 10$ a_2, $d_1 = 1.2$ $d_2 = 1.1$ d_3, $H_2:H_1 = 3$ and 4). The results are shown in Figure 13 and show clearly the various branches of the curve found experimentally in Figure 12. Direct comparison between experimental and the retical results is made in Figure 14 and it will be seen that the main deviations are a long wave lengths on the intermediate branch and at the long wave length (11.4 ft, 46 ft/sec) on the lowest branch. The deviations on the intermediate branch may be due variations in the properties of the clay with depth or to the sand layer being thicker than allowed for in the analysis. In practice, the sand layer had a thickness varying from 9 to 23 in. over the 200 ft length of section and measurements were made over length for which the nominal thickness was from 10 in. to 17 in.: this variation in thi ness along the line of measurement may also have influenced the results. The phase velocities along the lowest branch of the curve were becoming comparable with the velocity of shear waves in the clay and sand so that deviations were to be expected here because of the inadequacy of the analysis.

The factors which can be positively identified from the experimental data are:

1. The velocity of shear waves in the asphalt at a frequency of about 30,000 c/s; this enables the shear modulus of elasticity of the asphalt to be estimated.
2. The thickness of the asphalt layer.
3. The velocity of compressional waves in the sand.

In addition an estimate can be obtained of the velocity of compressional waves in th clay.

One item of practical interest has been to deduce changes occurring in the propert of the subbase of this construction under traffic. It is the intermediate branch of the phase-velocity-wave length relation which provides these data and experimental result obtained initially and about 7 months and 13 months after the road was opened to traff are shown in Figure 15. It will be seen that the value of a_2 increased from about 1, to 1,450 ft/sec during the winter and spring while there was a further increase to ab 1,950 ft/sec during the summer. These increases were due to compaction of the san subbase by the relatively high stresses generated below the thin construction. It is interesting to observe that there was a greater incremental increase during the summ months when the effective elastic moduli of the surfacing were relatively low so that the imposed stress was higher than in the colder periods of the year.

REFERENCES

Jones, R., "In-Situ Measurement of the Dynamic Properties of Soil by Vibration Methods." Geotechnique, pp. 1-21 (March 1958).

Jones, R., and Gatfield, E.N., "Testing Concrete by an Ultrasonic Pulse Technique." Department of Scientific and Industrial Research, Road Research Technical Paper No. 34, London (1955).

Lamb, H., "On Waves in an Elastic Plate." Proc., Roy. Soc. A., 93:116-128 (1916).

Miller, G.F., and Pursey, H., "The Field and Radiation Impedance of Mechanical Radiators on the Free Surface of a Semi-Infinit Isotropic Solid." Proc., Roy. Soc., 223:521-41 (1954).

Miller, G.F., and Pursey, H., "On the Partition of Energy Between Elastic Waves in a Semi-Infinite Solid." Proc., Roy. Soc., 233:55-69 (1955).

Pekeris, C.L., "Theory of Propagation of Explosive Sound in Shallow Water." Geol. Soc. Amer., Mem. 27 (1948).

Press, F., and Ewing, M., "Propagation of Elastic Waves in a Floating Ice Sheet." Trans, Am. Geophys. Union, 32:673-8 (1951).

Sezawa, K., and Kanai, K., "Discontinuity in the Dispersion Curves of Rayleigh Waves." Bull. Earthq. Res. Inst., Tokyo, 13:238-43 (1935).

Stoneley, R., "Rayleigh Waves in a Medium with Two Surface Layers." Monthly Notices of Roy. Astron. Soc. Geophys. Suppl., 6 (9):610-15 (1954).

Van der Poel, C., "Dynamic Testing of Road Constructions." J. Appl. Chem., 1 (7):281-90 (1951).

Non-Destructive Testing of Pavements

A.A. MAXWELL, Chief, Flexible Pavement Branch, Soils Division, US Army Engineer Waterways Experiment Station, Vicksburg, Mississippi

A vibratory-type machine was developed by the Royal Dutch Shell Company, Amsterdam, Holland, for non-destructive testing of pavements. This machine was made available to the Corps of Engineers for about six months, during which tests were made on pavements and unsurfaced soil areas. For the greater part of the time the tests were under the direct supervision of engineers from the Royal Dutch Shell Company. Evaluations of the pavements can be made based on two distinct principles. The machine can be made to serve as a source of vibrations from 10 to 2,000 cycles per second, and the wave velocity can be determined. The elastic modulus of the pavement can then be established based on accepted relationships between the velocity of the wave propagations and elastic constants. A second approach is a determination of the so-called stiffness factor, which is the relationship between a dynamic load and the resulting deflection of the pavement surface under a circular loaded area. This paper presents typical results obtained with the machine.

● THE SHELL ROAD vibration machine was developed at the Shell Laboratories in Amsterdam, Holland. The U.S. Air Force made arrangements with Shell for the use of the machine, and it was brought to this country in April 1958. The machine has been used at the Corps of Engineers' Rigid Pavement Laboratory in Cincinnati, Ohio, the Flexible Pavement Laboratory in Vicksburg, Miss., and the Columbus Air Force Base, Miss. William Heukelom and Theodorus W. Niesman accompanied the machine. Niesman returned to Amsterdam as soon as an operator had been trained, but Heukelom remained throughout most of the test program. Thus, almost all the tests were made under the supervision of Heukelom. Tests were made on three occasions at Columbus AFB by Corps personnel after Heukelom's departure for Holland. After completion of the tests at Columbus AFB, the machine was transferred to the custody of the Transportation Corps for use on the AASHO Test Road.

SHELL ROAD VIBRATION MACHINE

This paper presents the results of tests made with the Shell road vibration machine which furnish some measure of the accuracy of the method and some indications of its potential usefulness and limitations. The machine and the method of operation have been described fully in the papers in the list of references, and only the basic elements will be discussed in this paper.

Two quantities are measured with this machine, the "stiffness modulus" and the velocity of waves over a wide range of frequencies. The stiffness modulus is defined as the ratio of a dynamic load and the resulting deflection. It is expressed in kilogram per centimeter or tons per inch and is therefore similar to a spring constant.

The machine can be operated so as to induce vibration over a range of frequencies of about 5 to 2,000 cycles per second. Vibrations with frequencies of 5 to 60 cycles per second are produced by counter rotating eccentric weights powered by a gasoline engine. This vibrating mass is attached to a 30-cm-diameter circular plate and rests

the pavement surface. Forces up to about 4 tons can be applied with this low fre-
quency unit. This unit is used to determine the stiffness modulus as well as a source
low frequency waves which are required for other purposes.

Vibrations at frequencies of 40 to 2,000 cycles per second are induced by a high
frequency electromagnetic vibrator. This unit is used solely as a wave source, as the
forces developed are too small to determine the stiffness modulus.

VELOCITY MEASUREMENTS

In operation, a probe or pickup is placed on the ground or pavement surface at a
known distance from the source of vibrations. This pickup is wired through an oscillo-
scope on which the wave form can be viewed. Further, a phase mark is superimposed
n the wave so that the position of the pickup with respect to the crest and troughs of
the wave at the point of generation is immediately apparent. The distance between the
pickup and the source of vibration is changed a little at a time until the phase mark
appears exactly at the crest or trough of a wave. The distance is recorded and is then
increased until the phase mark appears at the next trough (one-half the wave length) or
crest (one wave length). Thus, the wave length is determined directly. Knowing the
frequency of vibration and the wave length, the velocity is given by the relation

$$V = Ln$$

in which

V = velocity in meters per second,
L = length in meters, and
n = frequency.

Usually, the probe is operated over a distance of several wave lengths, and distance
from the source is plotted against number of wave lengths. The slope of the line de-
fined by these points is the wave length. This method gives greater accuracy than the
measurement of a single wave length.

Questions have been raised by several investigators as to the type of waves generated.
They are generally thought to be shear waves, although the occurrence of Rayleigh or
other type waves is possible. The difference in velocity of shear and Rayleigh waves
is only a few percent and is not considered significant in this type of work. The veloc-
ity of propagation of shear waves in a medium is related to the modulus of elasticity
and Poisson's ratio of the medium in accordance with the following classic equation:

$$V = \sqrt{\frac{Eg}{\gamma (1 + \mu)}}$$

in which

V = velocity,
E = Young's modulus,
g = acceleration of gravity,
γ = unit weight, and
μ = Poisson's ratio.

Taking μ as 0.5, squaring, and transposing gives

$$E = \frac{3\gamma}{g} V^2$$

The shear modulus G can be computed from the relation

$$E = 2(1 + \mu) G$$

From the foregoing, it is apparent that the wave velocity V, the unit weight of the
soil γ, and Poisson's ratio must be known in order to compute the modulus of elasticity
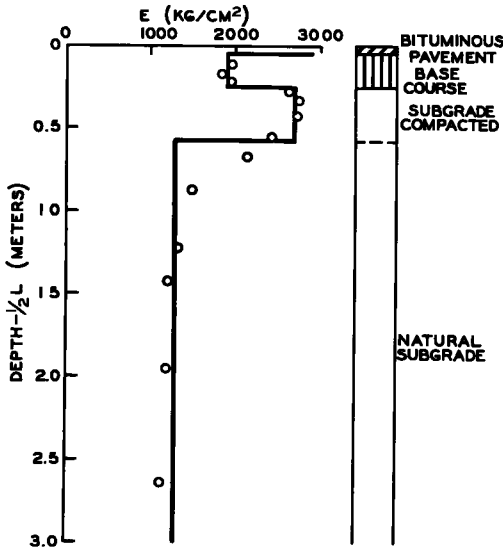E. The wave velocity is measured. The unit weight can be measured or in most cases

Figure 1.

estimated as a small variation has little effect on E. Poisson's ratio μ is probably more nearly 0.40 to 0.45, but, as with unit weight, small differences do not greatly affect the results.

In practice, the elastic moduli determined as outlined here are plotted against depth. It is known that waves induced by low frequency vibrations (long wave length) travel at relatively great depths, while waves induced by higher frequency vibrations (shorter wave length) travel at relatively shallow depths. Results of tests by the Royal Dutch Shell Company engineers

with the road vibration machine have shown that if the depth of travel is taken as one-half the wave length, the results agree remarkably well with known depths to the various layers in a pavement structure.

Figure 1 illustrates typical test results. It is a plot of E versus depth where the depth is taken as one-half the wave length. Each test point shown is based on a wave velocity measurement at a different frequency of vibration. The test point at the greatest depth was determined at a frequency of 60 cycles per second. The frequency was increased by steps up to 2,000 cycles per second.

The evaluation of a pavement structure is greatly facilitated if the subsurface materials can be separated into layers and specific properties assigned to these layers. It can be noted that lines have been drawn through the test points on Figure 1 with this end in view. It is necessary to determine the E-value of bituminous surface layers by laboratory methods.

Figure 2.

This determination was not made and no values are shown. A value of 1,900 is shown for the layer beneath the pavement to a depth of about 0.25 m. At this depth, the E-value increases to 2,700 and then shows with increasing depth a gradual decrease to about 1,300.

The data shown in Figure 1 are the results of measurements taken at a small municipal airport by Shell Oil Company personnel who had no knowledge of the subsurface conditions at the time the test was conducted. Figure 1 also shows a section showing the actual construction at this site. The bituminous pavement surface consists of 1 ½ in. of sand asphalt with about a ¼ - in. surface treatment. Below this is a 9 in. base of plastic clay gravel. The surface of the natural ground, a sandy silt, was compacted
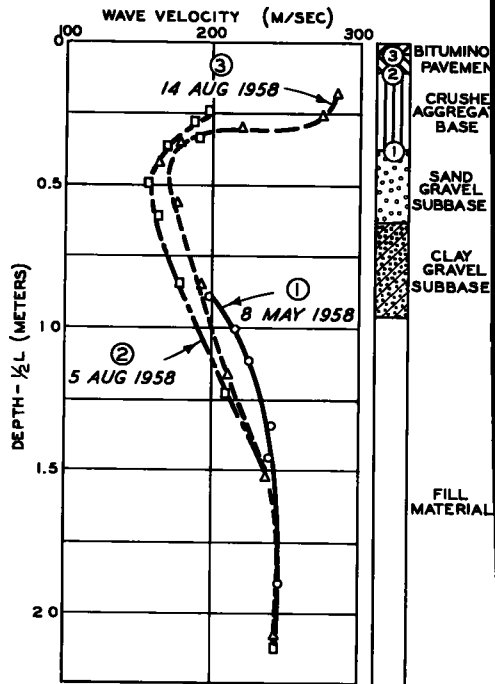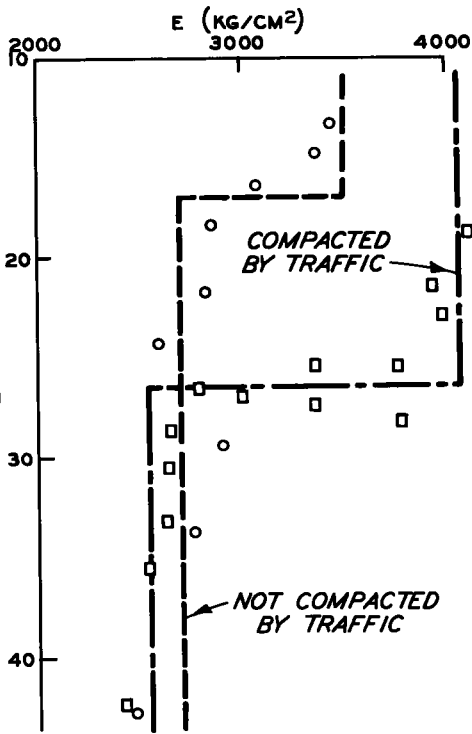
Figure 3.

prior to placement of the base course. The subsurface soils were not tested by conventional methods at the time of the vibration tests; however, it is known from pavement performance and from several series of earlier tests that the plastic clay gravel now has a high water content and a relatively low strength. It is considered that in this particular case, the results of the vibration tests agree satisfactorily with known relative strengths and depths to the subsurface layers.

Some idea of the capability of this method of exploration to resolve the subsurface properties adequately can be gained by an examination of Figure 2. Wave velocities are plotted against depth. Curve 1 was obtained from a test made May 8, 1958, at which time the surface was at point No. 1 on the log. The other curves were obtained from tests made after the addition of 11 in. of base course material and after construction of a 2 ½ - in. bituminous binder course. Obviously the curves are not coincident, but it should be remembered that the data were taken over a period from May 8 to August 27 as noted in Figure 2. It is suspected, and some supporting evidence is available, that a wetting and drying took place between May and August which may account for the differences occurring at the 40- to 60-in. depth interval. Even with no attempt to correct for such a possibility, the velocity values in the deeper layers before and after the addition of other layers at the surface are in good agreement.

Figure 3 shows that it is sometimes possible to detect changes in properties of the subsoil by means of velocity measurements. In this case, a portion of silty clay subgrade constructed under controlled conditions was subjected to traffic and other portions were not. These data show the increase in E-value caused by the effects of traffic. Data were also obtained from conventional soil tests made at depths of 2, 8, and 14 in. in trafficked and untrafficked areas and are given in Table 1 together with the E-value determined from vibration measurements.

TABLE 1

Depth (in.)	Before Traffic				After Traffic			
	γ	Water Content (%)	CBR	E	γ	Water Content (%)	CBR	E
2	108.7	13.8	41	-	110.2	10.6	70	-
8	107.6	13.2	44	2,600	108.5	11.8	68	4,100
14	105.5	12.1	36	2,600	106.3	12.3	38	2,500

At a depth of 8 in., traffic caused the CBR value to increase from 44 to 68, an increase of 55 percent. Referring to Figure 3, it can be seen that the E-value at the 8-in. depth, determined from vibration measurements, increased from about 2,600 to about 4,100, an increase of 58 percent. It should also be noted that at a depth of 14 in., both CBR and E-values indicate that little or no change occurred.
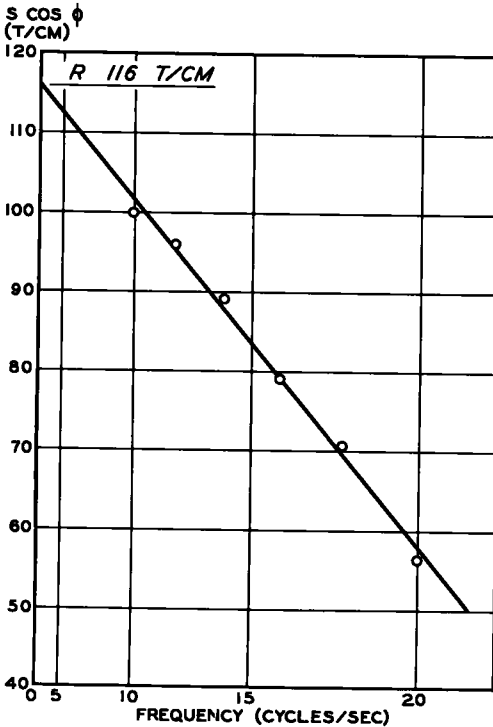
Figure 4.

STIFFNESS MODULUS

Data presented thus far have shown typical results that have been obtained from velocity measurements only and have indicated that such measurements can provide information on conditions throughout the depth of the construction except for the top several inches. As stated previously, a stiffness modulus for the whole system can be determined directly. This stiffness modulus was defined as the ratio of a dynamic load to the resulting deflection. The low frequency vibrator is used in this test because the forces developed are great enough to result in measurable deflections.

The force on the pavement is dependent on the frequency and the machine constant. Machine constants take into account the mass of the machine, eccentricity and mass of the rotating weights, and phase angle. The deflection is measured by electronic means. Further details are beyond the scope of this paper but are available in the references listed.

It is obvious that the higher the frequency at which the machine is operated the greater will be the force generated. Thus, a stiffness modulus as previously defined can be determined for each frequency used. Other investigators have found the stiffness modulus to vary with the frequency and that the variation is generally not linear. Heukelom showed that the value of the stiffness modulus depended on the mass of the soil in motion. In a system consisting of mass M, a spring R, and a dashpot, it can be shown that

$$S \cos \phi = R - W^2 M$$

in which

S = dynamic stiffness (stiffness modulus as previously defined)
ϕ = phase lag of the deflection with respect to the applied force
W = angular frequency ($2\pi n$ where n = frequency in cycles per second)

When $S \cos \phi$ is plotted against a function of the square of the frequency, a straight line through the experimental points intersects the $S \cos \phi$ axis at a value R which is called the elastic stiffness. Figure 4 shows such a plot. The data shown in this figure were obtained from tests made at the same location as the velocity measurements shown in Figure 1.

Returning now to Figure 1, it will be recalled that E-moduli of 1,900, 2,700, and 1,300 kg/cm^2 were found for the 9-in. base course, the compacted subgrade, and the deep soil, respectively, but that the E-modulus of the bituminous pavement was not determined. If this value was known, the elastic stiffness R of the entire system could be computed and this would permit a check on the R value determined as shown in Figure 4. The E-modulus of a bituminous pavement depends on the bitumen content, penetration value of the bitumen, temperature at the time of test, and rate of loading. Nijboer and others have developed theoretical methods whereby the E-modulus can be estimated, but a direct determination in the laboratory is much to be preferred. Fol-

owing Nijboer's method, the E-modulus was estimated to be 7,000 kg/cm². Using this value, and values for the underlying layers determined experimentally, R was computed to be 113 t/cm as compared with 116 t/cm determined from direct measurements. Too much significance cannot be given to the close check obtained in this particular case as it was necessary to estimate one of the one of the values used. The example was presented to illustrate that when all data are available, the determination of R by two different methods is possible which provides a check on the work. It is also evident that if the E-modulus of the surface layer is not known and cannot be accurately estimated, it can be treated as the "unknown" and determined, knowing the E-modulus of the underlying layers and the elastic stiffness of the whole system.

Several values of elastic stiffness in tons per centimeter, together with a brief description of the materials (to illustrate the range of values encountered) are given, as follows:

115-130 — unsurfaced, well-compacted, silty clay; CBR 40-60 percent.
160-170 — 5- to 10-in. crushed gravel over 24-in. clay gravel.
170-180 — 10- to 12-in. crushed gravel and slag over 10-in. sand gravel over clay-gravel subgrade.
200-210 — ¼-in. bituminous surface over 10- to 12-in. crushed gravel and slag over 10-in. sand gravel over clay-gravel subgrade.
250-400 — Heavy-duty airfield flexible pavement.

POTENTIAL USES

The material in this paper has been restricted to essentially a presentation of examples of the type of data obtained directly with the Shell road vibration machine and the initial treatment of these data. A study of the references will show that many uses can be made of these data. For example, actual deflections measured under given loads can be related to deflections to be expected under vehicles or aircraft of similar loadings. Also, with measured deflections, strains can be computed which can in turn be compared with strength available. Such uses involve assumptions and theories beyond the scope of this paper.

It appears highly probable that useful relations can be developed between the values determined from vibratory measurements and the conventional values used in design and evaluations, such as unconfined compressive strength, subgrade modulus (K, from plate bearing tests), density, CBR, and others. To establish such relationships, it is necessary to make the vibration measurements at locations where complete information on the subsurface conditions at the time of test is available.

The Shell road vibration machine has been used for sometime in Europe with considerable success. The Waterways Experiment Station had the use of the machine for about six months and based on the observations during that period, it is believed the machine has immediate application in the evaluation of airfield pavements. The machine is usually operated by a crew of three men; however, a fourth man is desirable when the test data are to be reduced in the field for immediate use. In a normal working day, a four-man crew can determine the stiffness moduli of the pavement at four locations. These determinations will show relative over-all strength and will permit definition of "weak" and "strong" areas. After stiffness moduli have been determined, velocity measurements can be made at selected locations dependent on the particular problem and information on the strengths of individual subsurface layers obtained to supplement the stiffness measurements. While proven methods are not presently available to relate results obtained with this machine directly to bearing capacity or performance, data obtained from satisfactory and unsatisfactory areas would permit an estimate of performance. It also appears highly probable that periodic measurements would provide useful information on the seasonal changes taking place in a pavement structure such as wetting and drying or feezing or thawing.

REFERENCES

. Nijboer, L.W., "Dynamic Investigations of Road Construction." Shell Bitumen Monograph No. 2.

2. Heukelom, W., and Niesman, T.W., "Method of Investigation and Apparatus Used by the Koninklijke/Shell Laboratorium, Amsterdam, Holland."
3. Heukelom, W., "Dynamic Testing of Pavements: Survey of Theoretical Considerations." (Unpublished.)
4. Heukelom, W., "Dynamic Testing of Pavements: Interpretation of Observed Data."
5. Heukelom, W., Miscellaneous unpublished data reports.
6. Heukelom, W., and Foster, C.R., "Dynamic Testing of Pavements."

A Non-Dimensional Approach to the Static and Vibratory Loading of Footings

R. L. KONDNER and R. J. KRIZEK, respectively, Instructor of Civil Engineering, The Johns Hopkins University, Baltimore, Md.; and formerly Research Assistant, The Johns Hopkins University, presently Instructor of Civil Engineering, The University of Maryland, College Park

An investigation of the surface deformations of rigid footings on homogeneous, cohesive soils under vertical static and vibratory loadings which is based on the methods of dimensional analysis in conjunction with small-scale model studies is reported. The physical quantities included are the strength and energy dissipation characteristics of the soil, the geometry of the footing, the magnitude of the static and dynamic loading, and the effects of frequency and amplitude of vibration. Practical illustrative examples are worked using the methods and data reported in this paper and the solutions are compared with those obtained for the conventional methods given by Housel, Kogler and Scheidig, and numerous authors in the field of soil mechanics.

THE BASIC PURPOSE of this paper is to report the results obtained from a small-scale laboratory investigation of the vertical static and vibratory loading of frictionless rigid footings on the surface of a homogeneous cohesive soil. Because the study is based on the methods of dimensional analysis and the results are presented in non-dimensional form, the results can be expected to hold for similar full-scale studies, provided all of the important variables have been included in the dimensional analysis and there is similitude between the corresponding non-dimensional parameters of the model and prototype. Thus, the seemingly impossible task of modeling is avoided. It must be recalled that dimensional analysis and model analysis are quite different, with dimensional analysis being a much more powerful and fundamental tool. Because of the complexity of soil as a structural material and the difficulty of soil problems in general, it is felt that a more extensive use of the methods of dimensional analysis will contribute to the field of soil mechanics.

Although some quantitative results are given, the results presented in this paper are intended to be qualitative indications of the possible results obtained using dimensional analysis as an experimental guide in problems in soil mechanics. The methods of dimensional analysis have been very successful in the field of hydraulics but their use in soil mechanics has been very limited, possibly because of the influence of boundary conditions, the water table, and the non-homogeneity and stratification of soils. The senior author intends to extend the present study to include the effects of stratification, eccentricity of loading, friction between the footing and the soil, single impulse loading, and the influence of a rigid ledge below the soil mass for both cohesionless and cohesive soils. It is felt that these difficult conditions can also be handled with the methods of dimensional analysis.

THEORETICAL CONSIDERATIONS

The methods of dimensional analysis as used to determine relationships among physical quantities which can be related by an equation are illustrated in a detailed manner in a companion paper by Kondner (12) on the static and vibratory cutting and penetration of soils.

37

The following physical quantities using the force-length-time system of fundamental units have been selected for use in the dimensional analysis:

x = sinkage (contact deformation or surface settlement), L;
t = time, T;
F_T = total applied force, F;
F_S = static force, F;
ω = forcing frequency, T^{-1};
p = natural frequency, T^{-1};
τ = maximum unconfined compressive strength of the soil, FL^{-2};
η = viscosity of soil, $FL^{-2}T$;
ρ = mass density of soil, $FL^{-4}T^2$;
g = acceleration of gravity, LT^{-2};
A = cross-sectional area of footing, L^2;
c = perimeter of footing, L; and
a = amplitude of vibration, L.

A discussion of the foregoing physical quantities is included in the paper previously mentioned (12).

Since there are 13 physical quantities and 3 fundamental units, there must be 10 independent, non-dimensional π terms. These π terms can be methodically obtained by choosing three physical quantities, which contain all three fundamental units and cannot be formed into a π term by themselves (for example, F_T, ω, and τ), and combining them with each of the remaining quantities, one at a time.

There is nothing unique about the form of the non-dimensional terms obtained; hence it is possible to algebraically transform them so long as the final π terms are non-dimensional and independent. Because of the great difficulty in experimentally determining the exact nature of the function F, the π terms obtained, by the method indicated, were algebraically manipulated into the following non-dimensional parameters. In this study the sinkage (x) is considered the dependent variable and hence occurs in only one π term.

$$\pi_1 = \frac{x}{c} \qquad\qquad \pi_7 = \omega t$$

$$\pi_2 = \frac{F_T}{A\tau} \qquad\qquad \pi_8 = \frac{g}{a\omega^2}$$

$$\pi_3 = \frac{c^2}{A} \qquad\qquad \pi_9 = \frac{\omega}{p} \tag{1}$$

$$\pi_4 = \frac{F_T}{F_S} = 1+R \qquad \pi_{10} = \frac{g\rho}{\tau}\sqrt{\frac{F_T}{\tau}}$$

$$\pi_5 = \frac{a}{c}$$

$$\pi_6 = \frac{\omega\eta}{\tau} \text{ or either of the convenient forms } \frac{\tau t}{\eta} \text{ and } \frac{F_T t}{A\eta}$$

The functional relationship among the various physical quantities can therefore be expressed as

$$x = c\,\Psi\left(\frac{F_T}{F_S},\, \frac{F_T}{A\tau},\, \frac{c^2}{A},\, \frac{a}{c},\, \frac{\omega\eta}{\tau},\, \frac{cw}{gt},\, \frac{\omega}{p},\, \omega t,\, \frac{g\rho}{\tau}\sqrt{\frac{F_T}{\tau}}\right) \tag{2}$$

The interpretations of the non-dimensional terms are similar to those given by the senior author for the static and vibratory cutting and penetration of cohesive soils (12).

By dropping from the study the π terms containing p and ρ (12), Eq. 2 can be reduced to the form

$$x = c \, \psi' \left(\frac{F_T}{F_S}, \frac{F_T}{A_T}, \frac{c^2}{A}, \frac{a}{c}, \frac{\omega\eta}{\tau}, \frac{c\omega}{gt}, \omega t \right)$$ (3)
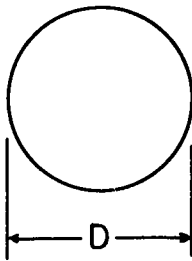
which is assumed to have a solution in an eight-dimensional space.

Although the natural frequency has been dropped from the functional relationship, it will be discussed qualitatively later in the paper. When comparing the relationship between any two π terms, the remaining π terms must not be forgotten. It must be noted that it is the value of the π term that is important and not its individual parts. Thus, the value x/c should be unique for constant fixed values of π_1 although the individual physical quantities composing the π terms may change.

$$\frac{c^2}{A} = 4\pi$$

inches	inches^2	inches
D	A	C
0.79	0.5	2.48
1.13	1.0	3.55
1.38	1.5	4.34
1.59	2.0	5.00
1.78	2.5	5.59
1.95	3.0	6.13

Figure 1.   Circular footings.

EXPERIMENTAL APPARATUS

Model Footings

The model footings used in the study are shown in Figures 1 and 2. They include a set of six circular footings of various diameters, a square footing, four rectangular footings, and a special footing in the form of a symmetric cross. The circular footings have cross-sectional areas of 0.5, 1.0, 1.5, 2.0, 2.5 and 3.0 sq in. and a value of c^2/A equal to 4π which is a constant for all circular footings and the geometric minimum value for c^2/A. The square footing has a cross-sectional area of 2 sq in. and a value of c^2/a equal to 16 which is a constant for all square footings. The rectangular footings and the cross-shaped footing all have constant cross-sectional areas of 2 sq in. but have variable values of c^2/A as shown in Figure 2. All of the model footings are made of aluminum and have a polished finish.

Static Test Apparatus

The two types of static test apparatus used are shown in schematic form in Figures 3 and 4. As shown in Figure 3, the static weight is applied to the footing through a ball bearing with the use of a lever system consisting of a rigid arm pivoted at point e.

The apparatus in Figure 4 operates as follows. The load is applied to the footing through a ball bearing and a shaft by placing weights on the loading platform. The shaft is free to move vertically in the guides. The sinkage is measured with an indicator dial.

Vibratory Test Apparatus

The vibratory test apparatus is schematically shown in Figure 5. The load is ap-
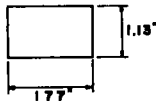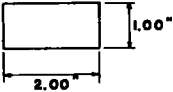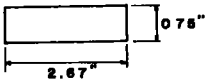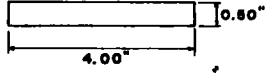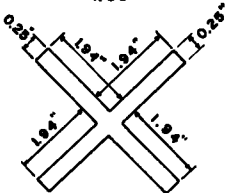
Footing	c	A	$\frac{c^2}{A}$
1.41", 1.41"	5.66	2.0	16
1.13", 1.77"	5.80	2.0	16.8
1.00", 2.00"	6.00	2.0	18
0.75", 2.67"	6.83	2.0	23.4
0.50", 4.00"	9.00	2.0	40.5
0.25", 1.94"	16.5	2.0	136

Figure 2. Footings of constant area and variable perimeter.

plied to the footing through a ball bearing and a solid shaft which is connected in series with a dynamometer and static weights both of which are attached to the moving coil of the electro-magnetic exciter. When the shaft is not bearing on the footing, the weight acting on the moving coil is transferred by small, leaf springs to the field coil which is suspended on the guide track by counter weights. By use of the adjustment reel the shaft is brought to bear on the footing. The position reel is used to raise or lower the exciter along the guide track in order to maintain an average relative displacement of zero between the field coil and the equilibrium position of the moving coil and thus a constant resultant static force. The output of the exciter used was limited to a maximum sinusoidal dynamic force amplitude of 10 lb for a frequency range of 20 to 60 cycles per second.

Static and dynamic forces are measured by the electric dynamometer whose response is amplified and viewed on a cathode-ray oscilloscope. The amplitude of vibration is measured with a piezoelectric crystal-type accelerometer and a vibration meter calibrated to read in micro-inches. The sinkage of the footing is measured by means of an indicator dial calibrated in thousandths of an inch with a range of 1 in.

MATERIAL TESTED

The soil used to date in this investigation is a Jordan buff clay obtained from the United Clay Mines Corporation. It is mined on US 40 approximately 6 miles north of Baltimore at Popular, Maryland. The deposit is a part of the Patapsco formation of the Potomac group which is of the lower Cretaceous period. The characteristics of the clay are as follows:

Liquid limit	42 %
Plastic limit	21 %
Plasticity index	21 %
Specific gravity	2.68
Optimum moisture content	15 %
Maximum dry density	114 pcf

(Modified AASHO)

Test samples were prepared to approximately the desired unconfined compressive strengths by a compaction process using moisture-density-strength relationships previously obtained (11).

EXPERIMENTAL RESULTS

Static Tests

Since this was the first time, to the authors' knowledge, that small-scale model

a loading platform   e pivot
b static weights   f ball joint
c lever arm   g footing
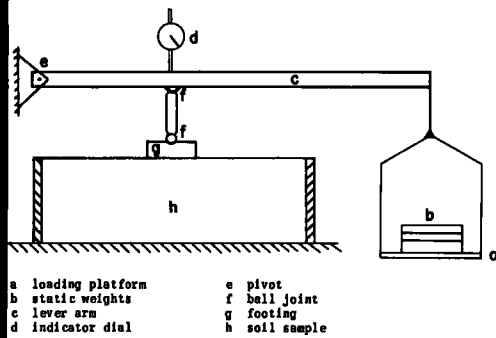d indicator dial   h soil sample

Figure 3. Schematic diagram of static
apparatus.

studies in conjunction with the methods of dimensional analysis had been used to investigate the loading of frictionless and rigid footings on the surface of a homogeneous cohesive soil, it was decided to first conduct experiments with only static loadings. Eqs. 1 and 3 show that the static load-sinkage relation can be expressed in the form

$$x = c \, \psi'' \left(\frac{F_T}{A\tau}, \frac{c^2}{A}, \frac{\tau t}{\eta} \right) \qquad (4)$$

The non-dimensional term $\tau t/\eta$ was obtained from Eq. 1 by dividing π_7 by π_6. Thus, Eq. 4 includes time effects which are known to be of great practical consequence. Those persons familiar with the use of rheological models in the field of high polymers will recognize the term η/τ as being proportional to the relaxation time for a Maxwell material and as being proportional to the retardation time of a Kelvin material. Thus, the non-dimensional term $\tau t/\eta$ controls the rate of sinkage in a static test. The present state of development of the field of soil mechanics is such that very little in a quantitative manner can be done with this term.   The senior author has recently initiated an extensive research program into the static and dynamic viscoelastic properties of soils and is hopeful that considerable progress can soon be made in stress-strain-time phenomena in soils (11).

Pressure Intensity, Soil Strength and Shape Effects. — To illustrate the convergent nature of the non-dimensional form of presenting the experimental data, load-sinkage tests were conducted on a very soft sample using circular footings. The effects of the cross-sectional area on the sinkage of footings was evaluated by using different values of A while maintaining a constant value of c^2/A. For circular footings of any diameter the value of c^2/A is equal to 4π. Thus, such tests will give the relationship between the dependent variable (x/c) and $F_T/A\tau$ for $c^2/A = 4\pi$.

Figure 6 is a conventional plot of the load-sinkage data for the aforementioned tests. The same data are plotted in the non-dimensional form of x/c versus $F_T/A\tau$ in Figure 7. It is important to note that the rate of loading for all of these tests was 1 kg per min with sinkage readings being taken at the end of the 1 min intervals. Although the load application rate was constant, the rate of stress application was not constant because of the difference in cross-sectional area. The senior author's recent work in stress perturbations about various stress levels indicates that the viscous response of the soil being studied is a function of the stress level; thus, the viscous nature of the soil is non-Newtonian and the time effects should be different
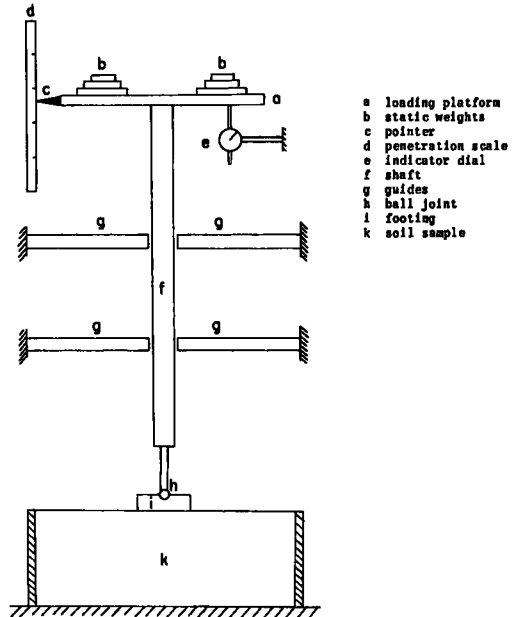

a loading platform
b static weights
c pointer
d penetration scale
e indicator dial
f shaft
g guides
h ball joint
i footing
k soil sample

Figure 4. Schematic diagram of static
apparatus.

a   position reel
b   vibration meter
c   exciter power supply, oscillator
d   amplifier
e   dual channel oscilloscope
f   counter balance weight for exciter
g   guide track
h   accelerometer
i   static weights

j   field coil
k   leaf springs
l   moving coil
m   electro-magnetic exciter
n   dynamometer
o   footing
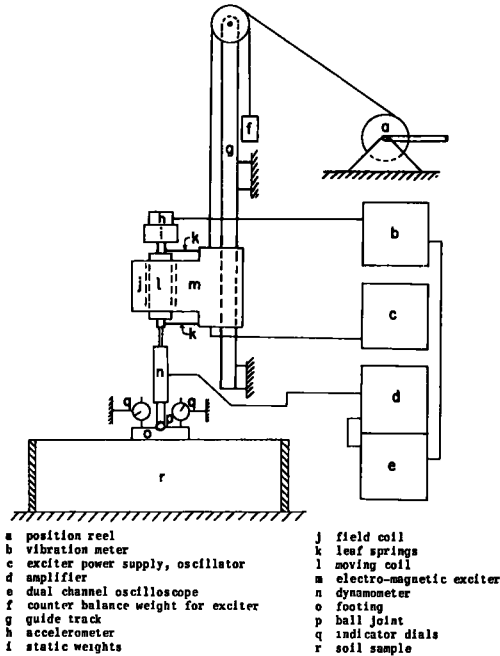p   ball joint
q   indicator dials
r   soil sample

Figure 5.   Schematic diagram of vibratory apparatus.

for the different footings. This means that to obtain a unique relationship between x/c and $F_T/A\tau$ a constant value of $\tau t/\eta$ would have been required for all of these tests. Theoretically, this could have been done by varying the loading rate for each test either by varying the load interval or by changing the time interval of loading. Unfortunately, the field of soil mechanics has not yet reached a state of development where such loading rates can be predicted. It may be that a reverse process could be used to investigate such viscous phenomena. Thus, the "scatter" in Figure 7 is probably due to viscous effects as well as experimental error.

Theoretically, the same curve of x/c versus $F_T/A\tau$ could be obtained by varying the value of τ for any one of the circular footings provided the remaining π terms are kept constant and equal to their values in the previous tests. Figure 8 is the result of such tests conducted on a stiff sample using the same loading rate as in the previous tests. Once again variations in the term $\tau t/\eta$ seem to prevent a complete agreement with the results of Figure 7.

If term $\tau t/\eta$ had been kept constant in the foregoing tests, the results obtained would have been expected to hold in the field. For circular cross-sections the only field data that was located is that reported (4) on the presentation of rigid plate bearing test data. Load versus sinkage data of subgrade for plate diameters ranging from 1 to 7 ft (4, Tables 3 and 5) have been plotted in non-dimensional form in Figure 9. The value of the unconfined compressive strength which was used was estimated from another paper connected with the same study (5). Figure 9 shows a surprisingly small amount of scatter for the wide range of plate sizes and pressures used. When compared with Figures 7 and 8, the best agreement is obtained with Figure 8. The results given in Figure 8 were obtained for a "stiff" soil sample having an unconfined compressive strength closer to that of the field tests. Therefore the viscous effects are less when comparing Figures 8 and 9 than when comparing Figures 7 and 9. The generally good agreement obtained from the non-dimensional plots for the wide range of cross-sectional areas, soil strengths and applied loads seems very encouraging.

To obtain the variation of the sinkage (x/c) as a function of c^2/A, a series of tests were conducted on footings of equal cross-sectional area but with different values of c^2/A for soil samples having approximately the same unconfined compressive strengths. The range of c^2/A tested was from the geometrical minimum of 4π for circular footings to a value of 136 for the cross-shaped footing of Figure 2. The results of these tests are given in Figures 10 and 11. Figure 10 is a plot of x/c versus $F_T/A\tau$ for various values of c^2/A. Figure 11 is a plot of x/c versus c^2/A for various values of $F_T/A\tau$. For a constant value of $F_T/A\tau$, the sinkage parameter (x/c) increases as c^2/A decreases. Thus, for a constant cross-sectional area, a circular-shaped footing has the most undesirable sinkage characteristics.

The results of Figures 7, 8, 9, 10, and 11 are in agreement with the observations on size effects reported by Taylor (15) and Tschebotarioff (18).

It must be recalled that the foregoing data were obtained from carefully controlled tests on homogeneous cohesive soil in which any eccentricities of loading were carefully avoided. Thus, the failure mechanism was such that failure occurred by a gradual sinkage without any tipping of the footing. In actual field studies the soil deposit may
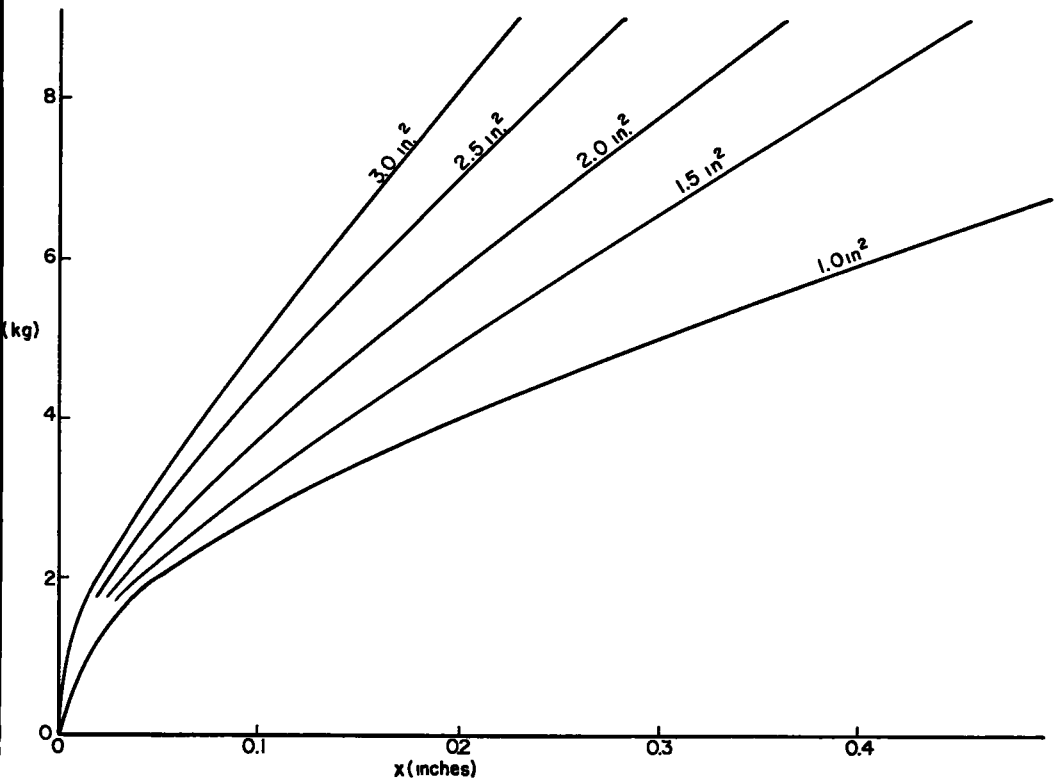
Figure 6. Sinkage versus load: circular footings.

not be homogeneous and the accentricities may be considerable, thus inducing different failure mechanisms for different cross-sectional shapes of constant area. There are two different phenomena to be considered; namely, the sinkage characteristics as indicated by Figure 11 and the stability characteristics which may be a function of the homogeneity of the cohesive soil and both the shape of the footing and the magnitude of the load eccentricity.

Load History and Creep Effects. — To get some qualitative indication of the importance of time effects on the study, a series of load history and creep tests were conducted on soft samples using a circular footing with a cross-sectional area of 2 sq in. The selection of a circular footing and a soft soil was to accentuate viscous effects through large sinkages and to increase stability against tipping of the footing.

The results of the creep tests for various stress levels are given in Figure 12 in the form of x/c versus t. Since the ratio of τ/η is approximately constant for any one creep test but not for different creep stress levels (non-Newtonian effects), the time t is approximately proportional to the non-dimensional term $\tau t/\eta$. Thus Figure 12 can be considered as giving in a qualitative manner the variation of x/c with $\tau t/\eta$ for different values of $F_T/A\tau$ and a constant value of $c^2/A = 4\pi$.

The slopes of these curves for various stress levels at constant times are an indication of the manner in which the strain rate varies as a function of the applied stress level. This indicates that the strain rate increases with the increase in stress level in a non-linear manner. Thus, the viscous response is non-Newtonian. The rate at which the strain rate is increasing with increase in stress level indicates a quasi-Bingham behavior (Fig. 13) for the soil being studied. This agrees with the senior author's preliminary results on the dynamic viscoelastic properties of the clay in question as reported to the U.S. Army, Corps of Engineers (11).
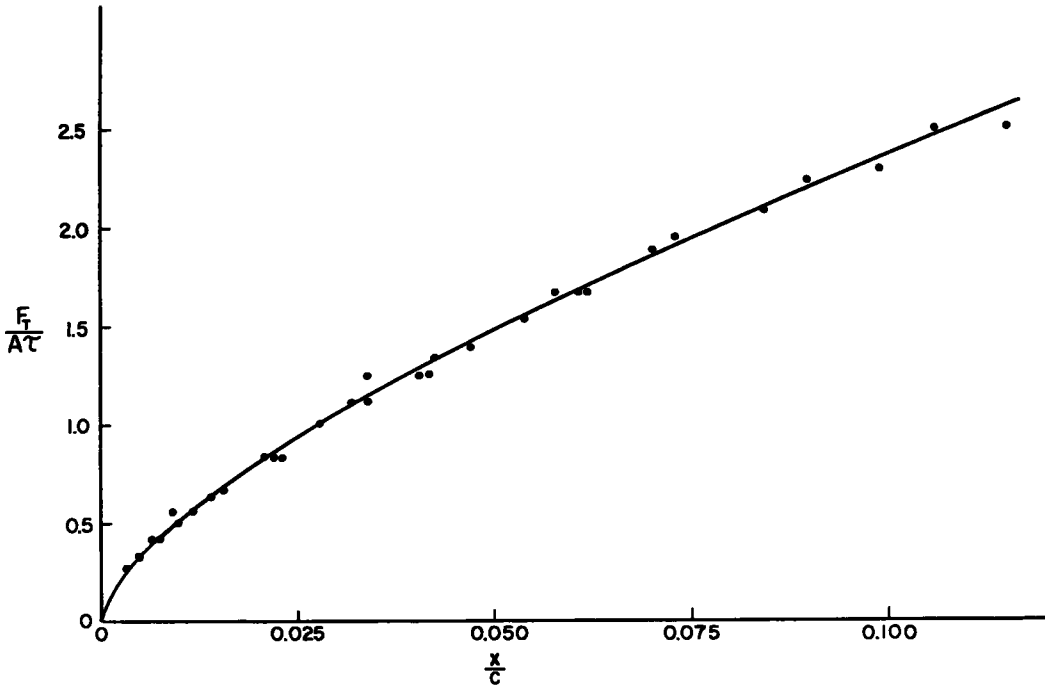
Figure 7. Non-dimensional plot for circular footings of x/c versus $F_T/A\tau$.

Figure 13 illustrates several kinds of viscous behavior. A Newtonian material has a linear relationship (from the origin) between stress and strain rate while non-Newtonian is any other curve. Bingham response is also linear but flow does not develop until a yield stress is reached. Note that the linear relationships mean a constant viscosity. The actual response of the soil considered is non-linear and each stress level is associated with a different viscosity.

The results of the tests conducted with different load histories are shown in Figure 14. The loading sequences used for these tests were 0.5 kg per min, 1.0 kg per 2 min, 2.0 kg per 4 min, and 4.0 kg per 8 min. Thus, for all of the tests, the average loading rate was 0.5 kg per min and the average rate at which the applied stress was being increased was 0.55 psi per min. A comparison of the values of x/c for times of 8 min and 16 min shows an increase in x/c for an increase in the loading sequence. A check of the unconfined compressive strengths showed that the larger load sequences were run on soils with slightly lower values of τ and consequently lower values of η. Since the applied stresses were equal at these times and the viscosity is lower for the large load sequences, the strains for the larger load sequences should be greater. This agrees with the larger values of x/c for the larger load sequences even though the average rate of stress increase was constant.

Although this study is primarily concerned with the rheologic characteristics (referred to by many as plastic, viscous, or secondary time effects) and not with "consolidation" phenomena, the results of this section agree with those obtained for consolidation studies. For the soil tested the smaller increments of load and hence the correspondingly larger number of increments gave smaller surface deformations. When the load is applied gradually the soil skeleton has time to reorient itself and hence to develop a greater resistance to the next increment of load than would be the case if a larger increment of load was applied.

The different results given in Figures 7, 8, 9, 12 and 14 can be reconciled by recalling that variations in τ and the applied stress F_T/A cause different changes in η
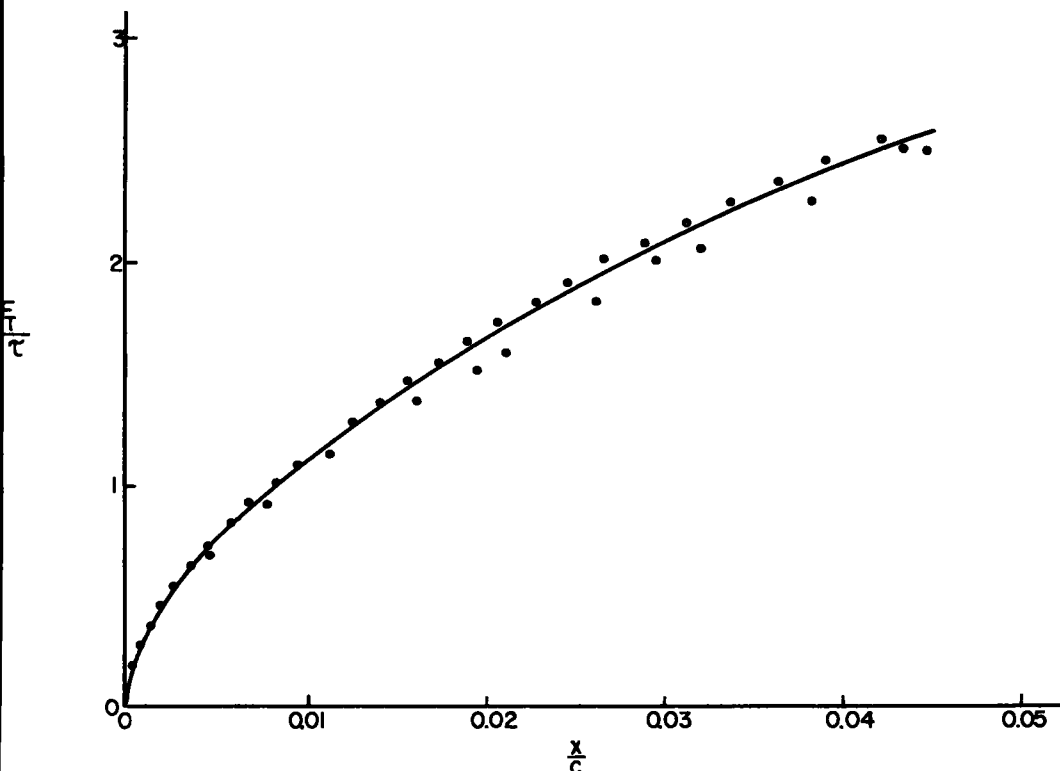
Figure 8. Non-dimensional plot for circular footings of x/c versus $F_T/A\tau$.

and that the various rates of stress application mean that different values of time should be used. Therefore the relationship between (x/c) and $F_T/A\tau$ for different size footings under different rates of stress application on cohesive soils having various unconfined compressive strengths will not be a unique relation until the non-dimensional parameters c^2/A and $\tau t/\eta$ or its equivalent expression $F_T t/a\eta$ are maintained constant.

Practical Applications

The authors believe that the methods of dimensional analysis offer considerable promise in the transformation from model studies to prototype response. To illustrate some of the possible applications of the results presented, several practical problems are solved using the methods presented and the solutions are compared with the solutions obtained using conventional methods of analysis. In this section the viscous effects expressed by the term $\tau t/\eta$ are neglected and it is assumed that Figures 10 and 10-a can be used to obtain the surface deformations under a rigid footing of a homogeneous, cohesive clay mass of any consistency as a function of the total applied vertical load regardless of the cross-sectional area of the footing for a variety of cross-section shapes. Figure 10-a is an enlarged detailed plot of the experimental data near the origin in Figure 10 for square footings.

Specific Problems. — Example A: Comparison with the Housel Method. The following example is taken from Andersen (1, p. 81). It is desired to design a square footing to transmit a load of 94 kips to a cohesive soil without exceeding a settlement of ½ in. Two tests are made with bearing areas of 1 ft by 1 ft and 2 ft by 2 ft; they give settlements of ½ in. for loads of 7,600 and 20,800 lb, respectively.

The solution by the Housel method gives the desired footing having a side length equal to 5 ft.
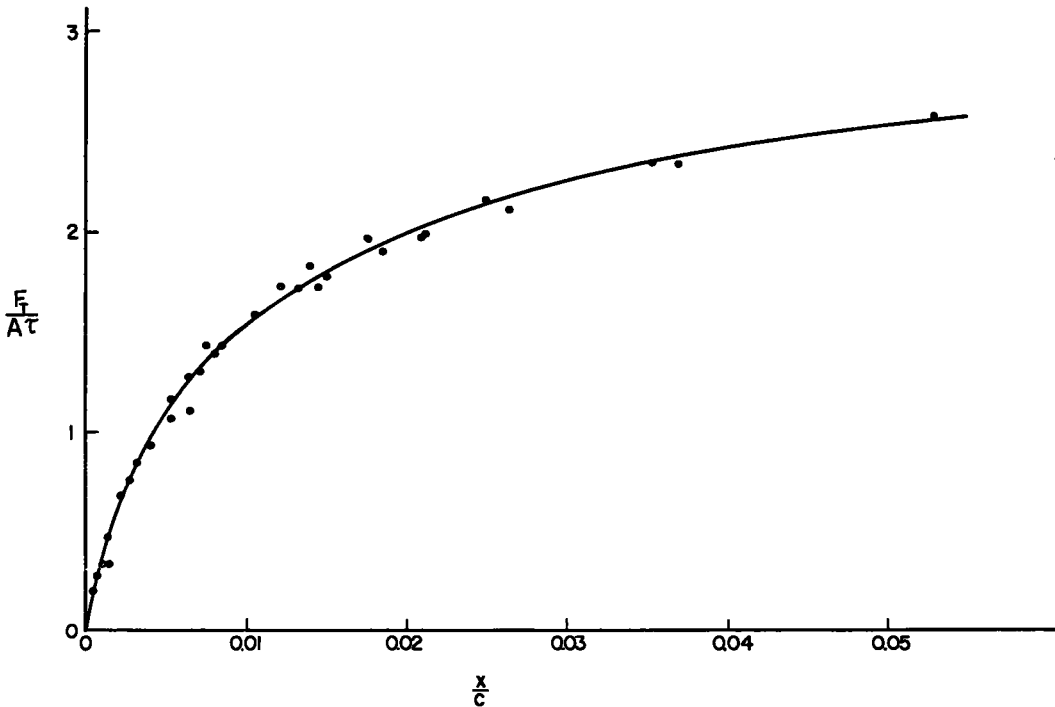
Figure 9. Non-dimensional plot of field data: x/c versus $F_T/A\,\tau$.

Using the non-dimensional method as expressed in Figure 10-a, the solution is as follows:

For the 1- by 1-ft test plate

$$\frac{F_T}{A\tau} = \frac{7600}{1\,\tau} \qquad \text{and} \qquad \frac{x}{c} = \frac{0.5}{48} = 0.01042$$

Entering Figure 10-a with x/c = 0.01042, one obtains a value of $F_T/A\tau$ = 0.614. The value of τ is obtained by equating the two values of $F_T/A\tau$. Inasmuch as the τ for the test plate and the footing is the same, this value is then substituted into the prototype expression and

$$\frac{F_T}{A\tau} = \frac{94,000 \times 0.614}{7,600\,b^2} = \frac{7.6}{b^2} \qquad \text{and} \qquad \frac{x}{c} = \frac{0.5}{48\,b}$$

With the use of Figure 10-a the solution of the two equations is easily obtained by trial and error to be b = 4.93 ft.

The same process can be used for the 2- by 2-ft test plate to obtain a solution of b = 5.01 ft.

The non-dimensional method required the data from only one load test. The agreement between the Housel and the non-dimensional method is excellent.

Example B: Comparison with the Housel Method. A second problem was selected from Andersen (1, p. 85, No. 4).

It is desired to design a square footing to transmit 328 kips to a cohesive soil without exceeding a settlement of $\frac{1}{4}$ in. Two tests are made with bearing areas of 1 ft by 1 ft and 2 ft 3 in. by 2 ft 3 in. They gave $\frac{1}{4}$ in. settlements for 7,600 lb and 25,000 lb respectively.

Figure 10. Non-dimensional plot of x/c versus $F_T/A\tau$ for constant values c^2/A.

Figure 10-a. Non-dimensional plot for square footings.

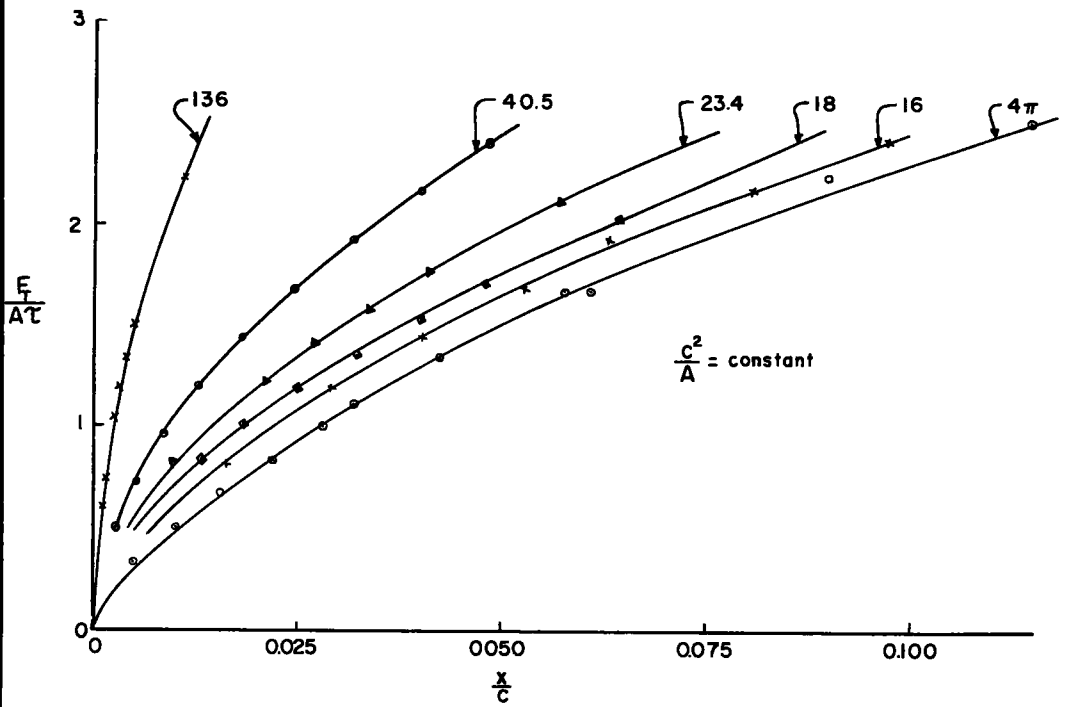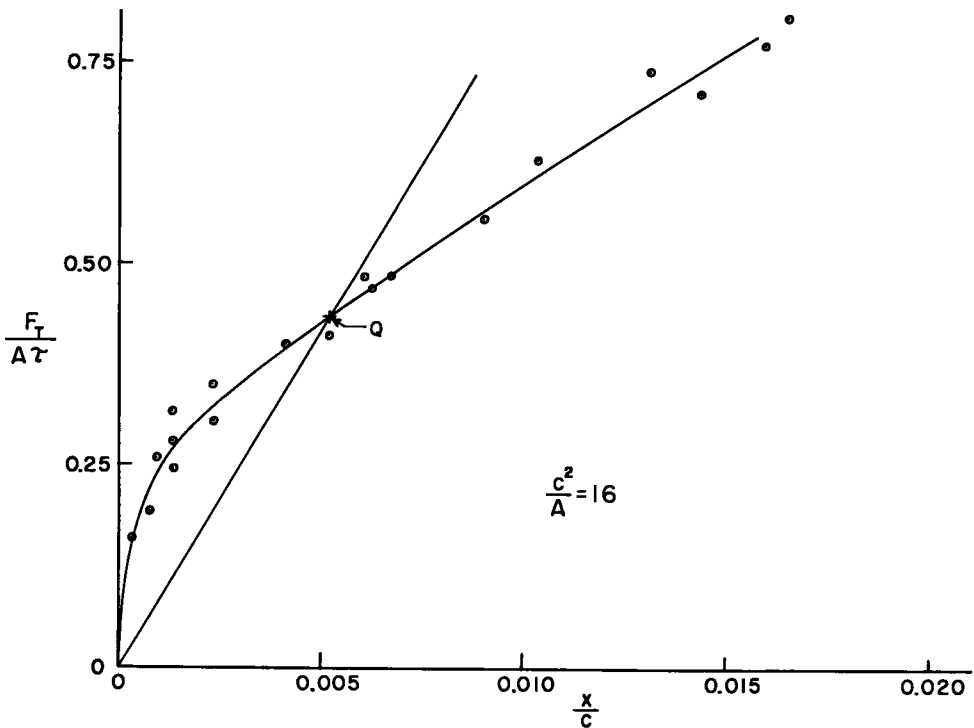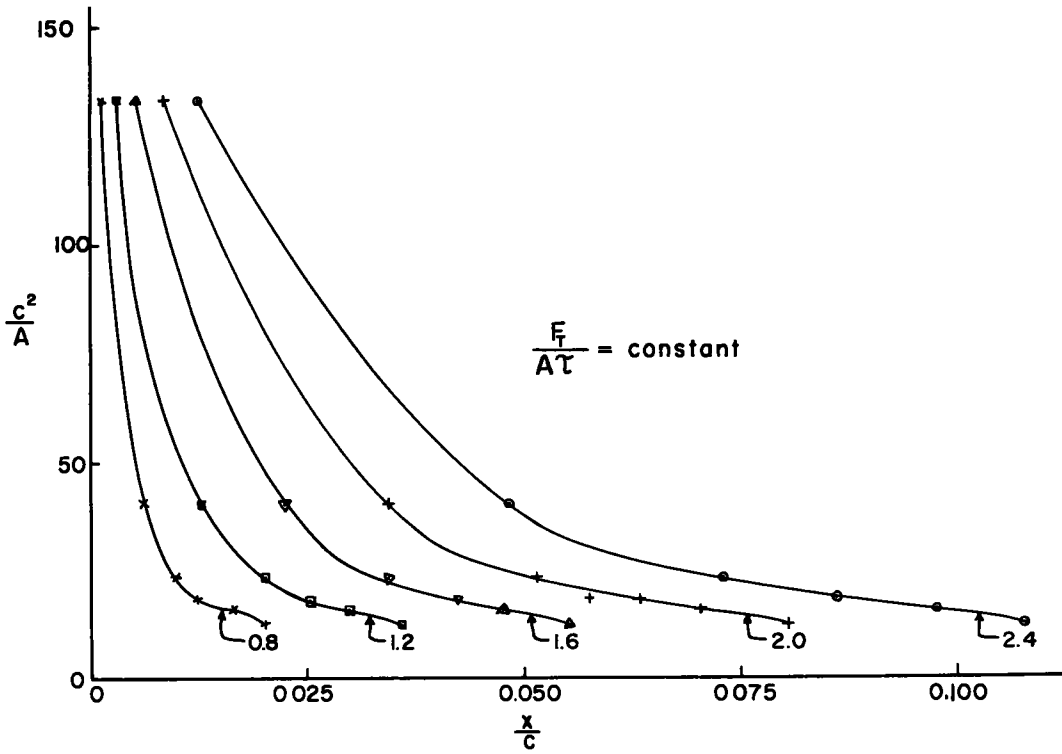Figure 11. Non-dimensional plot of x/c versus c^2/A for constant values of $F_T/A\tau$.

The solution by the Housel method is b = 10 ft and by the non-dimensional method, as previously illustrated, is approximately 10.4 ft. The agreement for this example is also fairly good.

Example C: Proportioning Footings to Prevent Differential Settlement. The foundation designer is frequently required to design spread footings for a structure such that harmful differential settlements are prevented. It is well known that footings of different sizes will settle unequally even though they carry the same unit pressure intensi The following problem is taken from Andersen (1, p. 84) where it is solved by the meth of Kogler and Scheidig.

It is desired to find the square contact areas for three single footings carrying, respectively, 36, 48, and 72 kips. The compressible layer in which the footings are resting extends 6 ft below the contact areas. It is assumed that a square footing of 9 sq ft will be used for the load of 36 kips and the other footings will be proportioned s that the final deflections will be approximately equal for the three loads.

The solutions given by Andersen using the Kogler and Scheidig method are

b = 3 ft for the 36-kip load,
b = 3.66 ft for the 48-kip load, and
b = 4.92 ft for the 72-kip load.

The solution obtained using the non-dimensional method is as follows. Because all three footings are on the same soil and the settlements are to be equal, the soil properties should not affect the solution. The 3-ft by 3-ft footing carrying the 36-kip load will be used in the same manner as the test plates in Examples A and B. Inasmuch a the settlement of the 3-ft by 3-ft footing is unknown, a value may be assumed (for example ½ in.).

$$\frac{x}{c} = \frac{0.5}{144} = 0.00347 \quad \text{and} \quad \frac{F_T}{A\tau} = \frac{36000}{9\tau}$$
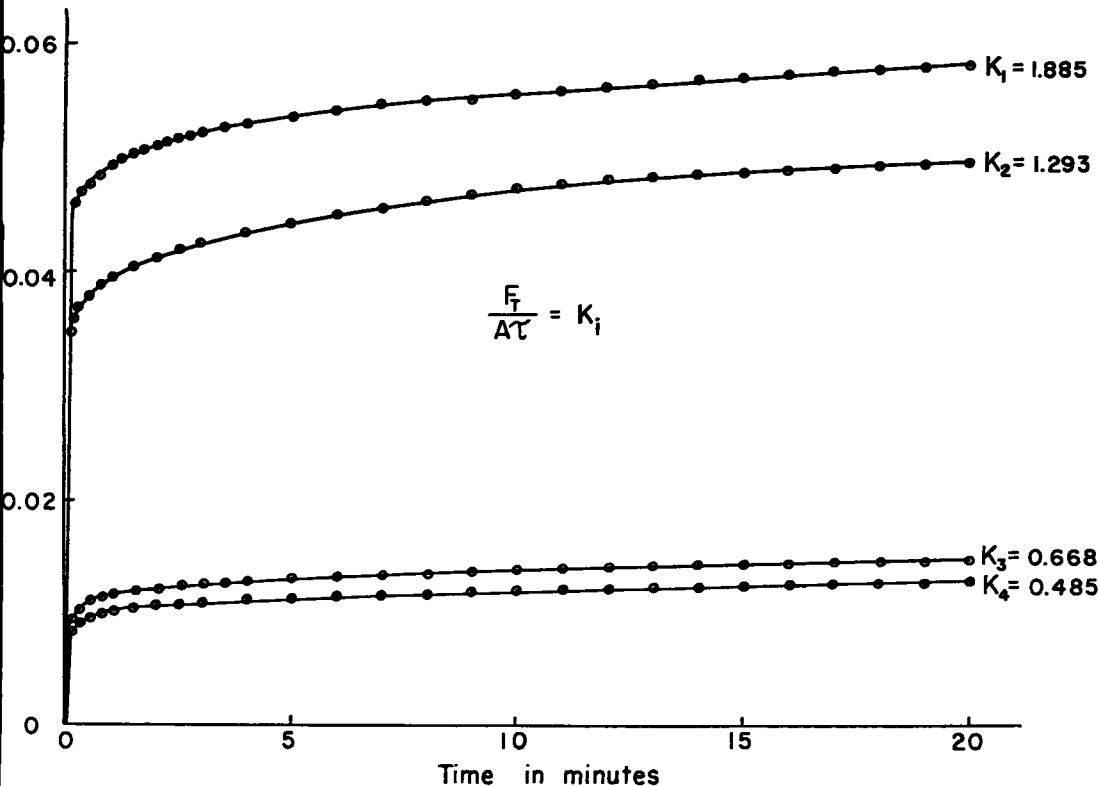
Figure 12. Static creep tests.

For $x/c = 0.00347$ Figure 10-a gives $F_T/A\tau = 0.37$. Following the procedure of illustrative Example A gives for the other two loading conditions

$$\frac{F_T}{A\tau} = \frac{4.45}{b^2} \quad \text{and} \quad \frac{x}{c} = \frac{0.5}{48\,b} \quad \text{for the 48-kip load,}$$

and

$$\frac{F_T}{A\tau} = \frac{6.67}{b^2} \quad \text{and} \quad \frac{x}{c} = \frac{0.5}{48\,b} \quad \text{for the 72-kip load.}$$

These two sets of equations can be solved by trial and error to give

b = 3.58 ft for the 48-kip load, and
b = 4.56 ft for the 72-kip load.

The solutions were repeated using assumed settlements of 1 and 2 in. with the following results:

For an assumed settlement of 1 in., b was equal to 3.58 ft and 4.67 ft for the 48-kip and 72-kip loads, respectively, while b was 3.66 ft and 4.87 ft, respectively, using an assumed settlement of 2 in.

It must be noted that the Kogler and Scheidig method was developed to include the depth of the soil to a rigid ledge. The senior author has not yet extended the non-dimensional method to include this condition although it should be done in the near future. In spite of this difficulty the largest discrepancy (assumed settlement of $\frac{1}{2}$ in. for 72-kip load) was only 7.3 percent. If one considers the location of the 10 percent pressure bulb as a function of the length of the side of the footing and with regard to the depth of
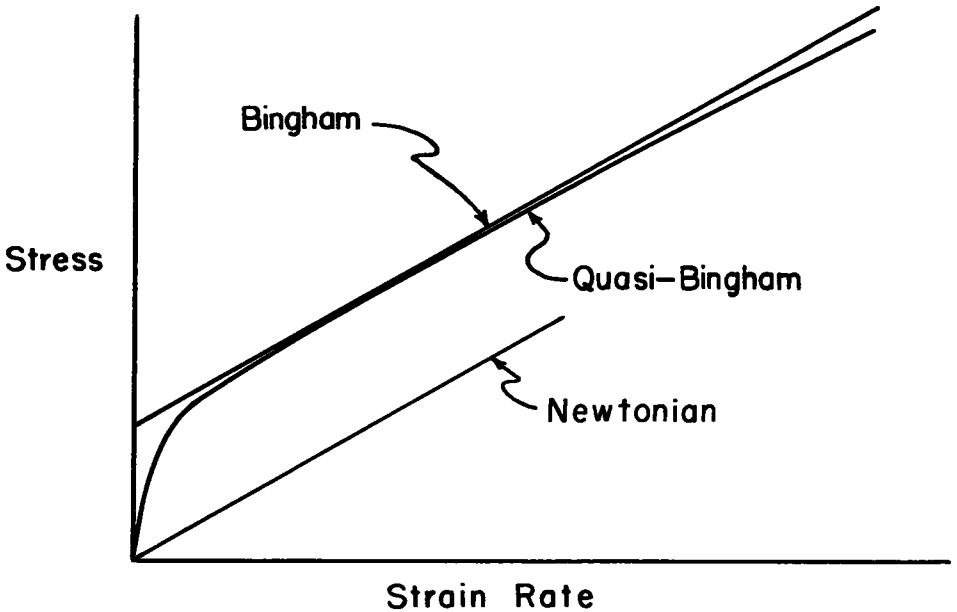
Figure 13. Bingham and quasi-Bingham material.

the soil layer given, such a small percent error is to be expected for the 48-kip load but a somewhat larger error would be expected for the 72-kip load.

Limited Generalizations. — The following are some generalizations obtained from the non-dimensional method.

Non-Linear Case. For a constant cross-sectional shape and a constant value of $F_T/A\tau$ (that is, for a constant applied pressure and the same soil), a constant value of x/c will be obtained regardless of the total load and the cross-sectional area. This does not involve any assumption regarding the linearity of the load versus surface deformation relationship. Therefore, under these conditions

$$\frac{x}{c} = \text{constant} = k .$$

For circular footings

$$\frac{x}{c} = \frac{x_1}{\pi d} = \frac{x_2}{\pi d_2} \qquad \text{or} \qquad \frac{x_1}{x_2} = \frac{d_1}{d_2} \qquad (5)$$

This agrees with observations attributed to Terzaghi by Andersen ($\underline{1}$). For square footings

$$\frac{x}{c} = \text{constant} = k_2 = \frac{x_1}{4\,b_1} = \frac{x_2}{4\,b_2}$$

or

$$\frac{x_1}{x_2} = \frac{b_1}{b_2} \qquad (6)$$
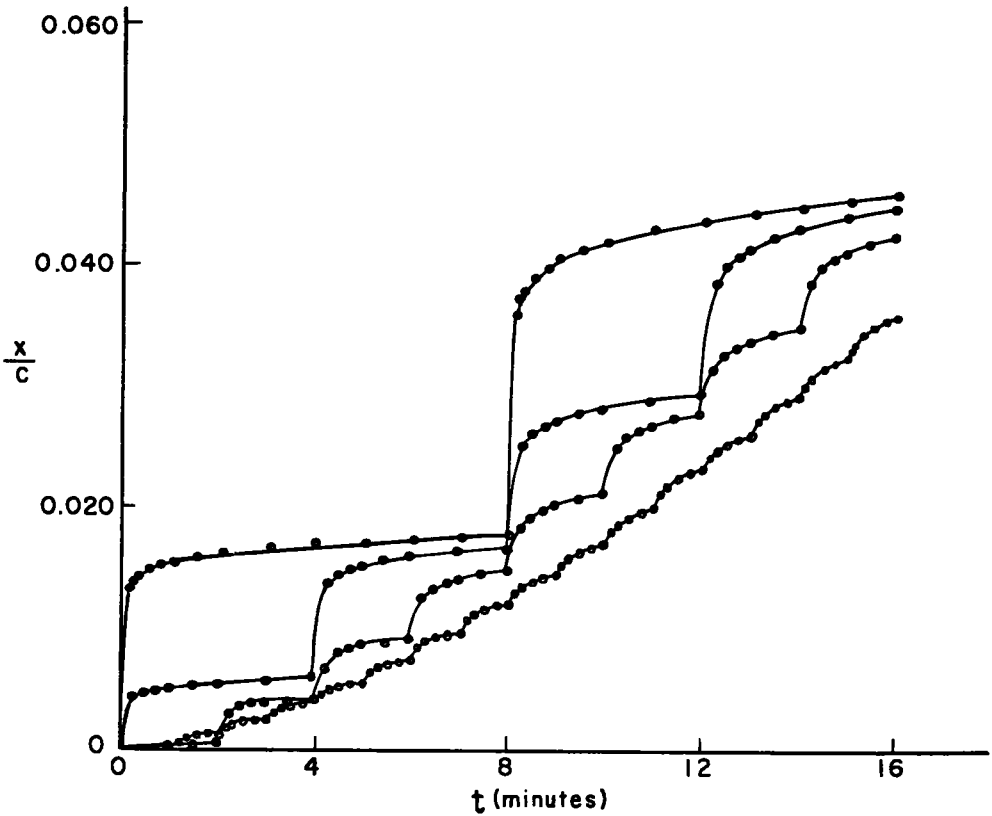
Figure 14. Load history tests.

For rectangular footings

$$\frac{x}{c} = \text{constant} = k_3 = \frac{x_1}{2b_1(1+a)} = \frac{x_2}{2b_2(1+a)}$$

or

$$\frac{x_1}{x_2} = \frac{b_1}{b_2} \tag{7}$$

in which a is the ratio of the length to the width of the footing and is a constant for both footings.

Linear Case. If one assumes an initially linear load versus settlement relationship, as numerous authors do ($\underline{14}$, Fig. 5: 18-b, p. 128), then the relationship for F_T/A_T versus x/c for a constant value of c^2/A can be written as:

$$\frac{\left[\dfrac{F_T}{A_T}\right]_M}{\left[\dfrac{F_T}{A_T}\right]_F} = \frac{\left[\dfrac{x}{c}\right]_M}{\left[\dfrac{x}{c}\right]_F} \tag{8}$$

in which subscripts M and F refer to the model (test plate) and the prototype footing, respectively. Note that for the linear assumption Eq. 8 can be used for any pressure
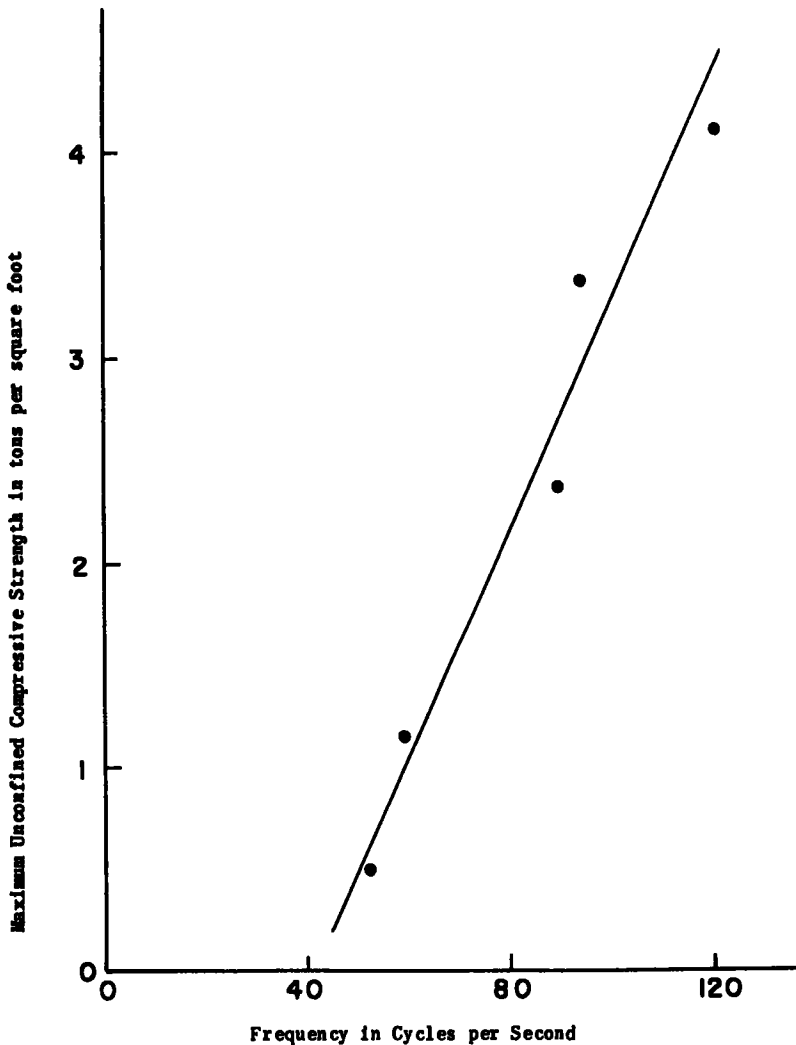
Figure 15. Natural frequency versus unconfined compressive strength.

intensity F_T/A. The validity of the linear assumption is discussed later. For constan pressure F_T/A and $\tau_M = \tau_F$ Eq. 8 reduces to Eqs. 5, 6 and 7 for circular, square, an rectangular footings, respectively. Various forms of Eqs. 5, 6, and 7 are given in th literature; for example, by Sowers and Sowers (14, Eq. 5: 12a, p. 129, and stated in words by others p. 583).

Discussion of Linearity. The following example illustrates some of the possible effects that the linearity assumption can have on the computed settlements.

A load test conducted on a clay with a 2- by 2-ft test plate gave a settlement of $\frac{1}{2}$ in. under a load of 12 kips. Estimate the surface settlement of an 8- by 8-ft rigid foo ing under a load of 128 kips.

It is important to note that the pressure intensities are 3 kips per sq ft and 2 kips per sq ft for the bearing plate and the footing, respectively. A first order approxima solution to this problem (which some people might use) would be to reduce the bearing plate data to that for a pressure intensity of 2 kips per sq ft (the same as that of the footing) by using the assumption of a linear relationship between the load and the surf settlement. Thus, for a pressure intensity of 2 kips per sq ft the bearing plate would
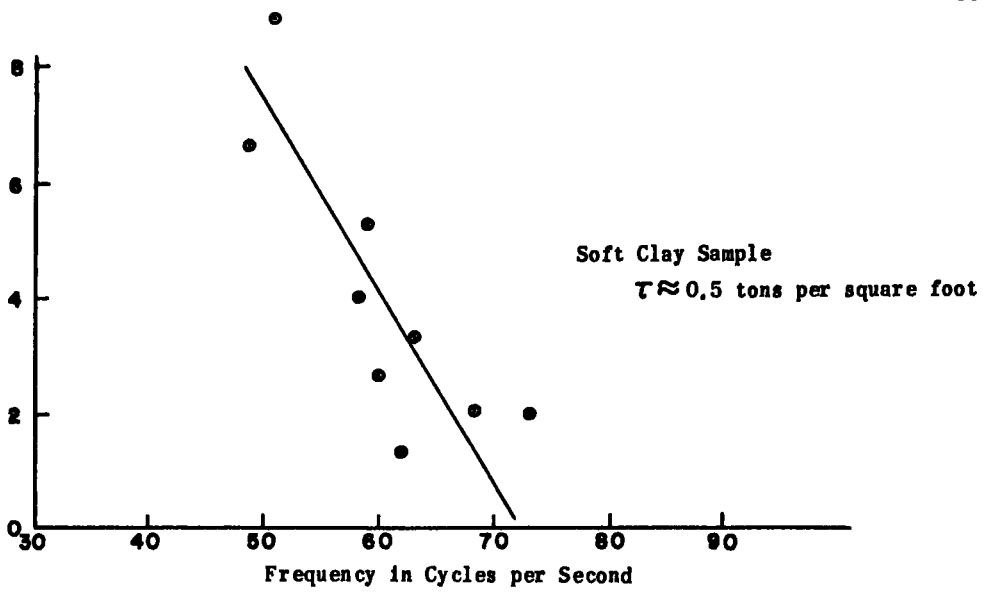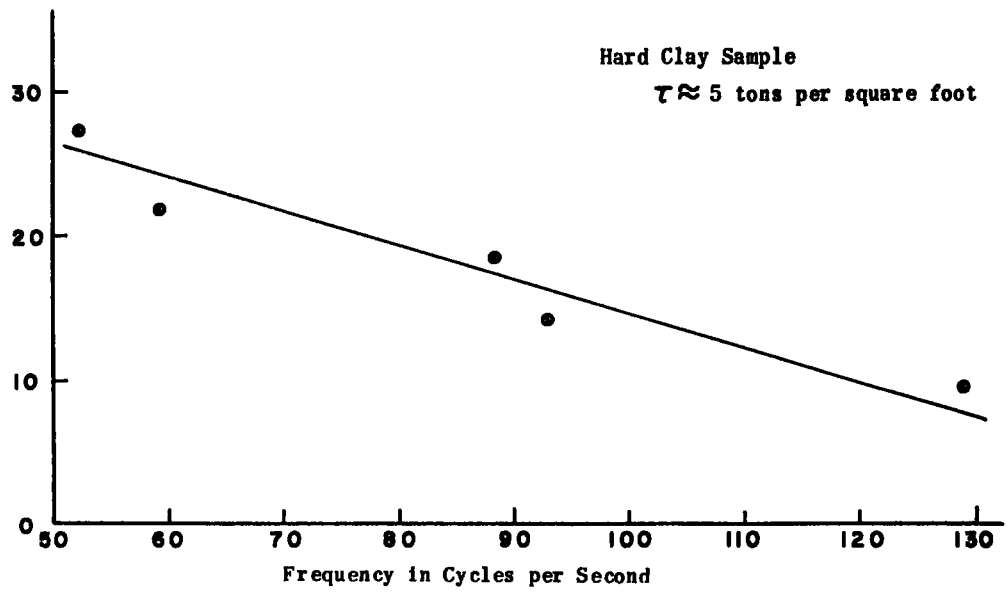
Figure 16. Natural frequency versus contact stress.

be assumed to give a surface settlement of $\frac{1}{3}$ in. Now that the pressure intensities are equal, Eq. 6 ($\underline{14}$, Eq. 5: 12a, p. 129) could be used to obtain a prototype surface settlement of 1.33 in.

With the linear assumption the non-dimensional method as expressed by Eq. 8 gives

$$\frac{\dfrac{12}{4\tau}}{\dfrac{128}{64\tau}} = \frac{\dfrac{0.5}{2 \times 48}}{\dfrac{x}{8 \times 48}}$$

$$x = 1.33 \text{ in.}$$
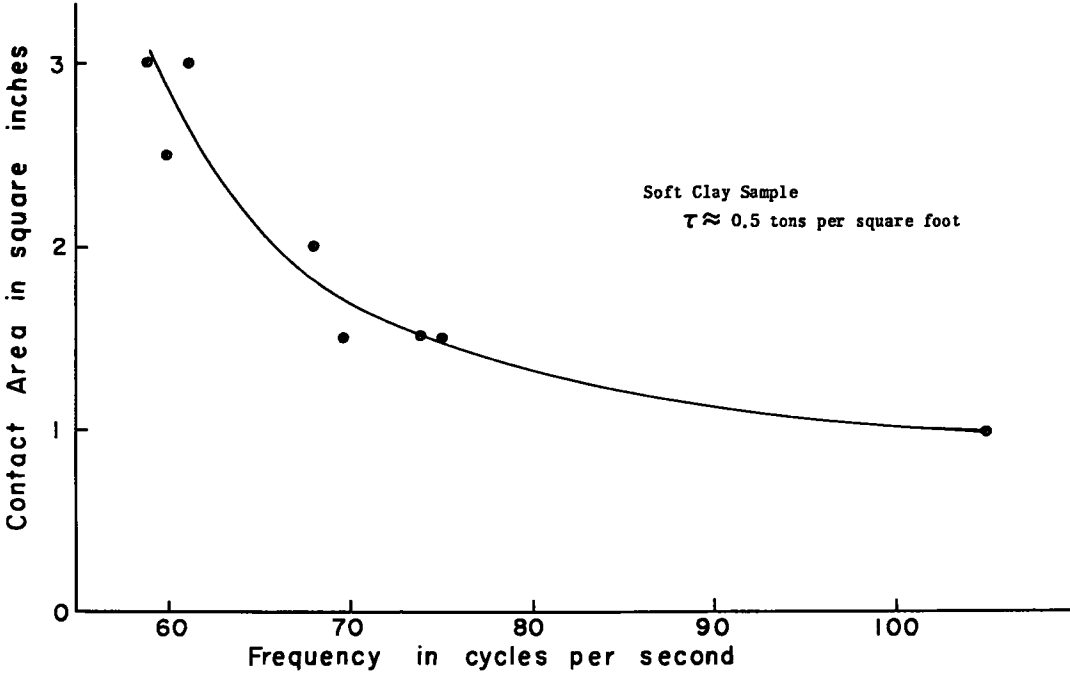
Figure 17. Natural frequency versus cross-sectional area for constant contact stress.

For comparison the same problem will be solved by the non-dimensional method without making the assumption of a linear load versus settlement curve. Neglecting the time effects, Figure 10-a for square footings may be considered to hold for any pressure intensity on a cohesive soil of any unconfined compressive strength.

From the load test data

$$\frac{F_T}{A_\tau} = \frac{12000}{4\tau}$$

and

$$\frac{x}{c} = \frac{0.5}{2 \times 4 \times 12} = 0.00521$$

For a value of $x/c = 0.00521$, Figure 10-a gives

$$\frac{F_T}{A_\tau} = 0.433 = \frac{12000}{4\tau}$$

Substituting for τ in the prototype footing gives

$$\frac{F_T}{A_\tau} = \frac{128000 \times 4 \times 0.433}{64 \times 12000} = 0.2886$$

For

$$\frac{F_T}{A_\tau} = 0.2886$$

Figure 10-a gives

$$\frac{x}{c} = 0.00164$$
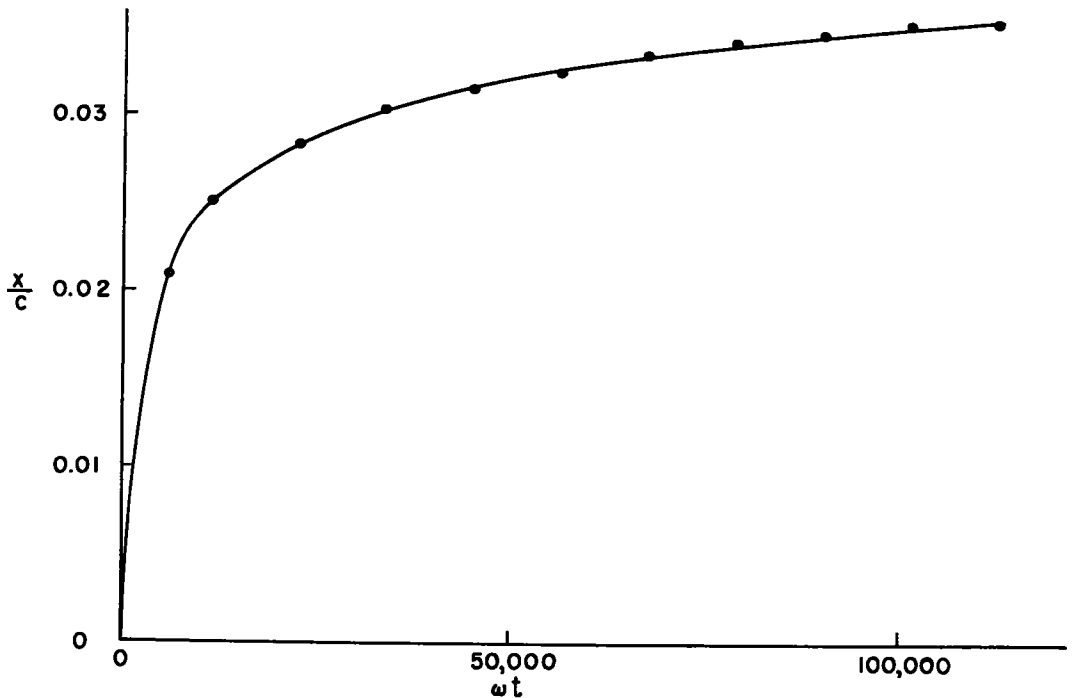
Figure 18. Dynamic creep curve.

Therefore

$$x = 0.00164\,c = 0.00164 \times 4 \times 12 \times 8 = 0.63 \text{ in.}$$

which is only 47.4 percent of the surface settlement estimated with the linear assumption.

The reason for the smaller value of the surface settlement, as given by the non-dimensional data of Figure 10-a, when compared with that obtained for the linear assumption, is as follows. The data from the load test are actually only one point (point Q of Fig. 10-a) on the non-linear curve of F_T/A_T versus x/c. The linear assumption gives a straight line from the origin through point Q. Therefore, for pressure intensities less than that of the load test the surface settlement predicted by Figure 10-a will be less than that obtained with the linear assumption, while for pressure intensities greater than that of the load test, the predicted values will be greater than those for the linear assumption.

Experimental evidence indicates considerable non-linear behavior in cohesive soils. Therefore considerable caution should be exercised in the use of linear approximations and it should be realized that such linear approximations are only valid over a limited range of variables. Such limitations are clearly pointed out in the literature. For example, when writing on loading tests on cohesive soil Terzaghi (16) states "...we always find that the ratio between the settlement and the unit load increases with increasing load." Terzaghi (16) also states, "the increase of the rate of settlement under higher loads is due to the fact that soils do not obey Hooke's law."

Because of the great number of variables involved, numerous authors in the field of soil mechanics have wisely expressed caution in the extrapolation of the results of small-scale loading tests to the surface settlements of prototype footings. The illustrative examples given in this section seem to indicate that the use of non-dimensional parameters obtained with the methods of dimensional analysis provide a rational basis for the transformation from model studies to prototype response. Although the examples given show very good agreement with the methods of Housel, Kogler and Scheidig, and
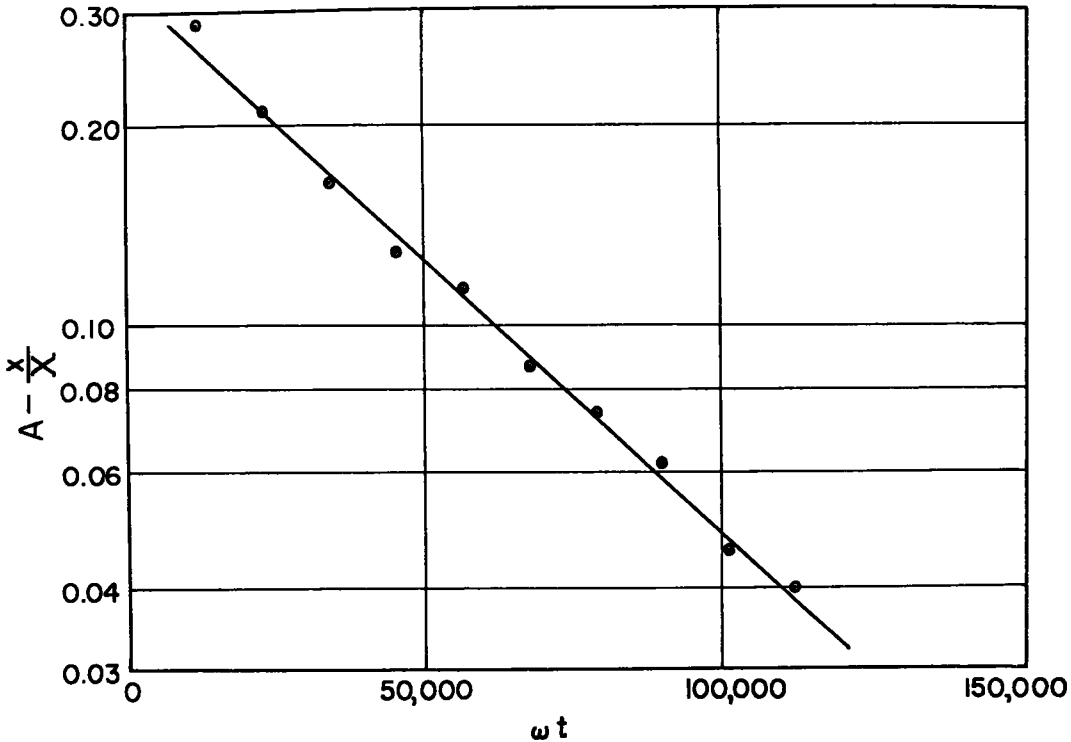
Figure 19. Semi-logarithm fit of dynamic creep data.

with some of the observations of Sowers, Taylor, Terzaghi, Tschebotarioff, Andersen, Peck, Krynine and others, the authors must caution the would-be user that the work reported in this paper is only the initial preliminary part of the study and much research is needed, particularly with regard to viscous effects, before any general quantitative results can be expressed and used with confidence.

Vibratory Tests

The vibratory experimental results presented in this section are of a qualitative nature only and no quantitative conclusions should be drawn until a more extensive research program is conducted.

Natural Frequency Tests. — In the interpretation of the non-dimensional parameters it was noted that the natural frequency of the soil-footing system is primarily a function of the magnitude and configuration of the equipment used and may be entirely different for model and prototype. Although the mechanical resonance of the system is important, the present study is more concerned with the response of vibratory loaded footings due to the basic frequency dependent properties of the soil. As a qualitative indication of field response and as a basis of comparison with the data yet to be given, the following information regarding the mechanical natural frequency is presented. The variation of the natural frequency of a circular footing with a cross-sectional area of 2.5 sq in. under a constant static force for changes in the unconfined compressive strength is given in Figure 15. The natural frequencies were obtained by measuring the free vibrations of the system as a function of time when the footing system was displaced from its equilibrium position by a small impulsive force. For the same soil type the natural frequency increases with an increase in the unconfined compressive strength. Whether, for simplicity, one considers a linear or a non-linear (soft) soil spring characteristic curve, the point value of the spring "constant" will increase with
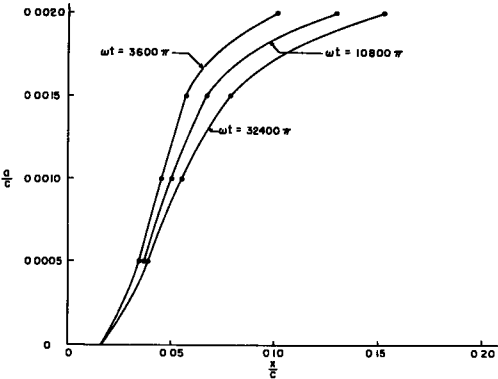
Figure 20. Sinkage parameter versus amplitude of vibration.

an increase in the unconfined compressive strength. Therefore the results of Figure 15 are to be expected. The results also agree with the increase of the compressive modulus with an increase in the compressive strength (11).

Figure 16 shows the variation of the natural frequency under different applied stresses for the same footing used in the foregoing on a hard sample (high τ) and a circular footing having area of 1.5 sq in. on a soft sample.

Figure 17 shows the variation of the natural frequency with the cross-sectional area of the footing for constant soil contact pressures on the same soil. The natural frequency decreases as the contact area increases. This agrees with the results given by Tschebotarioff (18). Although the results of Figures 16 and 17 seem to indicate a reduction in natural frequency because of an increase in the total oscillating mass, the possibility also exists that the effective spring characteristics of the soil are non-linear and also changing. Much additional research is required before any definite conclusions can be made regarding the aforementioned variations.

In addition to these results, it was found that the size of the bin used to hold the soil for the model footing tests can affect the value of the natural frequency.

Time Effects. — Figure 18 is a typical curve of x/c versus ωt and is actually a dynamic creep test. Note the similarity between Figure 18 and the shape of curves in Figure 12. The most consistent fit of such data was obtained by plotting log (a - x/X) versus ωt, as shown in Figure 19, where X is the ultimate sinkage and A is a constant. Inasmuch as the resultant curve is approximately a straight line, the sinkage can be expressed in the form

$$x = X (A - Be^{-2.3 S \omega t}) \tag{9}$$

where B and S are the intercept and slope of the curve. For a controlled set of tests it may be possible to get A, B, S and X as functions of the other π terms. To date such an ambitious test program has not been conducted.
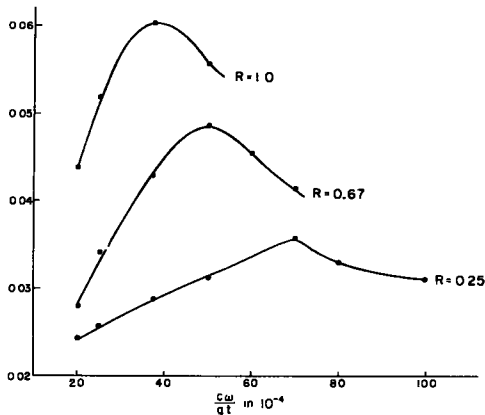
Figure 21. Sinkage parameter versus frequency parameter.

Figure 22. Sinkage ratio versus frequency parameter.
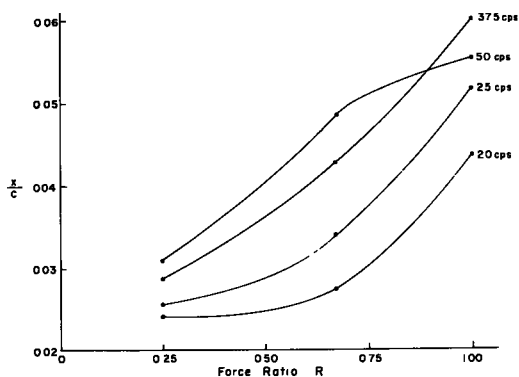
Figure 23. Sinkage parameter versus force ratio.
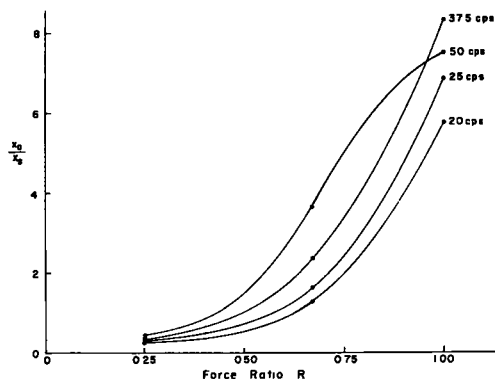
Figure 24. Sinkage ratio versus force ratio.

Amplitude Effects. — Figure 20 shows the variation of sinkage as a function of the amplitude of vibration for the same footing, static contact pressure and soil with a constant frequency of vibration at various values of ωt. The exponential increase in sinkage as a function of the amplitude agrees with the results obtained by the senior author, Kondner (11), for the vibratory unconfined compression testing of the soil being used. It must be remembered that the results of such a non-dimensional plot will change with variations in soil type and strength characteristics, frequency of vibration and magnitude of the stress level about which the stress perturbations are taking place.

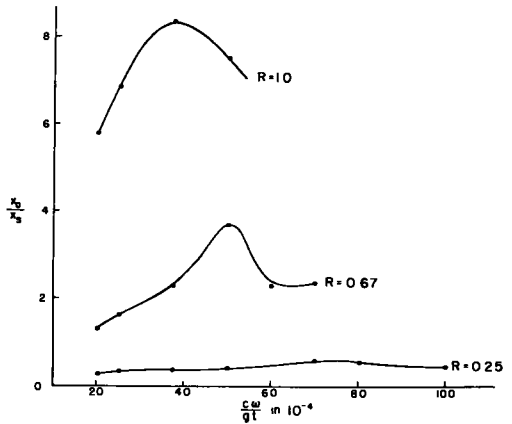**Frequency and Force Ratio Effects.** — The variation of the sinkage parameter (x/c) as a function of the frequency parameter $(c\,\omega/gt)$ is presented in Figure 21 for differen values of the force ratio R. The force ratio is the ratio of the dynamic to static contact stresses and its relation to the π_4 term is given by Eq. 1. These results were obtained on a soft sample with a footing having a cross-sectional area of 1.5 sq in. The total force (static plus maximum dynamic force amplitude) was kept constant for these tests. As a basis of comparison the natural frequencies of the footing for the various static stress levels used in the experiments were found by the free vibration method to be 63, 57, and 58 cycles per second for values of R = 1.0, 0.67, and 0.25, respectively. Figure 22 is a plot of the ratio of the dynamic sinkage to the static sinkage x_D/x_S as a function of the frequency parameter for constant force (stress) ratios. The variation of x/c and x_D/x_S as functions of the force ratio for various values of the frequency are presented in Figures 23 and 24. These figures show that the sinkage parameter, frequency term and the force ratio are all interrelated. Figure 21 shows a decrease in the frequency of the peak response for an increase in the force ratio while the natural frequency data show there should have been a slight increase in the peak response frequency. Thus, the influence of the amplitude of the dynamic force on the peak response is an indication of non-linear spring and damping characteristics.

The non-linearity seems to increase with an increase in the magnitude of the dynam force amplitude. When related to spring characteristics this indicates a "soft spring" response. This agrees with the results of the senior author's recent work on the dyna mic viscoelastic properties of the soil in question (11).

Figures 21 through 24 show that the dynamic sinkage is not necessarily a mechanic resonance phenomenon but may also be a function of the frequency and stress level de pendence of the soil properties. Although in many cases it is difficult to separate thei effects, it is believed that the frequency and stress level dependence is more importa in some cases than the mechanical resonance. Because of the limited power output of the vibratory apparatus currently being used, a wider range of force ratios and fre quencies could not be studied.

FAILURE MECHANISM

The failure mechanism involved in the vibratory sinkage of rigid footings on homo

geneous, cohesive soils is similar to that given by the senior author for the vibratory penetration of soils (12).

CONCLUSIONS

The method of dimensional analysis forms a rational basis for investigating the sinkage (surface settlement) of rigid footings on homogeneous cohesive soils under static and vibratory loads. Such a basis greatly enhances the transformation from model studies to prototype phenomena by avoiding the difficult task of model analysis.

Illustrative practical static problems have been solved using the non-dimensional method and the results were in very good agreement with the methods of analysis of Housel, Kogler and Scheidig and with some of the published observations of Sowers, Taylor, Terzaghi, Tschebotarioff, Andersen, Krynine and others.

Thus, the illustrative examples and the non-dimensional analysis of reported field data indicate that the static sinkage of rigid footings on homogeneous soils can be accurately predicted from x/c versus $F_T/A\tau$ relations as functions of c^2/A, regardless of the combination of total applied force, shape of footing and unconfined compression strength of the soil. The accuracy of the method seems to be somewhat affected by viscous time effects. These viscous effects seem to be not only a function of the soil considered, but also a function of the stress level applied to the soil. An extension of some of the tests reported, in conjunction with other rheological experiments, might possibly be used to obtain quantitative information about such phenomena.

The influence of the cross-sectional shape of the footing seems to be adequately taken into account in the non-dimensional method by the parameter c^2/A, where c is the perimeter and A the cross-sectional area of the footing. Some generalizations for relating the surface settlement and the size of footing have been obtained from the non-dimensional method and found to agree with those given by numerous authors. The senior author intends to extend the present study to include the effects of stratification, eccentricity of loading, friction between the footing and the soil, single impulse loading, and the influence of a rigid ledge below the soil mass for both cohesionless and cohesive soils. It is felt that these difficult conditions can also be handled with the methods of dimensional analysis.

The vibratory sinkage of footings is not only a function of the shape of the footing but also a function of the amplitude and frequency of vibration, the ratio of the dynamic stress to the static stress applied, and the dynamic viscosity of the soil. Although the natural frequency of the soil-footing system is important, considerable sinkage can be obtained at frequencies other than the mechanical resonance. Such response is believed to be due to the frequency and stress level dependence of soil properties. Thus, the sinkage of footings under vibratory loading is a highly non-linear problem and considerable investigation is needed before accurate predictions of field response can be made.

There is a necessity in the field of soil mechanics for more coordinated, comprehensive investigations of the rheological properties of soils both statically and dynamically. A systematic investigation should be conducted to determine the effects of moisture content, grain size distribution, mineral content, and nature of the pore water on the elasticity, anelasticity, creep and stress relaxation spectra, recovery behavior and dynamic frequency response of both cohesive and non-cohesive soils. Such studies will indoubtedly lead to a better understanding of stress-strain-time effects and hence to more rational solutions to many of the problems facing the field of soil mechanics.

REFERENCES

Andersen, P., "Substructure Analysis and Design." Ronald Press, New York, N.Y. (1948).

2. Ayre, R. S., and Kondner, R. L., "Laboratory Apparatus for Vibratory Cutting and Penetration of Soils, Preliminary Development." Technical Report No. 1 by The Johns Hopkins University to U. S. Army, Corps of Engineers, Waterways Experiment Station (Dec. 1957).

3. Ayre, R. S., and Konder, R. L., "Cutting and Penetration of Soils under Vibratory Loading: A Progress Report." HRB Proc., 37:506-516 (1958).

4. Benkelman, A. C., and Williams, S., "A Cooperative Study of Structural Design of Nonrigid Pavements." HRB Special Report 46 (1959).

5. Benkelman, A. C., and Olmstead, F. R., "A Cooperative Study of Structural Design of Nonrigid Pavements." Public Roads, 25: 2 (Dec. 1947).

6. Cowin, S. C., Kondner, R. L., and Ayre, R. S., "Bibliography Relating to Vibratory Cutting, Penetration and Compaction of Soils." Technical Report No. 2, by The Johns Hopkins University to U. S. Army, Corps of Engineers, Waterways Experiment Station (Jan. 1958).

7. Cowin, S. C., Kondner, R. L., and Ayre, R. S., "Bibliography Relating to Vibratory Cutting, Penetration and Compaction of Soils." (Supplement No. 1), Technical Report No. 3 by The Johns Hopkins University to U. S. Army, Corps of Engineers, Waterways Experiment Station (Feb. 1958).

8. Cowin, S. C., Kondner, R. L., and Ayre, R. S., "A Critical Review of Selected Literature Relating to the Vibratory Cutting, Penetration and Compaction of Soils." Technical Report No. 4 by The Johns Hopkins University to U. S. Army, Corps of Engineers, Waterways Experiment Station (April 1958).

9. Kondner, R. L., Ayre, R. S., and Chae, Y. S., "Laboratory Investigation of the Vibratory Cutting and Penetration of Soils (Part I)." Technical Report No. 5, by The Johns Hopkins University to U. S. Army, Corps of Engineers, Waterways Experiment Station (June 1958).

10. Kondner, R. L., and Ayre, R. S., "Study of Vibratory Cutting, Penetration and Compaction of Soils." Technical Report No. 6 by The Johns Hopkins University to U. S. Army, Corps of Engineers, Waterways Experiment Station (June 1958).

11. Kondner, R. L., "The Vibratory Cutting, Compaction and Penetration of Soils." Technical Report No. 7 by The Johns Hopkins University to U. S. Army, Corps of Engineers, Waterways Experiment Station (July 1959).

12. Kondner, R. L., and Edwards, R. J., "The Static and Vibratory Cutting and Penetration of Soils." HRB Proc., 39:583-604 (1960).

13. Krynine, D. P., "Soil Mechanics." McGraw-Hill, New York (1947).

14. Sowers, G. B., and Sowers, G. F., "Introductory Soil Mechanics and Foundations." Macmillan Co., New York (1951).

15. Taylor, D. W., "Fundamentals of Soil Mechanics." John Wiley, Chapter 19 (1948).

16. Terzaghi, K., "Theoretical Soil Mechanics," John Wiley and Sons, p. 401, New York (1943).

17. Terzaghi, K., and Peck, R. B., "Soil Mechanics in Engineering Practice." John Wiley and Sons, New York (1948).

18. Tschebotarioff, G. P., "Soil Mechanics, Foundations, and Earth Structures." McGraw-Hill, Chapters 9 and 18 (1951).

Stresses Under Circular Flexible Foundations

H. S. GILLETTE, Soils Engineer, Fort Worth, Texas

This paper outlines a new simple, and convenient method of
computing stresses underneath uniformly loaded flexible
circular foundation of a definite given radius: (a) along the
vertical axis underneath the circular surface flexible founda-
tion; and (b) along horizontal plane at any outward distance
from the vertical axis at right angles to it, and parallel to
the horizontal plane surface boundary.

● EMPLOYING the geometrical dimensions outlined in Figure 1, and the original pre-
limenary assumptions of Boussinesq (1) for point loads, Love (2) developed the basic
differential equations for the deflections and stresses beneath uniformly loaded flexible
circular surface foundations. To use these differential equations conveniently in practi-

$\overparen{\omega \omega}$ = omega-omega

$\overparen{\rho \rho}$ = rho-rho

$\overparen{ZZ}$ = zee-zee
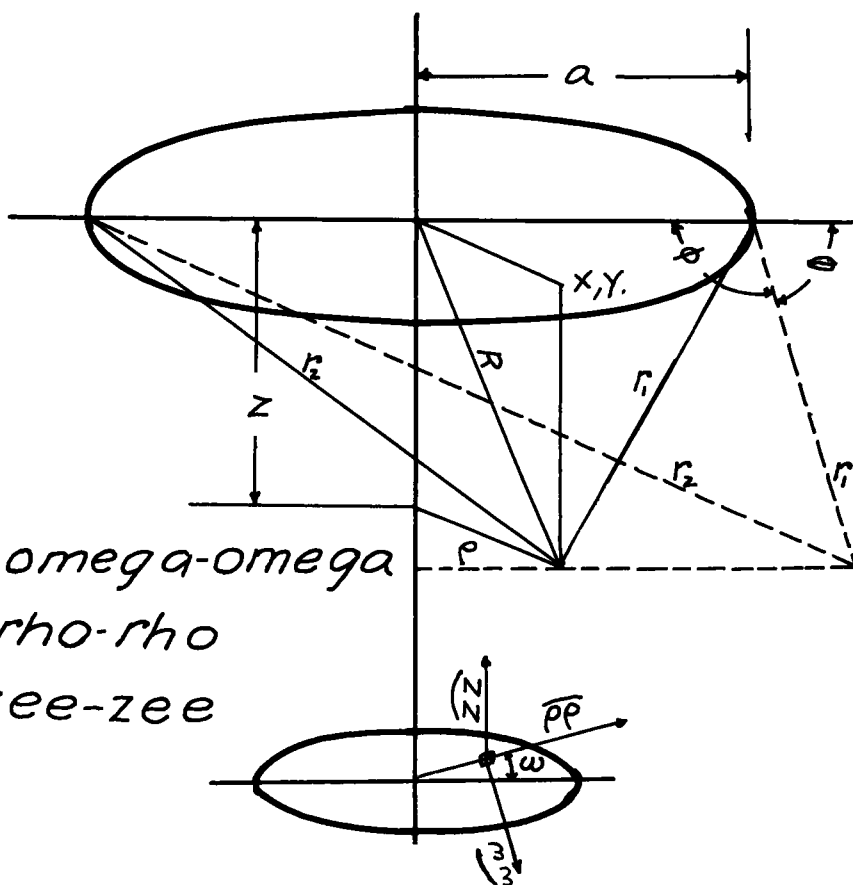
Figure 1. Geometrical dimensions used to develop theoretical stresses underneath a
circular area.

cal foundation design problems Tufts (3), employing eliptic integral tables, developed "influ ence values" (that is, expressing the differential equations in terms of dimensionless ratio the quantities being dimensions that can be measured from a load plan). In this form the righthand member of the equation can be solved for various values of the dimensionless ratios. These influence value tables are set forth in the Appendix.

With the aid of these influence tables in the Appendix the author drew up quickly and easily the stress contour curves outlined in Figures 2 to 16 for a flexible surface foun- dation of radius A and a definite uniform surface loading in pounds per square inch or square foot. These stress contour curves are self explanatory.

For purposes of this paper, the following nomenclature or symbols have been adopted:

a = radius of circular loaded area;
p = unit vertical pressure on loaded area;
z, ω, ρ = cylindrical coordinates (Fig. 1);
$\widehat{zz}$ = vertical normal stress;
$\widehat{\rho\rho}$ = radial normal stress;
$\widehat{\omega\omega}$ = tangential normal stress;
$\widehat{\rho z}$ = shear stress in the ρz plane;
T_I = major principal stress;
T_{II} = minor principal stress;
S = stress difference = $T_I - T_{II}$;
s = maximum shearing stress = $\frac{1}{2} S$; and
μ or σ = Poisson's ratio.

Attention is directed to the fact that the value of Poisson's ratio (μ) does not affect the stresses acting vertically but does cause stress variations in all stresses acting at an angle with the vertical.

The vertical stress contours have been found to be of considerable value in the design of flexible base courses for bituminous surfaces.
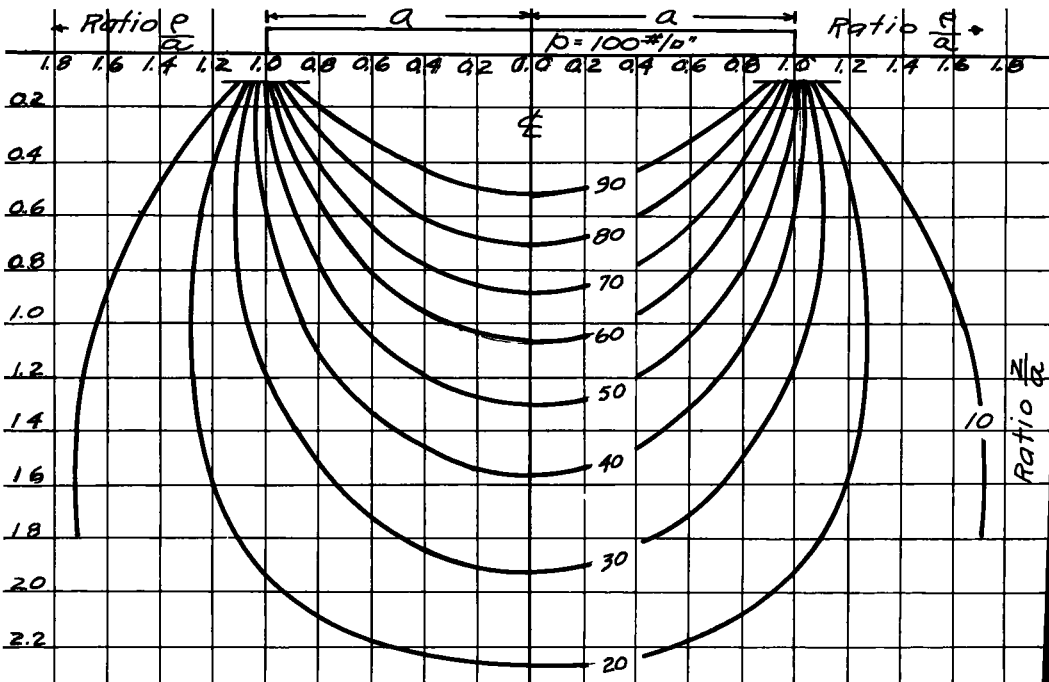
Figure 2. $\widehat{zz} = p_z$ contours of stress.
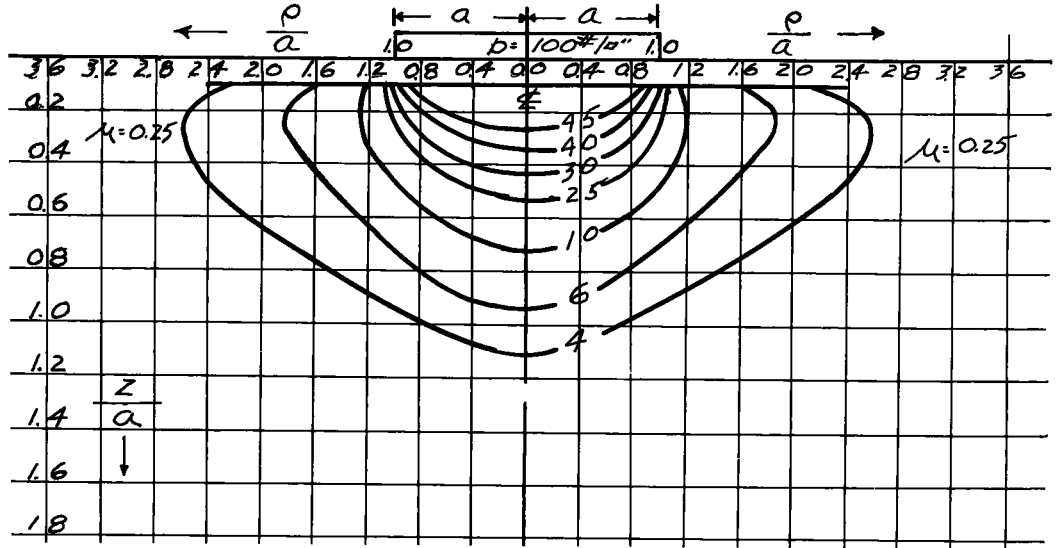
Figure 3. Tangential $\widehat{\omega\omega}$ stress contours.
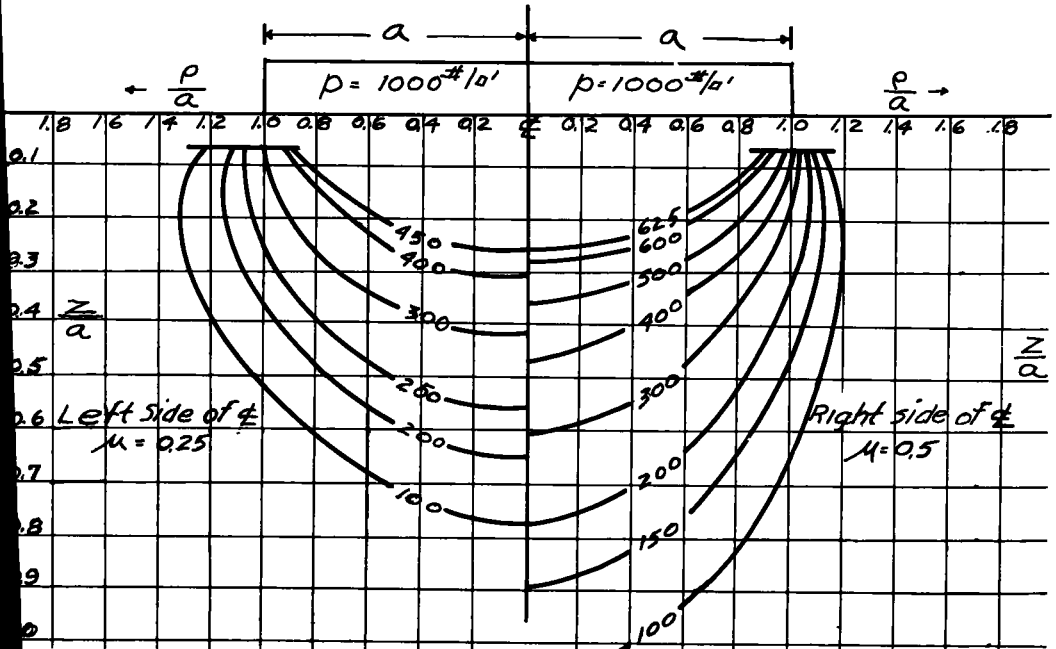
Figure 4. Tangential $\widehat{\omega\omega}$ stress contours.

64
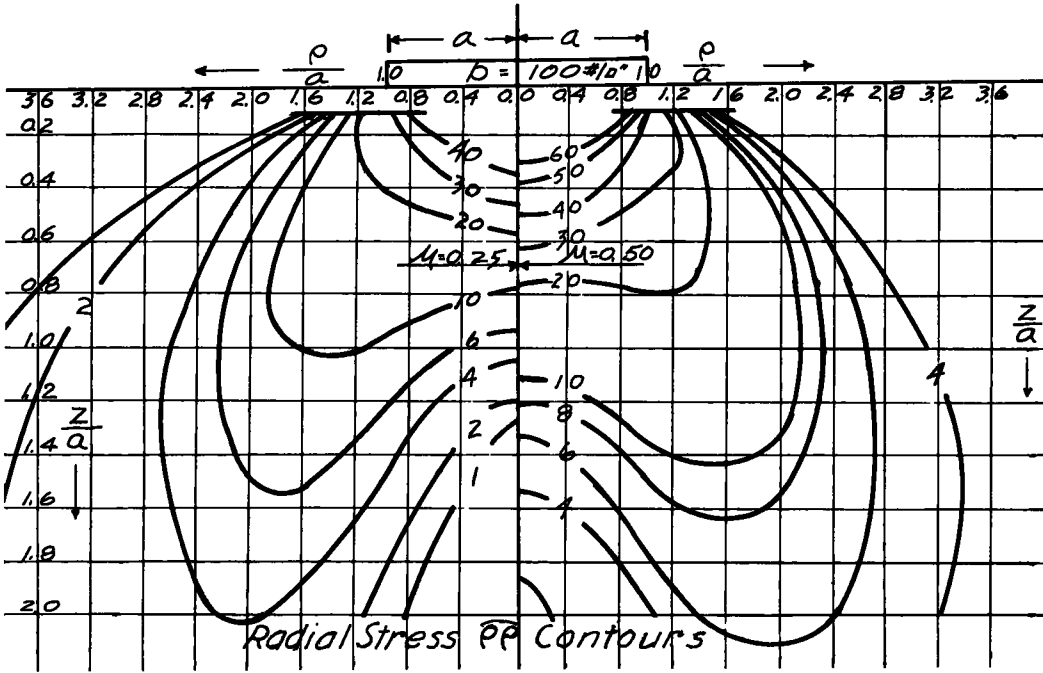
Figure 5.   Radial stress $\widehat{\rho\rho}$ contours.
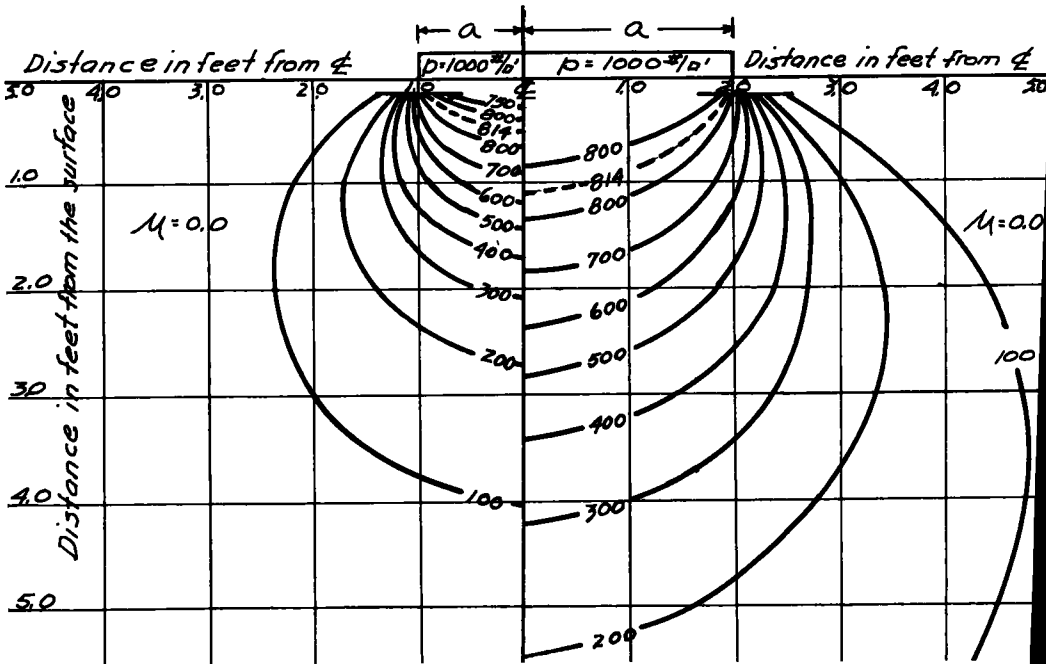
Figure 6.   Stress-difference (S) contours.
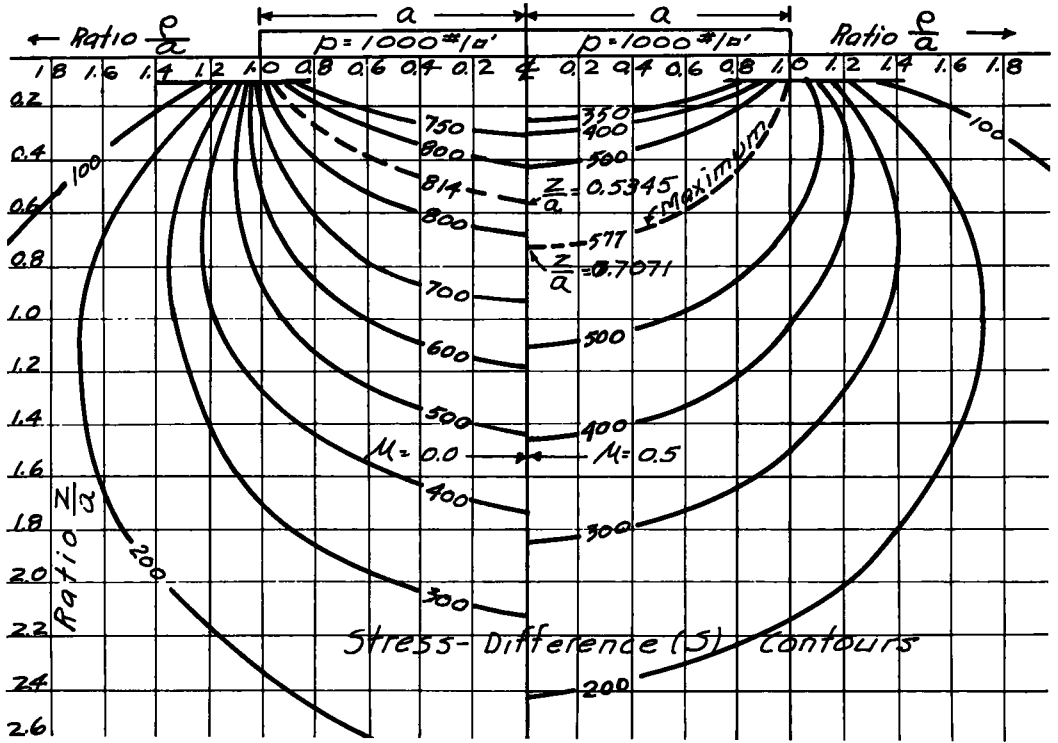
Figure 7. Stress-difference (S) contours.
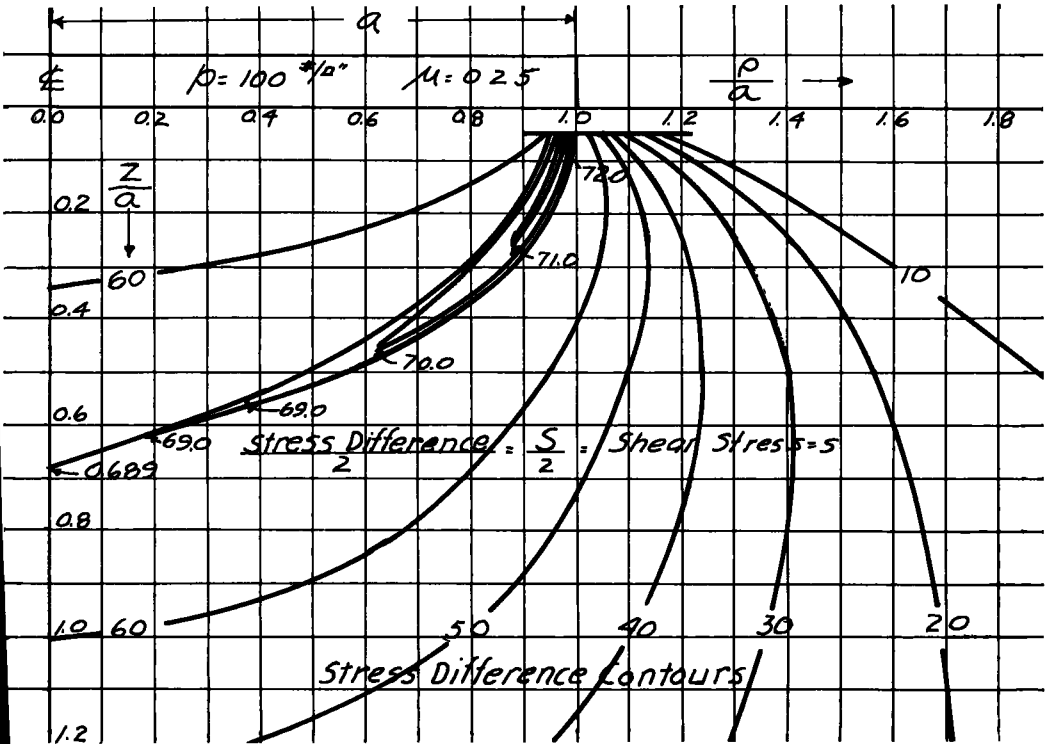
Figure 8. Stress-difference contours.
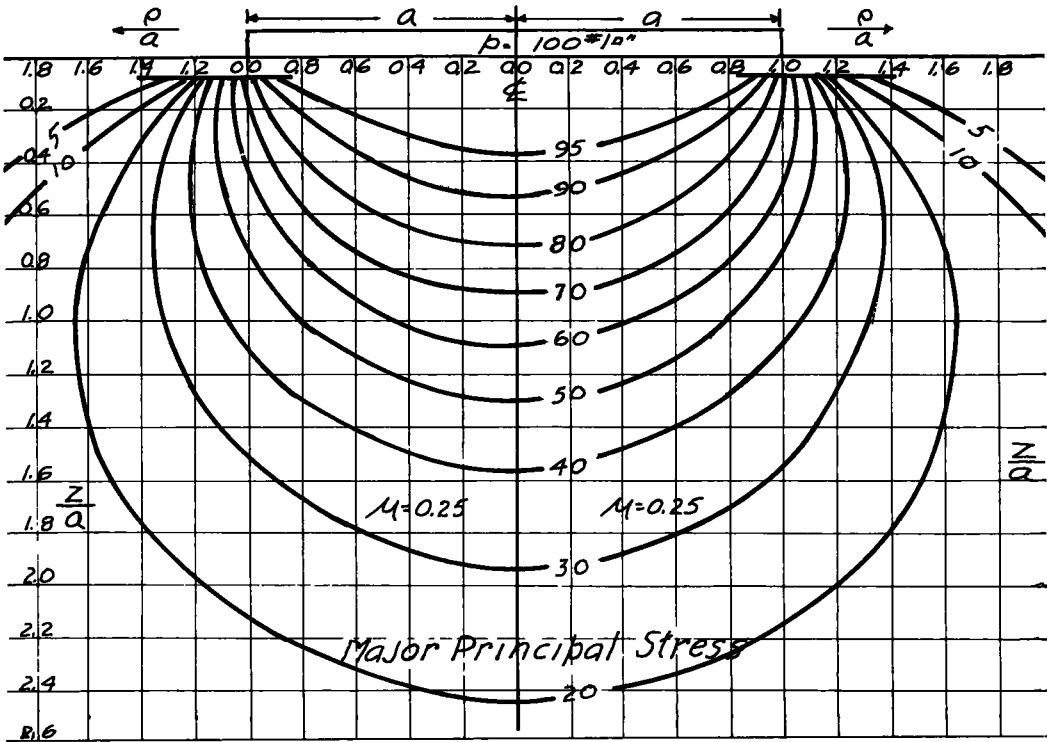
Figure 9. Major principal stress.
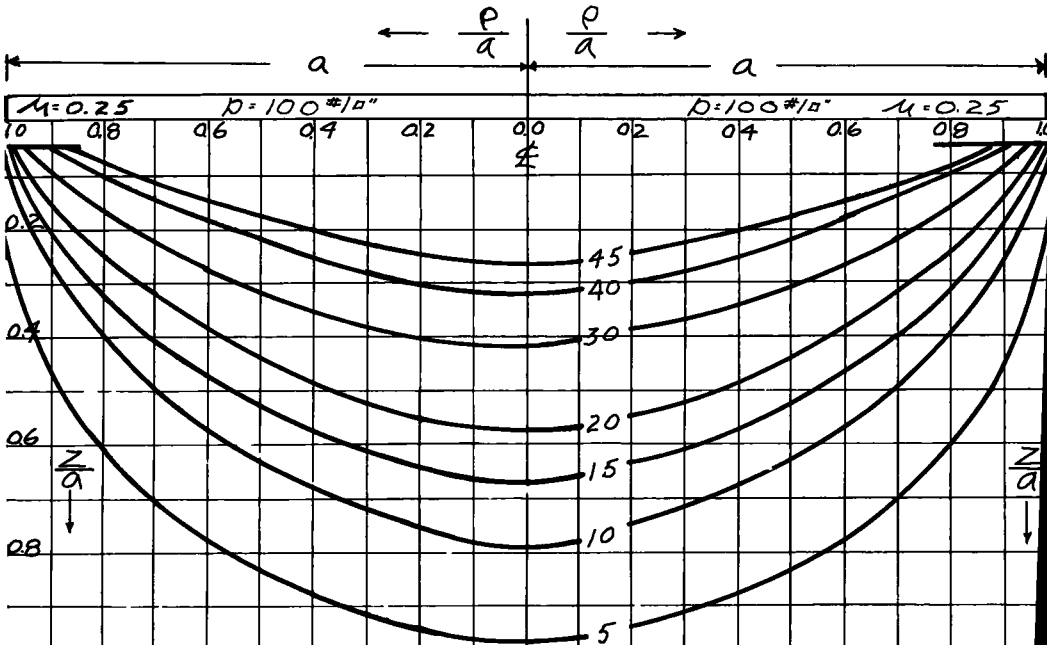
Figure 10. Minor principal stress contours.
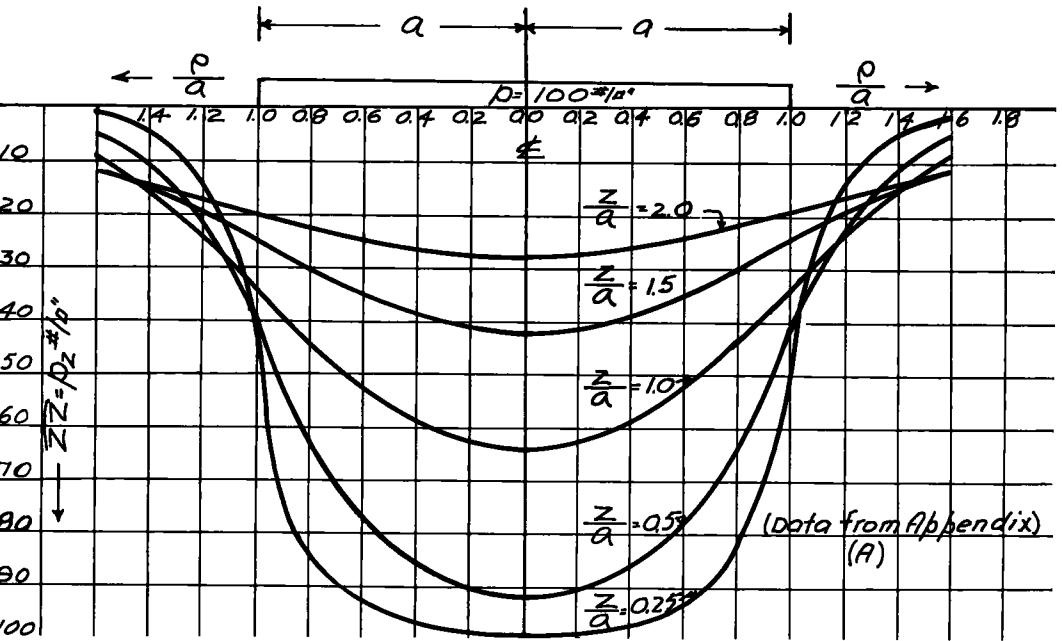
Figure 11. Vertical stress $\widehat{zz} = p_z$.
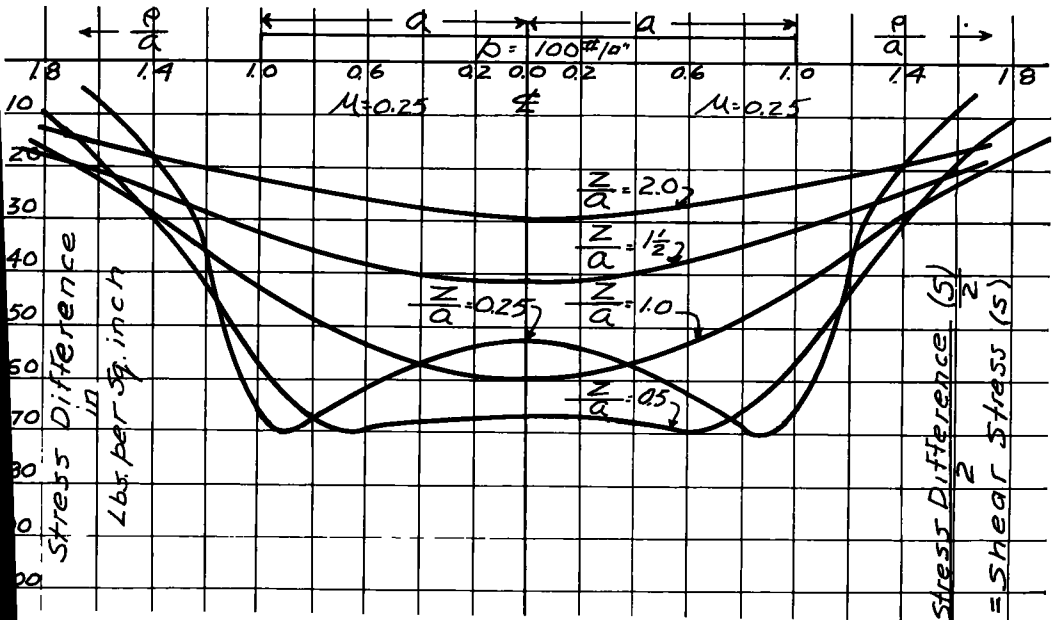
Figure 12. Stress difference (S) and shear curves = $\dfrac{S}{z}$ = s.

68
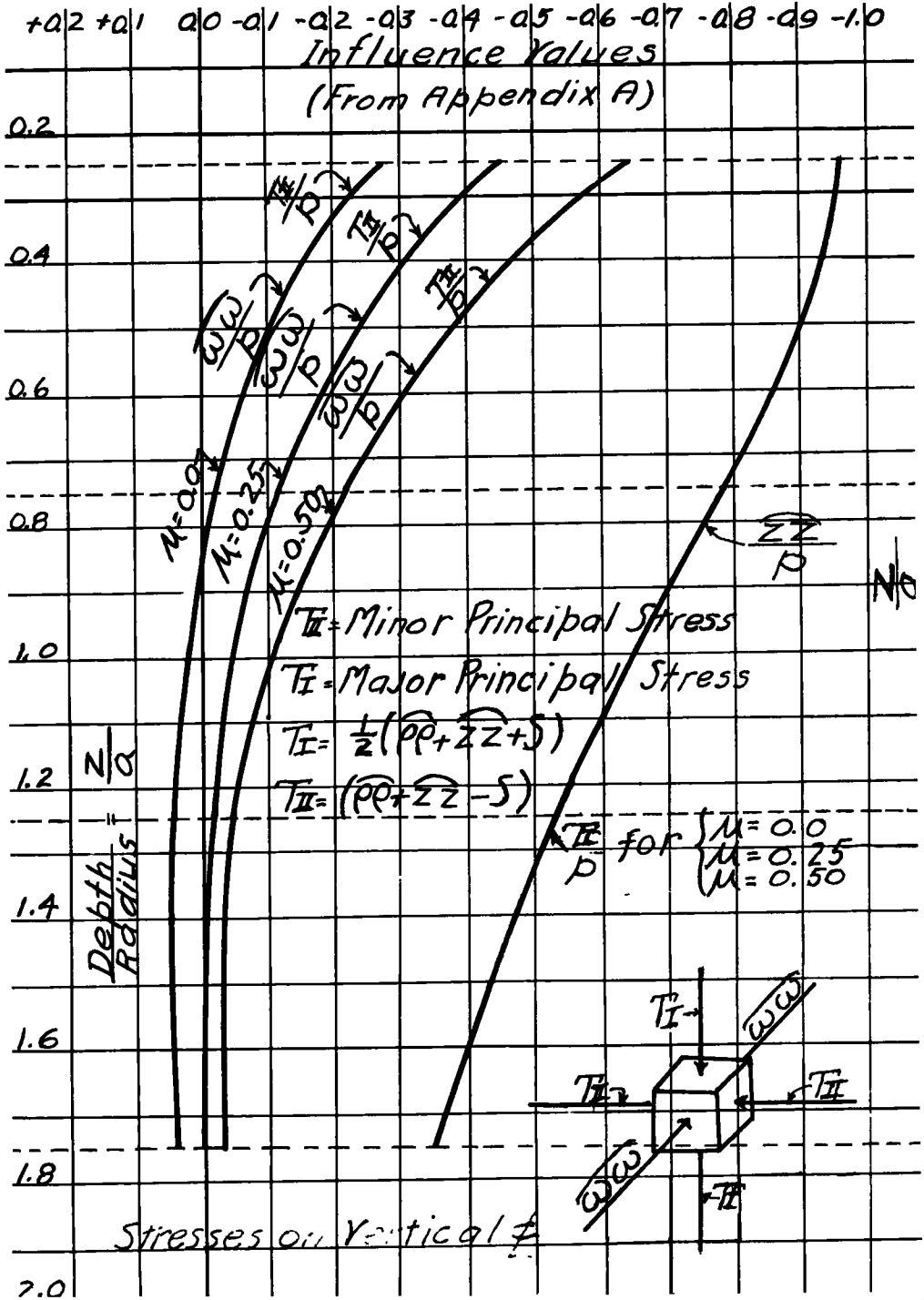
Figure 13. Stresses on vertical centerline.
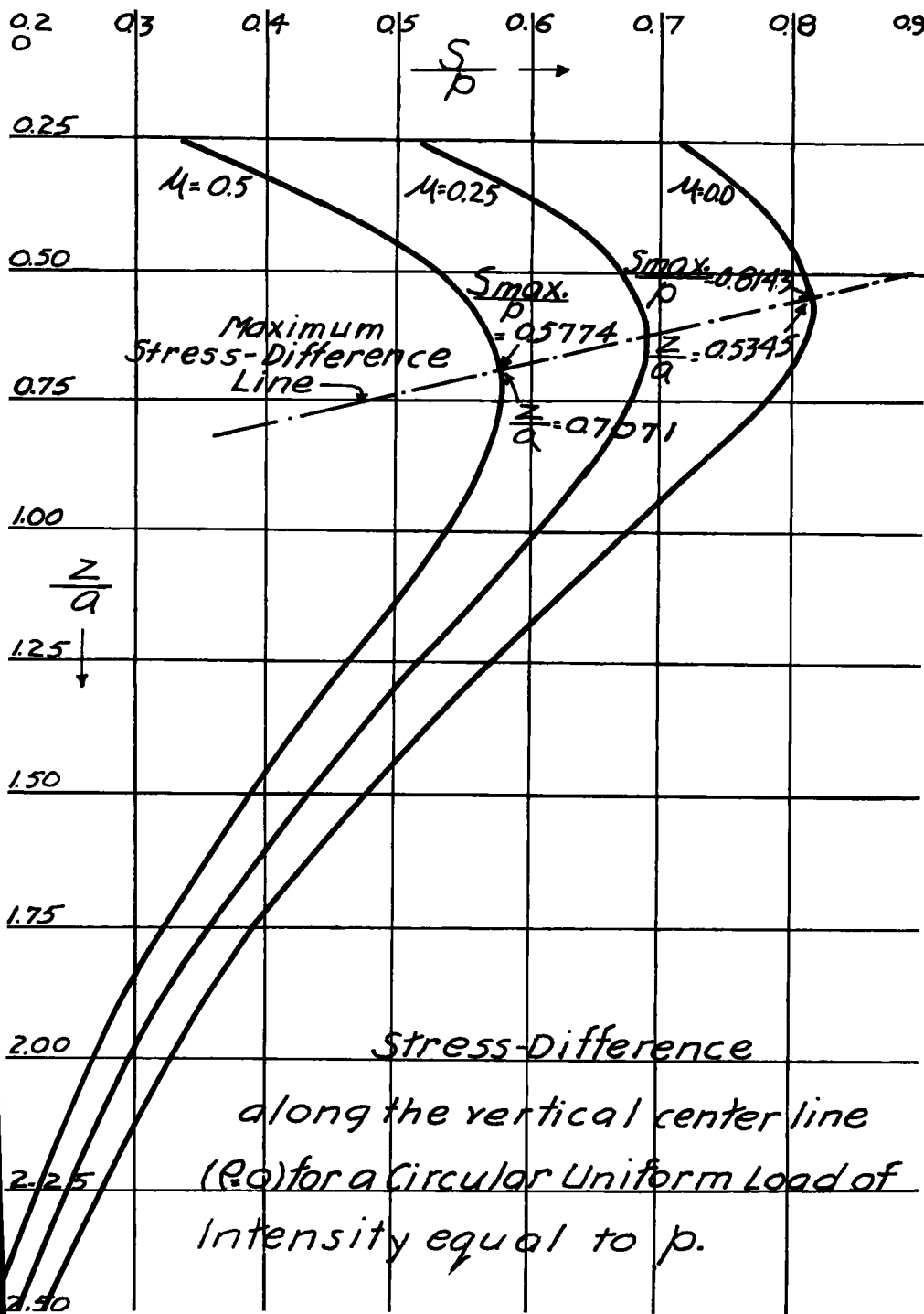
Figure 14. Stress-difference along the vertical centerline ($\rho = 0$) for a circular uniform load of intensity equal to p.
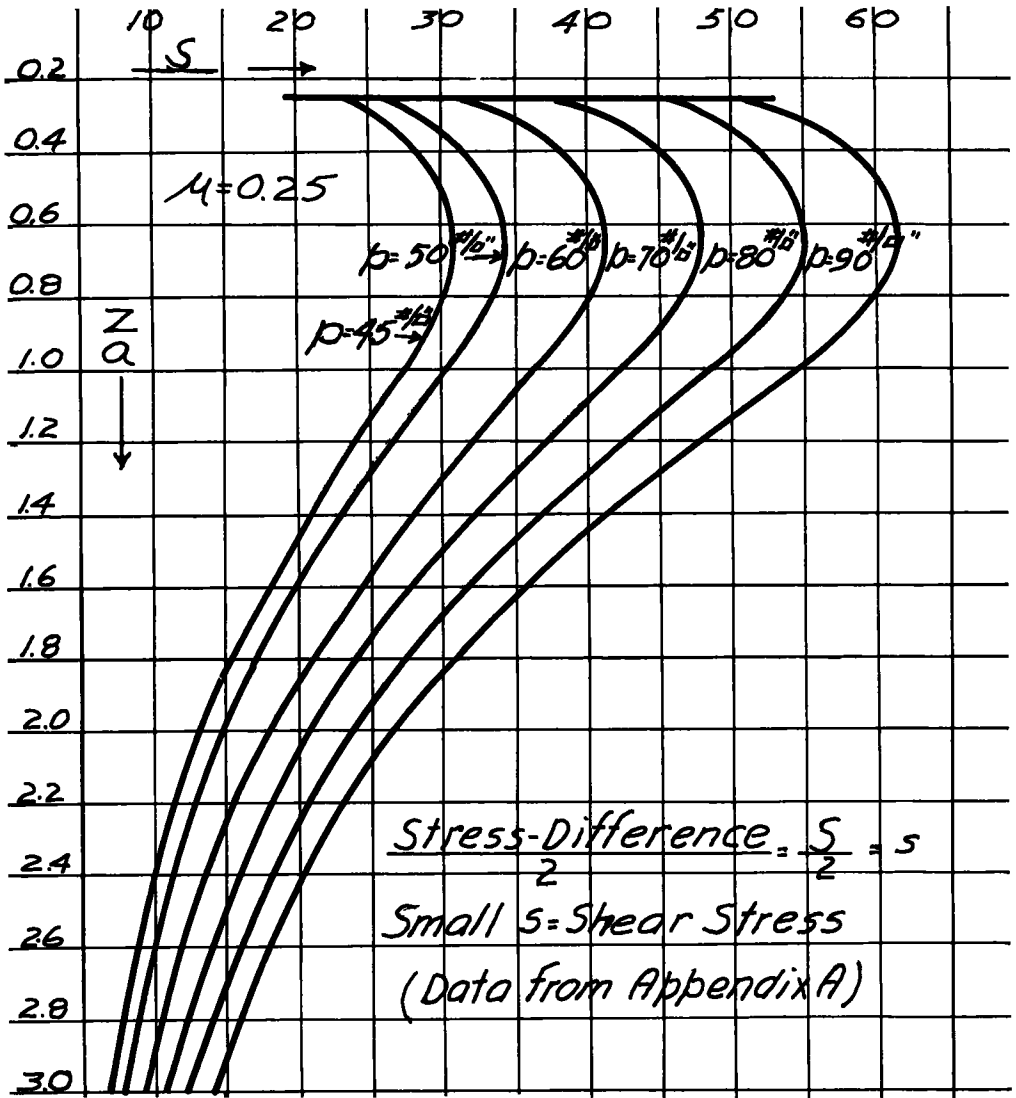
Figure 15. Stress-difference along vertical centerline beneath the circular foundatio

REFERENCES

1. Boussinesq, J.V., "Application des Potentiels a l'Etude de l'Equilibre et du Mouvement des Solides Elastiques." Gauthier-Villars, Paris (1885

2. Love, A.E.H., "The Stress Produced in a Semi-Infinite Solid by Pressure on Pa of the Boundary." Philosophical Trans., Royal Society (London, England), Series A, Vol. 228 (1929).

3. Tufts, W.M., "Public Aids to Transportation." Vol. 14, pp. 248-250, U.S. Gov Print. Off. (1940).

Figure 16. Vertical stress $\overline{zz} = p_z$ along centerline beneath the circular foundation.

Appendix

$\frac{\rho}{a}$	$\frac{\tilde{\rho}\tilde{\rho}}{p}$			$\frac{\tilde{\omega}\tilde{\omega}}{p}$			$\frac{\hat{z}\hat{z}}{p}$	$\frac{pz}{p}$	$\frac{s}{p}$		
	$M=0$	$M=0.25$	$M=0.5$	$M=0$	$M=0.25$	$M=0.5$			$M=0$	$M=0.25$	$M=0.5$

$$\frac{z}{a} = 0.25$$

$\frac{\rho}{a}$	$M=0$	$M=0.25$	$M=0.5$	$M=0$	$M=0.25$	$M=0.5$	$\frac{\hat{z}\hat{z}}{p}$	$\frac{pz}{p}$	$M=0$	$M=0.25$	$M=0.5$
0	-0.2613	-0.4540	-0.6133	-0.2646	-0.4540	-0.6133	-0.9857	0	0.7211	0.5318	0.3424
0.0670	-0.2611	-0.4538	-0.6428	-0.2633	-0.4576	-0.6119	-0.9855	-0.0034	0.7209	0.5318	0.3429
0.3131	-0.2431	-0.4304	-0.6177	-0.2576	-0.4405	-0.6224	-0.9801	-0.0294	0.7394	0.5529	0.3672
0.5670	-0.1828	-0.3649	-0.5471	-0.2401	-0.4027	-0.5652	-0.9542	-0.0781	0.7871	0.6097	0.4361
0.7500	-0.1111	-0.2846	-0.4580	-0.2173	-0.3469	-0.4765	-0.8838	-0.1397	0.8361	0.6702	0.5322
0.8834	-0.0696	-0.2333	-0.3970	-0.1978	-0.2820	-0.3662	-0.7243	-0.2562	0.8314	0.7097	0.6080
1.0000	-0.0822	-0.2335	-0.3849	-0.1832	-0.2131	-0.2430	-0.4596	-0.2988	0.7069	0.6390	0.6023
1.1166	-0.0892	-0.2252	-0.3613	-0.1735	-0.1553	-0.1371	-0.2086	-0.2342	0.4776	0.4628	0.4870
1.2500	-0.0957	-0.1635	-0.2812	-0.1620	-0.1149	-0.0677	-0.0737	-0.1297	0.2609	0.2745	0.3320
1.4330	+0.0116	-0.0842	-0.1800	-0.1435	-0.0859	-0.0284	-0.0211	-0.0525	0.1195	0.1311	0.1961
1.6869	+0.0044	-0.0286	-0.1015	-0.1172	-0.0638	-0.0105	-0.0034	-0.0227	0.0675	0.0509	0.1061
2.4178	+0.0460	+0.0079	-0.0301	-0.0668	-0.0341	-0.0014	-0.0005	-0.0037	0.0471	0.0113	0.0306

$$\frac{z}{a} = 0.50$$

$\frac{\rho}{a}$	$M=0$	$M=0.25$	$M=0.5$	$M=0$	$M=0.25$	$M=0.5$	$\frac{\hat{z}\hat{z}}{p}$	$\frac{pz}{p}$	$M=0$	$M=0.25$	$M=0.5$
0	-0.0975	-0.2357	-0.3739	-0.0975	-0.2357	-0.3739	-0.9106	0	0.8130	0.6749	0.5367
0.1340	-0.0951	-0.2327	-0.3703	-0.0961	-0.2329	-0.3698	-0.9066	-0.0292	0.8136	0.6764	0.5395
0.2859	-0.0848	-0.2208	-0.3567	-0.0932	-0.2246	-0.3559	-0.8913	-0.0654	0.8170	0.6832	0.5504
0.5000	-0.0628	-0.1938	-0.3249	-0.0851	-0.2009	-0.3168	-0.8396	-0.1287	0.8183	0.6951	0.5754
0.7688	-0.0474	-0.1615	-0.2875	-0.0736	-0.1532	-0.2328	-0.6775	-0.2259	0.7753	0.6813	0.5968
1.0000	-0.0752	-0.1809	-0.2864	-0.0701	-0.1054	-0.1406	-0.4175	-0.2621	0.6258	0.5721	0.5403
1.1820	-0.0914	-0.1836	-0.2758	-0.0726	-0.0769	-0.0811	-0.2224	-0.2143	0.4481	0.4303	0.4318
1.5000	-0.0559	-0.1261	-0.1962	-0.0736	-0.0510	-0.0283	-0.0604	-0.1019	0.2038	0.2140	0.2448
1.7141	-0.0267	-0.0848	-0.1430	-0.0685	-0.0420	-0.0146	-0.0268	-0.0590	0.1181	0.1316	0.1657
2.0722	+0.0138	-0.0355	-0.0848	-0.0593	-0.0324	-0.0053	-0.0085	-0.0260	0.0565	0.0586	0.0924
2.8660	+0.0175	-0.0075	-0.0324	-0.0394	-0.0202	-0.0010	-0.0013	-0.0069	0.0227	0.0142	0.0337
3.8356	+0.0175	+0.0035	-0.0106	-0.0237	-0.0105	+0.0024	+0.0026	-0.0019	0.0203	0.0039	0.0137

$$\frac{z}{a} = 0.75$$

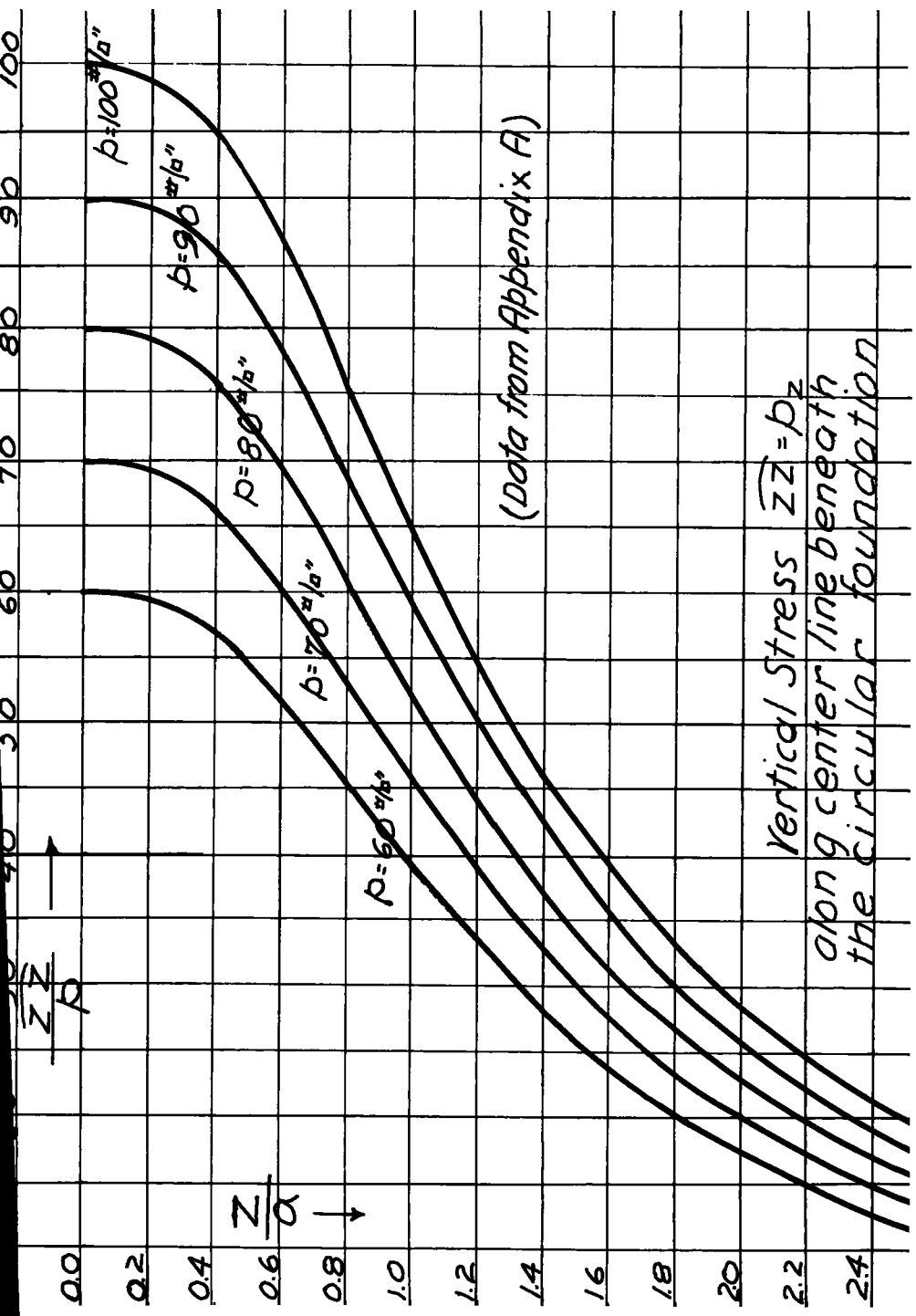| $\frac{\rho}{a}$	$M=0$	$M=0.25$	$M=0.5$	$M=0$	$M=0.25$	$M=0.5$	$\frac{\hat{z}\hat{z}}{p}$	$\frac{pz}{p}$	$M=0$	$M=0.25$	$M=0.5$
0	-0.0080	-0.1080	-0.2080	-0.0080	-0.1080	-0.2080	-0.7840	0	0.7760	0.6760	0.5760
0.1062	-0.0091	-0.1085	-0.2079	-0.0065	-0.1060	-0.2056	-0.7803	-0.0294	0.7734	0.6743	0.5753
0.3707	-0.0063	-0.1031	-0.1999	-0.0071	-0.0975	-0.1879	-0.7354	-0.1045	0.7585	0.6660	0.5749
0.5670	-0.0100	-0.1025	-0.1951	-0.0073	-0.0846	-0.1620	-0.6621	-0.1601	0.7264	0.6447	0.5662
0.7990	-0.0287	-0.1138	-0.1889	-0.0104	-0.0661	-0.1212	-0.5241	-0.2101	0.6506	0.5884	0.5326
1.0000	-0.0546	-0.1316	-0.2087	-0.0166	-0.0510	-0.0854	-0.3745	-0.2211	0.5457	0.5054	0.4722
1.2010	-0.0730	-0.1412	-0.2094	-0.0247	-0.0398	-0.0548	-0.2353	-0.1940	0.4206	0.3993	0.3889
1.4330	-0.0722	-0.1304	-0.1886	-0.0328	-0.0318	-0.0309	-0.1241	-0.1412	0.2872	0.2825	0.2897
1.7500	-0.0492	-0.0956	-0.1419	-0.0380	-0.0260	-0.0139	-0.0872	-0.0804	0.1652	0.1610	0.1698
2.0711	-0.0292	-0.0662	-0.1031	-0.0378	-0.0222	-0.0066	-0.0639	-0.0448	0.0960	0.0895	0.0977
2.6084	-0.0039	-0.0300	-0.0561	-0.0328	-0.0175	-0.0022	-0.0367	-0.0186	0.0495	0.0377	0.0418
3.7990	+0.0082	-0.0057	-0.0196	-0.0212	-0.0108	-0.0003	-0.0130	-0.0091	0.0227	0.0110	0.0105

$$\frac{z}{a} = 1.00$$

$\frac{\rho}{a}$	$M=0$	$M=0.25$	$M=0.5$	$M=0$	$M=0.25$	$M=0.5$	$\frac{\hat{z}\hat{z}}{p}$	$\frac{pz}{p}$	$M=0$	$M=0.25$	$M=0.5$
0	-0.0303	-0.0429	-0.1161	-0.0303	-0.0429	-0.1161	-0.6464	0	0.6768	0.6036	0.5303
0.1609	-0.0276	-0.0449	-0.1174	-0.0315	-0.0410	-0.1132	-0.6378	-0.0429	0.6708	0.5990	0.5273
0.4228	-0.0200	-0.0503	-0.1205	-0.0272	-0.0373	-0.1019	-0.5864	-0.1081	0.6438	0.5781	0.5136
0.6360	-0.0047	-0.0620	-0.1287	-0.0224	-0.0317	-0.0858	-0.5103	-0.1521	0.5981	0.5417	0.4880
0.9125	-0.0247	-0.0850	-0.1453	-0.0127	-0.0242	-0.0612	-0.3773	-0.1813	0.5059	0.4658	0.4305
1.1763	-0.0499	-0.1031	-0.1563	-0.0013	-0.0191	-0.0396	-0.2461	-0.1713	0.3948	0.3712	0.3306
1.4663	-0.0594	-0.1046	-0.1499	-0.0101	-0.0163	-0.0225	-0.1363	-0.1325	0.2760	0.2670	0.2654
1.8391	-0.0180	-0.0844	-0.1205	-0.0193	-0.0149	-0.0105	-0.0595	-0.0812	0.1627	0.1642	0.1734
2.4281	-0.0223	-0.0476	-0.0732	-0.0230	-0.0132	-0.0034	-0.0173	-0.0398	0.0698	0.0760	0.0892
3.1445	-0.0079	-0.0233	-0.0397	-0.0206	-0.0108	-0.0011	-0.0050	-0.0138	0.0277	0.0327	0.0444
4.7321	+0.0076	-0.0043	-0.0131	-0.0132	-0.0067	-0.0001	-0.0060	-0.0029	0.0077	0.0068	0.0137

ρ/a	$\frac{\rho\bar{\rho}}{p}$			$\frac{\bar{\omega}\bar{\omega}}{2}$			$\frac{\bar{z}\bar{z}}{p}$	$\frac{\bar{p}z}{p}$	$\frac{S}{p}$		
	$\mu=0.0$	$\mu=0.25$	$\mu=0.50$	$\mu=0.0$	$\mu=0.25$	$\mu=0.50$			$\mu=0.0$	$\mu=0.25$	$\mu=0.50$

$$\frac{z}{a} = 1.25$$

ρ/a	$\mu=0.0$	$\mu=0.25$	$\mu=0.50$	$\mu=0.0$	$\mu=0.25$	$\mu=0.50$	$\bar{z}\bar{z}/p$	$\bar{p}z/p$	$\mu=0.0$	$\mu=0.25$	$\mu=0.50$
0	-0.0428	-0.0120	-0.0668	-0.0428	-0.0120	-0.0668	-0.5239	0	0.5667	0.5119	0.4571
0.1247	-0.0389	-0.0143	-0.0686	-0.0443	-0.0104	-0.0650	-0.5197	-0.0276	0.5623	0.5083	0.4545
0.4141	-0.0305	-0.0224	-0.0752	-0.0380	-0.0104	-0.0595	-0.4774	-0.0878	0.5373	0.4877	0.4388
0.6651	-0.0123	-0.0378	-0.0878	-0.0326	-0.0087	-0.0499	-0.4100	-0.1263	0.4921	0.4499	0.4094
0.8906	-0.0083	-0.0550	-0.1017	-0.0248	-0.0074	-0.0396	-0.3322	-0.1451	0.4349	0.4013	0.3706
1.1096	-0.0271	-0.0700	-0.1130	-0.0164	-0.0067	-0.0298	-0.2534	-0.1463	0.3699	0.3453	0.3246
1.4550	-0.0446	-0.0812	-0.1179	-0.0036	-0.0069	-0.0174	-0.1470	-0.1224	0.2657	0.2537	0.2466
1.8753	-0.0435	-0.0731	-0.1027	-0.0074	-0.0080	-0.0085	-0.0696	-0.0811	0.1644	0.1623	0.1656
2.4897	-0.0261	-0.0476	-0.0691	-0.0142	-0.0086	-0.0030	-0.0233	-0.0393	0.0786	0.0822	0.0909
3.1651	-0.0112	-0.0267	-0.0422	-0.0150	-0.0081	-0.0011	-0.0080	-0.0182	0.0365	0.0409	0.0499
4.4343	+0.0003 +0	-0.0089	-0.0181	-0.0120	-0.0061	-0.0002	-0.0017	-0.0054	0.0110	0.0130	0.0196

$$\frac{z}{a} = 1.50$$

ρ/a	$\mu=0.0$	$\mu=0.25$	$\mu=0.50$	$\mu=0.0$	$\mu=0.25$	$\mu=0.50$	$\bar{z}\bar{z}/p$	$\bar{p}z/p$	$\mu=0.0$	$\mu=0.25$	$\mu=0.50$
0	-0.0440	+0.0020	-0.0399	0.0440	0.0020	-0.0399	-0.4240	0	0.4680	0.4260	0.3840
0.1340	-0.0416	-0.0000	-0.0417	0.0499	0.0031	-0.0387	-0.4203	-0.0235	0.4642	0.4229	0.3815
0.4540	-0.0310	-0.0094	-0.0499	0.0398	0.0022	-0.0355	-0.3833	-0.0746	0.4404	0.4025	0.3653
0.7355	-0.0127	-0.0255	-0.0637	0.0332	0.0019	-0.0294	-0.3240	-0.1060	0.3979	0.3661	0.3357
1.0000	-0.0048	-0.0422	-0.0777	0.0251	0.0011	-0.0229	-0.2560	-0.1191	0.3449	0.3202	0.2976
1.2645	-0.0233	-0.0556	-0.0879	0.0166	-0.0000	-0.0167	-0.1892	-0.1165	0.2860	0.2685	0.2540
1.5960	-0.0338	-0.0626	-0.0914	0.0083	-0.0016	-0.0114	-0.1292	-0.1019	0.2250	0.2144	0.2073
1.8660	-0.0366	-0.0616	-0.0866	0.0007	-0.0032	-0.0072	-0.0800	-0.0798	0.1624	0.1576	0.1567
2.2587	-0.0318	-0.0527	-0.0736	-0.0054	-0.0047	-0.0040	-0.0435	-0.0551	0.1108	0.1106	0.1143
2.7876	-0.0215	-0.0380	-0.0545	-0.0085	-0.0057	-0.0019	-0.0197	-0.0322	0.0694	0.0669	0.0732
3.5981	-0.0095	-0.0212	-0.0329	-0.0107	-0.0057	-0.0007	-0.0066	-0.0146	0.0294	0.0327	0.0393
4.2186	-0.0042	-0.0135	-0.0227	-0.0101	-0.0052	-0.0003	-0.0032	-0.0085	0.0170	0.0198	0.0195

$$\frac{z}{a} = 1.75$$

ρ/a	$\mu=0.0$	$\mu=0.25$	$\mu=0.50$	$\mu=0.0$	$\mu=0.25$	$\mu=0.50$	$\bar{z}\bar{z}/p$	$\bar{p}z/p$	$\mu=0.0$	$\mu=0.25$	$\mu=0.50$
0	0.0410	0.0080	-0.0249	0.0410	0.0080	-0.0249	-0.3455	0	0.3865	0.3535	0.3206
0.1840	0.0387	0.0061	-0.0266	0.0409	0.0084	-0.0241	-0.3406	-0.0251	0.3826	0.3502	0.3179
0.5311	0.0270	-0.0045	-0.0361	0.0364	0.0074	-0.0216	-0.3058	-0.0663	0.3583	0.3292	0.3006
0.8469	0.0097	-0.0200	-0.0496	0.0298	0.0061	-0.0177	-0.2532	-0.0902	0.3188	0.2948	0.2719
1.1531	-0.0077	-0.0350	-0.0623	0.0221	0.0044	-0.0134	-0.1997	-0.0978	0.2706	0.2525	0.2362
1.4689	-0.0212	-0.0458	-0.0704	0.0141	0.0023	-0.0095	-0.1386	-0.0921	0.2184	0.2062	0.1963
1.8160	-0.0294	-0.0500	-0.0717	0.0066	0.0002	-0.0062	-0.0901	-0.0769	0.1657	0.1589	0.1549
2.2254	-0.0289	-0.0469	-0.0652	0.0008	-0.0018	-0.0036	-0.0523	-0.0568	0.1160	0.1137	0.1143
2.7500	-0.0225	-0.0373	-0.0522	-0.0049	-0.0034	-0.0018	-0.0253	-0.0361	0.0723	0.0732	0.0769
3.4993	-0.0129	-0.0240	-0.0351	-0.0076	-0.0042	-0.0007	-0.0102	-0.0187	0.0375	0.0399	0.0449
4.7529	-0.0036	-0.0108	-0.0180	-0.0076	-0.0039	-0.0002	-0.0027	-0.0069	0.0139	0.0160	0.0206

$$\frac{z}{a} = 2.00$$

ρ/a	$\mu=0.0$	$\mu=0.25$	$\mu=0.50$	$\mu=0.0$	$\mu=0.25$	$\mu=0.50$	$\bar{z}\bar{z}/p$	$\bar{p}z/p$	$\mu=0.0$	$\mu=0.25$	$\mu=0.50$
0	0.0367	0.0103	-0.0161	0.0367	0.0103	-0.0161	-0.2835	0	0.3211	0.2947	0.2683
0.2721	0.0331	0.0071	-0.0189	0.0363	0.0105	-0.0153	-0.2767	-0.0285	0.3150	0.2894	0.2640
0.6973	0.0213	-0.0037	-0.0287	0.0316	0.0091	-0.0135	-0.2430	-0.0606	0.2907	0.2682	0.2461
1.3527	-0.0093	-0.0306	-0.0519	0.0180	0.0050	-0.0080	-0.1459	-0.0802	0.2107	0.1975	0.1859
1.7279	-0.0196	-0.0386	-0.0575	0.0101	0.0027	-0.0084	-0.0996	-0.0721	0.1649	0.1566	0.1502
2.1547	-0.0234	-0.0401	-0.0565	0.0043	0.0005	-0.0033	-0.0612	-0.0571	0.1201	0.1161	0.1143
2.6782	-0.0217	-0.0352	-0.0488	-0.0011	-0.0014	-0.0018	-0.0329	-0.0393	0.0794	0.0786	0.0802
3.3835	-0.0151	-0.0256	-0.0361	-0.0047	-0.0029	-0.0008	-0.0145	-0.0226	0.0453	0.0466	0.0502
4.4681	-0.0068	-0.0142	-0.0215	-0.0061	-0.0032	-0.0003	-0.0097	-0.0100	0.0201	0.0222	0.0261

$\frac{\rho}{a}$	$\frac{\bar{\rho}\rho}{p}$			$\frac{\bar{\omega}\omega}{p}$			$\frac{\bar{z}z}{p}$	$\frac{\bar{\rho}z}{p}$	$\frac{s}{p}$		
	μ=0.0	μ=0.25	μ=0.50	μ=0.0	μ=0.25	μ=0.50			μ=0.0	μ=0.25	μ=0.50
					$\frac{z}{a}=2.50$						
0	0.0283	0.0104	-0.0075	0.0283	0.0104	-0.0075	-0.1996	0	0.2278	0.2100	0.1921
0.3301	0.0254	0.0078	-0.0098	0.0278	0.0104	-0.0070	-0.1935	-0.0212	0.2230	0.2057	0.1885
0.7813	0.0159	-0.0010	-0.0179	0.0241	0.0090	-0.0062	-0.1681	-0.0442	0.2091	0.1890	0.1742
1.2187	0.0034	-0.0123	-0.0290	0.0189	0.0071	-0.0048	-0.1327	-0.0553	0.1759	0.1635	0.1524
1.6699	-0.0076	-0.0218	-0.0360	0.0131	0.0048	-0.0035	-0.0955	-0.0577	0.1420	0.1337	0.1264
2.1658	-0.0146	-0.0270	-0.0394	0.0078	0.0026	-0.0023	-0.0621	-0.0481	0.1073	0.1024	0.0988
2.7505	-0.0164	-0.0269	-0.0374	0.0025	0.0006	-0.0013	-0.0357	-0.0359	0.0743	0.0723	0.0718
3.500	-0.0136	-0.0220	-0.0303	-0.0013	-0.0010	-0.0006	-0.0174	-0.0227	0.0456	0.0457	0.0472
4.5704	-0.0081	-0.0142	-0.0204	-0.0035	-0.0019	-0.0002	-0.0066	-0.0117	0.0234	0.0246	0.0271
					$\frac{z}{a}=3.00$						
0	0.0218	0.0089	-0.0039	0.0218	0.0089	-0.0039	-0.1462	0	0.1680	0.1551	0.1423
0.7375	0.0148	0.0025	-0.0098	0.0199	0.0083	-0.0032	-0.1300	-0.0281	0.1554	0.1440	0.1327
1.2625	-0.0056	-0.0060	-0.0175	0.0159	0.0066	-0.0027	-0.1046	-0.0392	0.1353	0.1261	0.1172
1.8038	-0.0036	-0.0141	-0.0245	0.0113	0.0047	-0.0020	-0.0761	-0.0414	0.1101	0.0135	0.0976
2.3989	-0.0098	-0.0190	-0.0282	0.0067	0.0027	-0.0013	-0.0497	-0.0366	0.0833	0.0793	0.0762
3.5173	-0.0115	-0.0184	-0.0254	0.0010	0.0002	-0.0005	-0.0203	-0.0225	0.0458	0.0450	0.0452
					$\frac{z}{a}=4.00$						
0	0.0136	0.0061	-0.0013	0.0136	0.0061	-0.0013	-0.0868	0	0.1005	0.0931	0.0856
0.2947	0.0121	0.0049	-0.0023	0.0141	0.0066	-0.0009	-0.0856	-0.0058	0.0984	0.0912	0.0840
1.0000	0.0086	-0.0015	-0.0056	0.0124	0.0058	-0.0009	-0.0761	-0.0176	0.0918	0.0825	0.0789
1.7053	0.0028	-0.0038	-0.0105	0.0096	0.0044	-0.0008	-0.0564	-0.0239	0.0760	0.0710	0.0663
2.4559	-0.0029	-0.0031	-0.0148	0.0066	0.0030	-0.0006	-0.0463	-0.0243	0.0653	0.0651	0.0580
3.3094	-0.0061	-0.0112	-0.0164	0.0036	0.0016	-0.0004	-0.0355	-0.0205	0.0504	0.0477	0.0452
4.3564	-0.0071	-0.0113	-0.0156	0.0010	0.0003	-0.0005	-0.0258	-0.0144	0.0343	0.0322	0.0305

THE National Academy of Sciences—National Research Council is a private, nonprofit organization of scientists, dedicated to the furtherance of science and to its use for the general welfare. The Academy itself was established in 1863 under a congressional charter signed by President Lincoln. Empowered to provide for all activities appropriate to academies of science, it was also required by its charter to act as an adviser to the federal government in scientific matters. This provision accounts for the close ties that have always existed between the Academy and the government, although the Academy is not a governmental agency.

The National Research Council was established by the Academy in 1916, at the request of President Wilson, to enable scientists generally to associate their efforts with those of the limited membership of the Academy in service to the nation, to society, and to science at home and abroad. Members of the National Research Council receive their appointments from the president of the Academy. They include representatives nominated by the major scientific and technical societies, representatives of the federal government, and a number of members at large. In addition, several thousand scientists and engineers take part in the activities of the research council through membership on its various boards and committees.

Receiving funds from both public and private sources, by contribution, grant, or contract, the Academy and its Research Council thus work to stimulate research and its applications, to survey the broad possibilities of science, to promote effective utilization of the scientific and technical resources of the country, to serve the government, and to further the general interests of science.

The Highway Research Board was organized November 11, 1920, as an agency of the Division of Engineering and Industrial Research, one of the eight functional divisions of the National Research Council. The Board is a cooperative organization of the highway technologists of America operating under the auspices of the Academy–Council and with the support of the several highway departments, the Bureau of Public Roads, and many other organizations interested in the development of highway transportation. The purposes of the Board are to encourage research and to provide a national clearinghouse and correlation service for research activities and information on highway administration and technology.